Lawrence Berkeley National Laboratory
Lawrence Berkeley National Laboratory

Title

Cycle-Life Improvement of Zn/NiOOH Cells by the Addition of Ca(OH)2 to the Zinc Electrode

Permalink

https://escholarship.org/uc/item/8nb1575t

Author

Jain, R.

Publication Date

1989-08-01

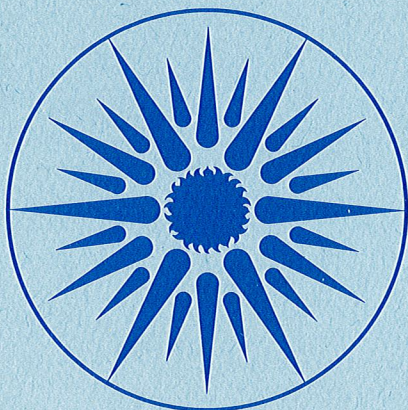Peer reviewed

Lawrence Berkeley Laboratory
UNIVERSITY OF CALIFORNIA

APPLIED SCIENCE DIVISION

Cycle-Life Improvement of Zn/NiOOH Cells by the Addition of $Ca(OH)_2$ to the Zinc Electrode

R. Jain,[*] F.R. McLarnon, and E.J. Cairns

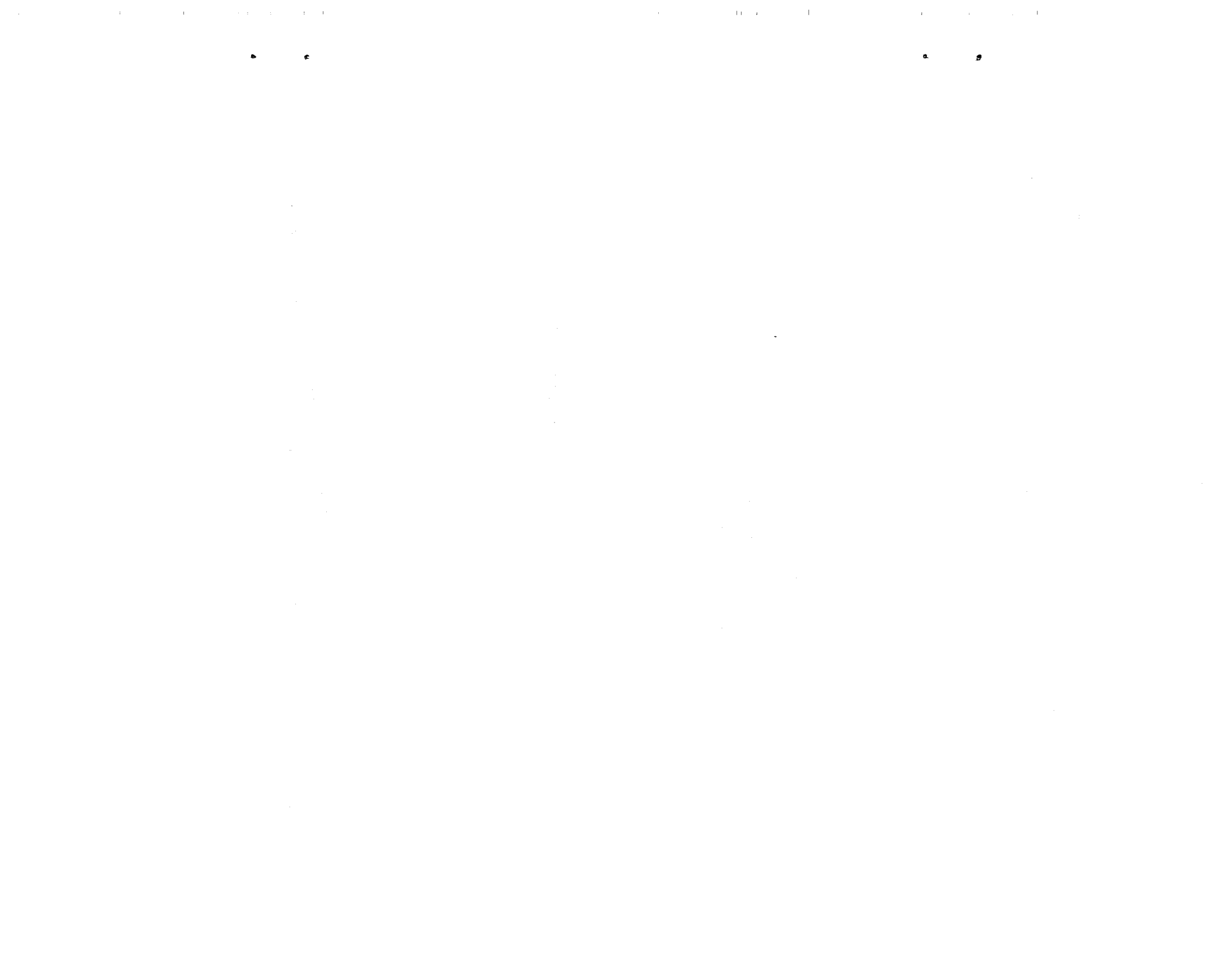[*](M.S. Thesis)

August 1989

APPLIED SCIENCE
DIVISION

Cycle-Life Improvement of Zn/NiOOH Cells by the Addition of Ca(OH)$_2$ to the Zinc Electrode

by

Rajiv Jain, Frank R. McLarnon and Elton J. Cairns

Applied Science Division
Lawrence Berkeley Laboratory
University of California
Berkeley, California 94720

Cycle-Life Improvement of Zn/NiOOH Cells by the Addition of $Ca(OH)_2$ to the Zinc Electrode

Rajiv Jain

Abstract

The addition of $Ca(OH)_2$ to the zinc electrode of Zn/NiOOH cells was investigated in order to determine its effect on reducing the rate of Zinc redistribution. Cells containing 0, 10, 25, and 40 mol% $Ca(OH)_2$ in the zinc electrode were constructed and tested. $Ca(OH)_2$ was found to form a calcium zincate complex with the zincate-supersaturated KOH solution created during the discharge half-cycle. As $Ca(OH)_2$ is insoluble in the electrolyte, the formation of this complex (containing two Zn atoms to one Ca) significantly reduces the Zinc redistribution rate. Electrodes with only 10% $Ca(OH)_2$ were found to contain insufficient $Ca(OH)_2$ to complex with enough Zinc to make a dramatic improvement in cycle life. The 25%-$Ca(OH)_2$ electrodes, however, were found to retain their capacity beyond 150 deep discharge cycles, with indication that any further Zinc redistribution would occur very slowly. The Zinc utilization of the Ca-containing electrodes showed dramatic improvement over the Ca-free zinc electrodes.

Another factor influencing the rate of Zinc redistribution was found to be the proximity of the separator seal to the edges of the zinc electrode. The closer the seal, the lower the rate of Zinc migration. Material balances performed on the cells showed that over 90% of the Zinc leaving the zinc electrode migrates to the NiOOH electrodes. There are indications that the Zinc may be complexing or binding with $Ni(OH)_2$ or NiOOH.

Acknowledgements

I want to express my thanks for the help and support given to me by my fellow researchers, Mark Isaacson, Robert Goldberg, Kenneth Miller and Thomas Adler. In addition, I am indebted and grateful to Marco Katz and James Nichols for their considerable work in establishing the Zn/Ni battery laboratory, the cycling equipment and the basic procedures. Their theses were essential in this work. I would also like to give my tender thanks to Susan Lauer for her indispensable help in creating the figures, tables, and final corrected, formatted thesis. My research advisors, Dr. Elton Cairns and Dr. Frank McLarnon, have my respect and gratitude for their many hours of consultation required in the performance of this project.

My special thanks go to my family, friends and relatives, who would not let me drop the thesis, no matter how hard I begged.
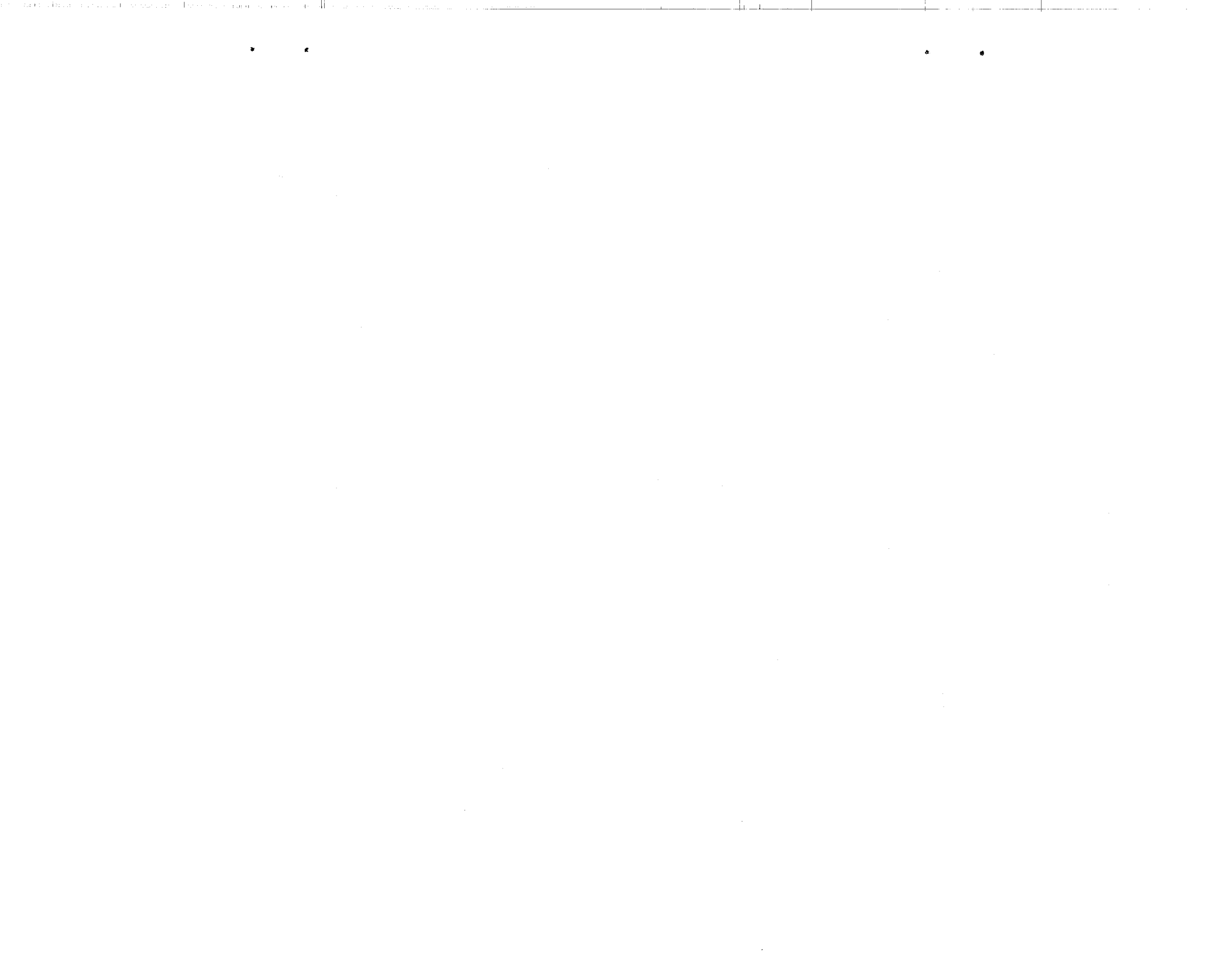
The experimental portion of this thesis was performed between October 1982 and October 1985.

Table of Contents

Chapter 1

Introduction

As the world's population grows and advances to more technological economies, more and more demand is made of the energy resources. As recently as in the 1960's most of the demand for petroleum and other sources of energy came from the more-developed nations. But now, even in poor third-world nations such as India, many of the rapidly growing middle class are able to purchase motor vehicles and other energy-consuming devices such as air conditioners, refrigerators and television sets. This not only leads to the quickened depletion of oil resources, but also to increased air pollution in cities and construction of expensive power plants to handle "peak" power consumption.

To meet the energy demand, non-petroleum energy sources such as nuclear, hydroelectric, thermal, wind, solar, coal and others are being developed and utilized. Unfortunately, these energy sources are feasible only for stationary power generation and would not decrease the demand for, and pollution caused by, gasoline usage in vehicles.

Many other methods for powering vehicles have been considered but due to the high energy density, low cost, and large supply requirements, in addition to safety considerations, very few viable alternatives to gasoline are available. The most promising option is the use of rechargeable batteries, thus creating the "electric" car. These battery-powered automobiles would basically be similar to electric golf carts and electric fork-lift trucks which currently use rechargeable batteries. Rechargeable batteries are those that once discharged (depleted of energy) only have to be charged with elec-

tricity to reestablish their energy content.

Batteries are an ideal candidate for vehicle propulsion because they cause negligible environmental pollution at the point of usage and are recharged with electricity, which can be produced using a variety of primary energy sources, such as nuclear. The power plants which produce electricity for the batteries would still be sources of pollution; however, it is much easier and less expensive to install pollution-control devices at large plants than in millions of individual cars. Another advantage of using batteries is that since an electric motor would weigh less than a gasoline engine, less primary energy would be required to propel electric vehicles. In addition, as vehicles are generally driven during the day, the batteries would be recharged at night and thus consume energy during times when power plants have excess capacity. This would help balance the load requirements of power plants. Batteries are also currently being considered to directly load level power plants by being used to store the excess energy available at night and release that energy during the day. An added value of batteries is that once the energy is delivered to them, they are over 70% efficient in returning the energy.

Developing a battery for electric vehicles, though, has proven difficult. The rechargeable Cd/NiOOH batteries used in portable consumer products, are much too expensive for use in electric cars. Also, there is not expected to be enough Cadmium available to convert a significant number of gasoline-powered vehicles to electric. The most common rechargeable battery, the lead-acid battery, weighs too much for the amount of energy it delivers. If you put wheels on a lead acid battery, it could barely pull itself, let alone a car with a driver over an extended distance. Generally, it is expected that for a battery to be practical for electric vehicles, it would have to weigh

less than one third of the total weight of the vehicle, provide a 200 km vehicle range between recharging, and accept at least 800 charges. To meet these goals, many types of batteries are being investigated. These include both ambient-temperature and high-temperature batteries. A popular and very attractive candidate is the Zn/NiOOH battery.

The Zn/NiOOH battery has a sufficiently high theoretical specific energy (326 Wh/kg - watt hours per kilogram) that it is expected to be able to deliver the desired minimum of 75 Wh/kg when assembled into a complete battery. In addition, it exhibits very high specific power (required for acceleration) and operates well even during very cold ambient conditions (-20°C). Zinc and Ni are common and fairly inexpensive materials and are not highly toxic. Much research has been done to develop this battery but problems still remain. One is that the cost of the battery is still fairly high due to the cost of the NiOOH electrode. Another problem is O_2 and H_2 evolution in the battery. Safety and maintenance considerations would probably require that the developed battery be sealed, and that it have a recombination electrode to recreate the H_2O. However, the most significant problem is the lifetime of this battery; it rarely completes more than 100 to 200 full-capacity cycles before failing. Failure is caused mainly by two phenomena: Zinc dendrites shorting to the NiOOH electrode and Zinc material redistribution.

In this paper, Zinc (capitalized) refers to zinc in any form it may be in, i.e. as zinc metal, ZnO, zincate etc.. In the same way, Calcium (capitalized) refers to calcium in any form (usually either calcium hydroxide or calcium zincate).

Zinc dendrites have been controlled somewhat by improved separators and optimized cycling conditions, and thus are not often the main cause of failure (but they are

still of concern). Zinc material redistribution (shape change) is the gradual movement of the Zinc across the face of the electrode. This results in regions which are very dense with Zinc and regions which have very little or no Zinc. This causes problems because the NiOOH electrode will only charge and discharge efficiently if there is Zinc material directly opposing. Also, the dense Zinc areas are less porous leading to higher overpotentials and decreased Zinc utilization. These dense areas can also cause punctures in the separator leading to shorts.

The cause of shape change is not certain, but there are theories which offer an explanation. McBreen proposes that there are uneven current distributions during charge and discharge which lead to concentration gradients which in turn ultimately lead to the movement of Zinc.[1] A model by Choi, Bennion, and Newman suggests that osmotic and electro-osmotic forces result in convective currents due to the movement of water.[2] The convective flows cause the movement of soluble Zinc species, and as the electrolyte level is low during discharge and high during charge, the active Zinc material should slowly move to the lower regions of the electrode with cycling. Experimental results obtained by Gunther and Bendert also indicate that electrolyte movement is a large factor in Zinc redistribution.[3] Neither of these two models can fully account for the shape change phenomenon, however they both predict that if the amount of Zinc in solution is decreased, the rate of Zinc redistribution will decrease. Zinc solubility in the electrolyte is considered to be a major cause of shape change.

The overall cell reaction is:

$$Zn + 2NiOOH + H_2O \rightleftarrows ZnO + 2Ni(OH)_2$$

The half cell reaction for the NiOOH electrode is:

$$2NiOOH + 2H_2O + 2e^- \rightleftarrows 2Ni(OH)_2 + 2OH^-$$
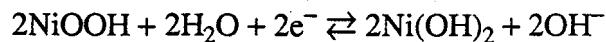
The net half cell reaction which takes place at the zinc electrode is:

$$Zn + 2(OH)^- \rightleftarrows ZnO + H_2O + 2e^-$$
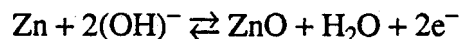
The Zn is expected to react with the KOH electrolyte to create $Zn(OH)_4^{2-}$ (zincate) in solution, which in turn precipitates as ZnO.[4]

$$Zn + 4OH^- \rightleftarrows Zn(OH)_4^{2-} + 2e^- \quad \text{Dissolution}$$

$$Zn(OH)_4^{2-} \rightleftarrows ZnO + 2OH^- + H_2O \quad \text{Precipitation}$$
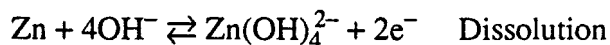
Concentrated hydroxide electrolyte is required for an efficient NiOOH electrode, but the more concentrated the electrolyte, the greater the amount of Zinc which will be dissolved at equilibrium. Although the electrolyte is saturated with ZnO before cell assembly, it is thought that during electrochemical discharge, the electrolyte may become supersaturated with Zinc, which would promote shape change. According to Dirkse, the appearance of "supersaturated" zincate solutions occurs because the zinc electrode oxidizes to form zincates ($K_2Zn(OH)_4$). These zincates are metastable with respect to ZnO and decompose very slowly. Because of this slow decomposition, "supersaturation" can occur.[4]

In order to decrease the rate of this Zinc redistribution, much research has been and is being performed to reduce Zinc solubility in the electrolyte. In this research group, James Nichols has investigated the use of various concentrations of KOH electrolytes and combination electrolytes such as KOH-KF.[5] Results indicate an improvement with KOH-KF electrolyte vs. KOH alone. Research in this area is continuing. Mark Issacson has investigated the use of KOH-organic electrolyte combinations, but

the results were discouraging.[6] Another method of attack has been alternative charging methods such as pulse charging. This was investigated by Marco Katz and is also being currently examined by Thomas Adler.[7,8] Robert Goldberg has considered alternative current collector designs and materials and currently Mark Issacson is developing methods to determine local concentrations in a working cell in order to help in developing a better theoretical model of the cell.[6,9] Another researcher, Kenneth Miller, is working on a mathematical model for this cell.[10]

This research project took a different approach than changing the electrolyte to decrease the Zinc solubility. Instead, the goal was either to prevent the Zinc from dissolving, or to cause the Zinc to redeposit in a uniform manner. The method used was to change the properties of the electrode rather than the electrolyte. In order to do this, it was desired to add compounds to the electrode which would create an insoluble complex with the ZnO, but would still allow the ZnO to revert to Zn when the cell was charged. It was decided to examine $Ca(OH)_2$ as the complexing agent as there were indications in the literature that $Ca(OH)_2$ would form a precipitate with ZnO when added to concentrated zincate solutions.[11-16,20-23] Also, there are numerous patents which list $Ca(OH)_2$ as an additive in the zinc electrode. Kawamura and Maki's experiments indicated that the other alkaline earth metals were not effective in complexing with ZnO/zincate, and no other elements or compounds with similar properties were found in a literature review.[11] Calcium hydroxide is an ideal candidate as it is insoluble in hydroxide solutions and thus would retain its initial distribution. Also, $Ca(OH)_2$ would be a safe and inexpensive additive.

Chapter 2

The Calcium-Zinc Complex

Since the basis for the addition of $Ca(OH)_2$ to the zinc electrode is the formation of this calcium zincate complex, it was decided that basic experiments with $Ca(OH)_2$ and ZnO were necessary to better understand the complex and its formation. Understanding the complex better would help in designing the cell and in analyzing the cycling postmortem data. First, the literature was searched to see what information about the complex existed.

The paper by Kawamura and Maki indicated that when $Ca(OH)_2$ was added to a zincate-saturated KOH solution, a Ca-Zn complex was produced.[11] This complex was shown, by calculations based upon atomic absorption results, to contain 2 Ca atoms for every 3 Zn atoms and had a distinctive powder X-ray diffraction pattern (Figure 1). An article by W.J. van der Grinten indicates that when $Ca(OH)_2$ is added to a zinc electrode, a complex of one Ca to one Zn is produced.[12] As these two groups of authors created the complex in a fairly similar manner, the significant difference in their formula for the complex indicates that more experiments were required. In addition, powder X-ray diffraction patterns obtained by Liebau and Amel-Zadch and by Schwick were similar to the one by Kawamura and Maki but indicated that the complex was 1 Ca to 2 Zn.[17,18] Sharma also found the complex to be 1 Ca to 2 Zn atoms.[16]

To investigate the calcium-zincate complex, various methods were used in attempting its formation. To examine its possible benefit in a Zn/NiOOH cell, the reaction rate and other properties were observed qualitatively. The first was simply mixing
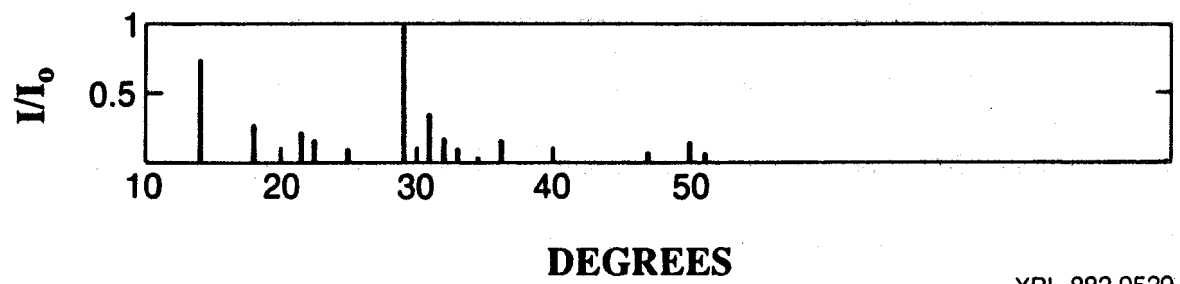
Figure 1. Powder X-ray diffraction pattern of calcium zincate complex.[9,12,13]

the dry $Ca(OH)_2$ powder with dry ZnO powder. After a few days this mixture was observed, by powder X-ray diffraction, to be only the combination of the $Ca(OH)_2$ spectrum with the ZnO spectrum. The next experiment was the mixing of the powders in a beaker of deionized H_2O. After a day of mixing, this yielded the same result. That neither of these experiments produced any calcium zincate indicates that the reaction is probably not a solid-state reaction and likely requires the Zinc to be in solution as zincate ion.

Further experiments were performed in zincate-saturated KOH solutions. As 31% KOH was used in the cell-cycling experiments (see Section 3.3), these also used a 31% KOH solution. In the first experiment, a small amount of $Ca(OH)_2$ was added to the zincate-saturated KOH solution. After a few hours of stirring, there was no indication of any reaction. However, after 24 hours, powder X-ray diffraction analysis of the precipitate indicated that some calcium zincate had formed. The second consisted of placing a small amount of $Ca(OH)_2$, which was sealed into a packet using a single layer of separator, into a stirred beaker of KOH solution and excess ZnO powder. After one day of stirring, there was no indication of any complex.

The next tests employed more complex procedures. A flat-bottom crystallizing dish bisected by a 1 to 2 mm high wall of epoxy was used. A thin layer of $Ca(OH)_2$ powder was put on one side and ZnO on the other. Both sides were then first filled with zincate-saturated KOH solution until the solutions were near the top of the epoxy but not in contact. After 20 hours, samples taken from the $Ca(OH)_2$ side showed no reaction. More zincate-saturated KOH was then added, avoiding any mixing of the two sides due to convection, until the two solutions came into contact and the liquid level

was at least 1 to 2mm above the epoxy. Samples were taken from both sides and at various distances from the center. There was no reaction seen in the first 24 hours except for a very small amount of Zinc found in the $Ca(OH)_2$ side. After 5 days, the region near the epoxy on the $Ca(OH)_2$ side became "stringy". By using energy dispersive spectroscopy for X-ray detection (EDS) in a scanning electron microscope (SEM) this area was found to have much more Zinc than that seen at 24 hours, however there was still no indication of crystals and there was still a large amount of unreacted $Ca(OH)_2$. Crystals were sought because, as will be seen, other experiments produced calcium zincate crystals. Also, calcium zincate crystals were found by other researchers.[15,16] This indicated that the $Ca(OH)_2$ was drawing the Zinc over to its side of the dish, but at a very slow rate.

After a sample was taken on day 5, the crystallization dish was shaken for one minute to create convective motion, mixing a small amount of powder together. A sample taken on the $Ca(OH)_2$ side 24 hours later contained a crystal which by EDS analysis was determined to be calcium zincate. There were not many crystals however. After allowing the mixture to stand for a few more days with occasional stirring, it was filtered using a fine-mesh screen to remove the powder while retaining the crystals. There were many more crystals than were observed after 24 hours. They were of hexagonal shape (see Figure 2) and were found by powder X-ray analysis to have the same calcium zincate spectrum observed by other investigators.[11,17,18] The fact that crystals form indicates that $Ca(OH)_2$ or the complex must be sparingly soluble, however, all indications are that their solubilities are very small.

30μ
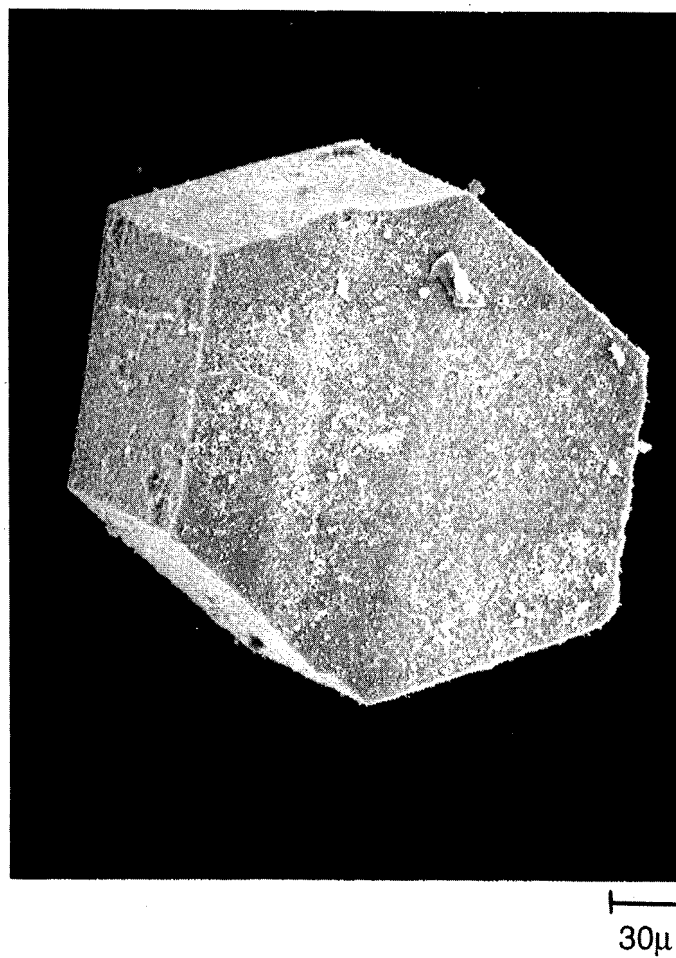
XBB 8910-8956

Figure 2. Hexagonal-shaped calcium zincate crystal, produced in zincate-saturated 31% KOH.

Another similar experiment performed was the continuous mixing for 24 h of $Ca(OH)_2$ and ZnO powders in the KOH solution. The analysis of the mixed powders showed some very small crystals which appeared to be the complex, but mostly the reactants remained unchanged.

The experiments described above indicate that the reaction to form calcium zincate in 31% KOH is slow. This agrees with the results obtained by other researchers, who claim that $Ca(OH)_2$ is more effective in lowering the zincate concentration in solutions of lower KOH concentrations.[13-16] At 31% KOH concentration, the $Ca(OH)_2$ was found to be ineffective in substantially lowering the zincate concentration. However, this research was not concerned with lowering the equilibrium zincate concentration but in having the $Ca(OH)_2$ bond with the excess ZnO (excess in the sense that it is not needed to saturate the electrolyte). Unfortunately, as charge/discharge cycling occurs in the scale of hours and to stop Zinc migration the $Ca(OH)_2$ would have to react with the ZnO within the given half cycle, the long reaction times (+24 h) observed so far, were discouraging. There was still one important experiment left, however, and that was examining the reaction rate in a supersaturated solution.

As was mentioned in the introduction, it is believed that the electrolyte in the immediate vicinity of the zinc electrode becomes supersaturated with zincate on discharge, although the degree of supersaturation has not yet been quantified. To examine the effects of supersaturation, 10 to 20 ml of deionized H_2O was added to a beaker containing 100 ml of 31% KOH and a few grams each of ZnO and $Ca(OH)_2$. Within a few minutes, the appearance of the mixture changed. After 30 minutes, very small crystals could be seen with the unaided eye, and within a few hours large crystals,

~0.5mm long, were observed. Adding deionized H_2O to the KOH solution supersaturates the mixture with regard to zincate because although the total volume is now greater, the lowered KOH concentration results in an actual decrease in the amount of dissolved ZnO required for saturation. These crystals were of a diamond shape (see Figure 3a) and exhibited the same powder X-ray pattern as that seen for the hexagonal crystal and as reported.[11,17,18] Gagnon and Sharma also found the complex as diamond shaped crystals.[15,16] These often were aggregated into fan-like structures - Figure 3b. These structures when broken would yield the diamond shapes.

An additional experiment was performed to determine if the increase in the reaction rate was due to supersaturation and not just due to the lowering of the KOH concentration. This experiment was performed by taking the liquid from the last experiment (now less concentrated than 31% KOH) and adding fresh ZnO and $Ca(OH)_2$ (although there still had been excess). After one day, no crystals could be found with a magnifying glass; the mixture appeared the same as when newly mixed. Thus, the large increase in reaction rate and rapid formation of crystals was almost certainly due to supersaturation.

The calcium zincate crystals themselves are also fairly stable. When calcium zincate crystals were added to pure 46% KOH (no ZnO or $Ca(OH)_2$), some remained undissolved after 3 hours. Attempts to perform X-ray crystallography failed as the crystals—both diamond and hexagonal—were too small for the equipment available. It is interesting to note that although the hexagonal and diamond crystals are indeed different crystal structures, as can be seen by the crystalline dislocations observed in Figures 4a and 4b, they have the same powder X-ray diffraction pattern. In addition, by

chemical analysis using atomic absorption and X-ray fluorescence, the Zn to Ca ratio for the two agree within 5%. For the diamond crystal the ratio is 2.0 and for the hexagonal crystal it is 2.1. Very little of the hexagonal crystal was produced so the analysis of it is less accurate. The ratio of one Ca to 2 Zn agrees with the formulae given in the powder X-ray diffraction handbook and by Sharma.[16-18] In addition, the density of the diamond crystal was experimentally determined and found to be 2.63 g/cm^3 compared to the handbook value of 2.62 g/cm^3 by Liebau and Amel-Zadch and 2.60 g/cm^3 by Schwick. The overall structure of the complex also appears to be closer to that calculated by Liebau, $CaZn_2(OH)_6 \cdot 2H_2O$, or Schwick, $Ca(Zn(OH)_3)_2 \cdot 2H_2O$ than that considered by Kawamura, $2Ca(OH)_2 \cdot 3Zn(OH)_2 \cdot 5H_2O$, and van der Grinten, $CaZn(OH)_4 \cdot H_2O$. Further confirmation was obtained by a hydrogen analysis which indicated 3.26% H, the same as that from Liebau's and Schwick's formulae. Unfortunately, a thermogravimetric balance was not available, so water of hydration could not be determined.

The hexagonal crystal structure was only observed when the complex was allowed to form very slowly (over a period of days) in a saturated solution. The diamond structure is observed when the complex forms quickly due to supersaturation. Thus, it is expected that when used in Zn/NiOOH cells, the calcium zincate will be observed in the diamond structure. As supersaturation is expected to occur in the zinc electrode, the experiments described above indicate that addition of $Ca(OH)_2$ may indeed be able to reduce the rate of Zinc redistribution and extend cell life. Table 1 is a summary of the experiments on the formation of the calcium zincate complex.

50μ

60μ
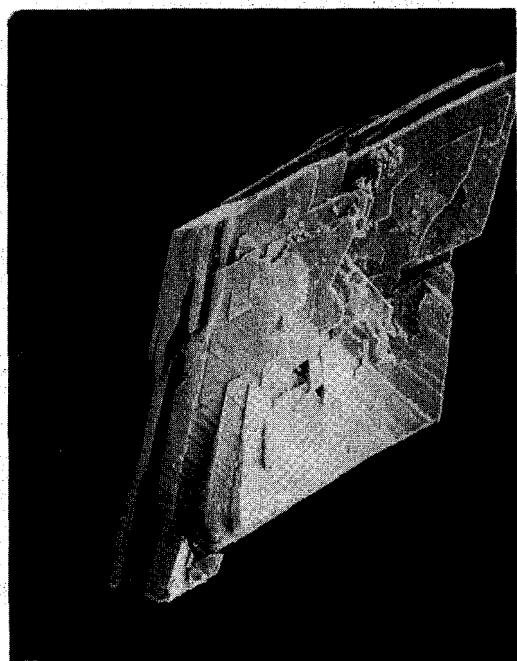
(a)   (b)

XBB 8910-8996

Figure 3. Diamond-shaped calcium zincate crystals - produced in zincate-supersaturated 31% KOH solution.
(a) Diamond shape of crystal.
(b) Fan-like structure created from an aggregate of diamond-shaped crystals.

(a) (b)
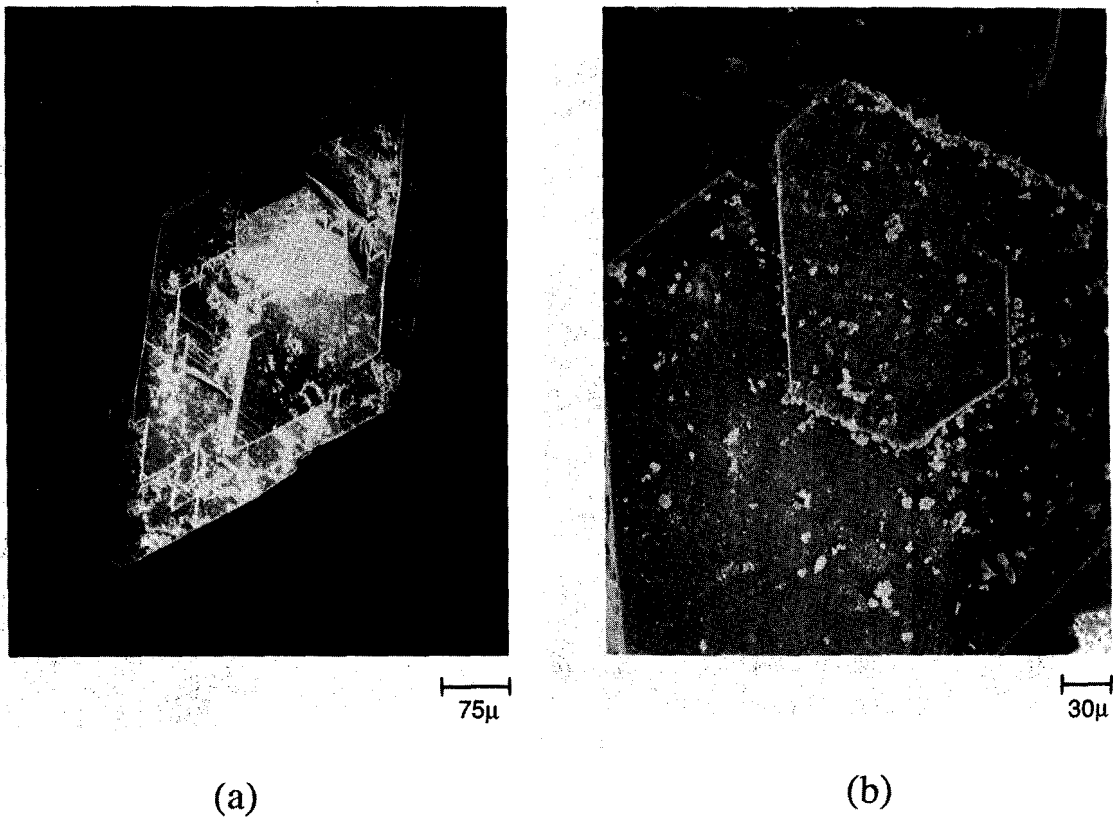
XBB 8910-8984

Figure 4. Stacking dislocations in complex crystals highlighting crystal structure.
(a) Diamond-shape dislocation.
(b) Hexagonal-shape dislocation.

TABLE 1			
Complex Formation Experiments			
Solution	**Powders Present**	**Elapsed Time (hrs)**	**Result**
No liquid	$Ca(OH)_2$, ZnO	72	No reaction
Deionized H_2O	$Ca(OH)_2$, ZnO	24	No reaction
Zincate-saturated 31% KOH	$Ca(OH)_2$	3	No reaction
" "	$Ca(OH)_2$	24	Slight amount calcium zincate
" "	ZnO, $Ca(OH)_2$-sealed in a separator	24	No reaction
" "	ZnO, $Ca(OH)_2$ stirred	24	Hexagon complex crystals
Zincate-supersaturated KOH - unknown %	$Ca(OH)_2$, ZnO	0.5	Many small complex crystals - diamond shaped
Zincate-saturated KOH % as above	$Ca(OH)_2$, ZnO	24	No reaction
46% KOH	Calcium zincate	3	Still some undissolved complex crystals

Chapter 3
Experimental Procedure and Apparatus

In order to determine the effect of $Ca(OH)_2$ addition on the zinc electrode of the Zn/NiOOH cell, experimental cells were constructed, cycled for extended periods, and then examined in detail.

3.1. Types of Electrodes Cycled

As a base case, a normal "100% Zn" Zn/NiOOH cell was cycled. For simplicity, the percentage figures reported are based on the mol% Zn and Ca in the uncycled electrode and ignores all other materials, unless otherwise implied from the context. From the determined calcium zincate stoichiometry, one Ca atom will react with two Zn atoms. Thus, for theoretically converting all the Zinc to calcium zincate, the electrode must be 33% Ca. To observe the effects of different amounts of Calcium, electrodes of 10%, 25%, and 40% $Ca(OH)_2$ by moles were synthesized and tested. Most experiments were performed in duplicate to determine the repeatability of the results. Table 2 lists the types of cells examined in this research project.

3.2. Zinc and Nickel Oxide Electrodes

A cell consisted of a zinc electrode held between two NiOOH electrodes (see Figure 5a), each NiOOH electrode being of one-half the cell design capacity. The reason that this layout was chosen is that in a battery the negative and positive electrodes alternate, thus an individual electrode would have an opposing electrode on each face. These opposing electrodes would contribute one half each to the sandwiched electrode.

TABLE 2	
Types of Electrode Cycled	
Cell Name	**Type of Zinc Electrode**
Zn1	100% Zn
Zn2	100% Zn
10Ca1	10% $Ca(OH)_2$
10Ca2	10% $Ca(OH)_2$
10Ca3	10% $Ca(OH)_2$
25Ca1	25% $Ca(OH)_2$
25Ca2	25% $Ca(OH)_2$
40Ca1	40% $Ca(OH)_2$
40Ca2	40% $Ca(OH)_2$

Therefore, for the cell to best approximate a battery, each opposing electrode should only be one half the design capacity. The design capacity was 1.32 Ah and the size of each electrode was 70 by 62 mm.

The zinc electrode consisted of ZnO as the active material. An electrode is defined as containing the current collector and all the active and inactive material bound to it (ZnO, Calcium, PbO, binder, etc.), but not any separator of wick. For the 100% Zn cell, sufficient ZnO was incorporated into the electrode to yield a theoretical capacity of 300% of the design capacity. Thus, a 200% excess of Zinc was included. This is required because as Zinc redistribution and material loss from the zinc electrode occurs, the capacity will decrease unless some excess Zinc is present. Also, without some excess ZnO there would be excessive overpotentials near the end of the charge half-cycle. Too much excess Zinc is undesirable, however, as this will result in a heavier battery (reduced specific energy) and thus make it unattractive for electric vehicle use. Three hundred percent of the design capacity was used because this would allow comparison with James Nichols' experiments and because 300% is comparable to

the practice of other researchers.[5]

For all the experiments, the total initial weight of the zinc electrode was kept constant. So, as $Ca(OH)_2$ was added to the electrode, less ZnO was incorporated, resulting in a decrease in the amount of excess Zinc. The 100% Zn electrode had 6.00 g ZnO. As the 10% $Ca(OH)_2$ electrode had 0.55 g $Ca(OH)_2$, it contained only 5.45 g ZnO. The 25% $Ca(OH)_2$ electrode had 1.4 g $Ca(OH)_2$ with 4.60 g ZnO, and the 40% $Ca(OH)_2$ electrode with 2.27 g $Ca(OH)_2$ had only 3.74 g ZnO. All weights were accurate to within 5% in the finished electrode. Table 3 is a summary of the compositions of the various types of zinc electrodes cycled, along with the resulting amount of excess Zinc. As was mentioned, the amount of excess Zinc is an important variable, since cycle life decreases rapidly with decreasing amounts of excess Zinc in conventional all-Zn electrodes.

In addition to the ZnO and $Ca(OH)_2$, the zinc electrode also contained 2% PbO powder and 4% to 6% polytetrafluoroethylene (PTFE). PbO is added as a H_2 gas suppressant. PTFE is added as a binder, and was added at a level of 4% of the active material weight for the 100% Zn and 10% $Ca(OH)_2$ electrodes. Since the density of $Ca(OH)_2$ is 2.24 g/cm^3 compared to 5.61 g/cm^3 for ZnO, the 25% $Ca(OH)_2$ and the 40% $Ca(OH)_2$ electrodes had a greater volume and thus required more binder. Five percent PTFE was used for the 25% $Ca(OH)_2$ electrode and 6% for the 40% $Ca(OH)_2$ electrode. The PTFE used was TFE-30 (produced by E.I. DuPont De Nemours and Co.), which is a dispersion of PTFE with 5.5% Triton X-100, as a wetting agent, in H_2O.
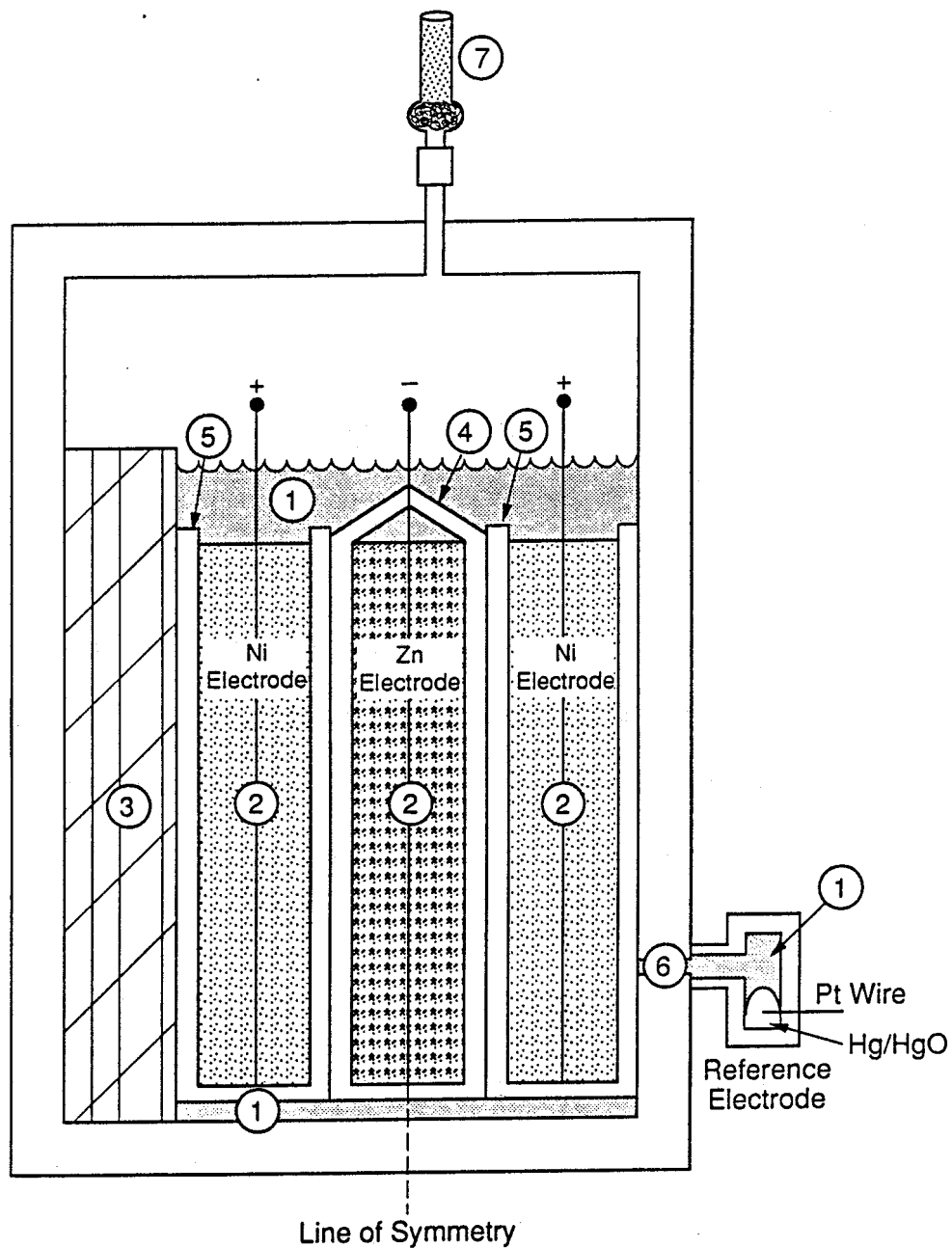
Figure 5a. Cross section of the Zn/NiOOH cell.
(1) Electrolyte. (2) Current Collector. (3) Non-porous PTFE spacers. (4) Separator.
(5) Wick. (6) Electrolyte conduit. (7) Column to remove CO_2 from air.

TABLE 3 Composition of Electrodes						
Cell Type	**Ca(OH)₂**	**ZnO**	**PbO**	**PTFE**	**Excess ZnO**	
	(g)	**(g)**	**(g)**	**(g)**	**(g)**	**(%)**
100% Zinc	0	6.0	.13 (2%)	.26 (4%)	4.0	200
10% Ca(OH)₂	0.55	5.45	.13	.26	3.45	175
25% Ca(OH)₂	1.40	4.60	.13	.32 (5%)	2.60	130
40% Ca(OH)₂	2.27	3.74	.13	.38 (6%)	1.74	85

The current collector for the zinc electrode is a lead-plated "expanded-metal" Cu mesh. The original Cu sheet thickness was 4 mils and the designation for the mesh used is 4-Cu-7, produced by Die Mesh Corporation of Mount Vernon, New York. The mesh was cut to the size of the electrode, 7.0 by 6.2 cm, then a strip of 10-mil thick Cu sheet, ~1 cm by 6 cm, was spot welded to a corner of the mesh. The total area of the mesh covered by the tab is roughly 1 cm^2. The current collector was then cleaned in isopropanol and in nitric acid solutions followed by electroplating with 0.3 g of Pb from an aqueous lead fluoroborate solution. The Pb plate was roughly 4-μm thick. No voids visible to the unaided eye were present in the Pb plating on the current collector.

Basically, the procedure for creating the zinc electrode consists of first blending the weighed amounts of ZnO, Ca(OH)$_2$, PbO, and PTFE with roughly 60 ml deionized H$_2$O and 10-ml acetone. An excess of 15 to 30% of material is used at this point to provide for loss in production. One half of this suspension is then poured onto filter paper on a vacuum table. The active material layer deposited on the filter paper is shaped by a frame mounted on the vacuum table to the size of the electrode. The suspension is filtered to make a moist cake. This procedure is repeated using the other half of the suspension. The two cakes are then placed together with the current collector between them. The resulting sandwich is pressed to the desired thickness/porosity in a hydraulic

press with the aid of shims. The detailed electrode fabrication procedure is provided in the appendix.

The wet-pressing procedure was used to insure consistent porosity and thickness over the entire electrode. Porosity is calculated by taking the volume of the final electrode (from its dimensions) and subtracting the volume of the current collector calculated from its weight. The volume calculated from the weight and densities of the ZnO, $Ca(OH)_2$, PbO, and PTFE in the electrode is then divided by the resultant volume determined above and subtracted from unity (1) to yield the porosity. The porosity of the 100% Zn and 10% $Ca(OH)_2$ electrodes was 75%. For the 25% $Ca(OH)_2$ and the 40% $Ca(OH)_2$ electrodes, the porosity was decreased to 70% as the filter cakes were themselves fairly dense. A completed zinc electrode can be seen in Figure 21b. All zinc electrodes were X-rayed before cycling to insure uniformity (see Figure 21a).

The NiOOH electrodes were composed of sintered Ni powder on a Ni screen into which $Ni(OH)_2$ was deposited. These electrodes were purchased from Eagle Picher Co. as sheets and were cut to the required size. It was assumed that the NiOOH electrode capacity would be 0.95 electrons per atom of Ni in the active material (based on previous work in the laboratory). As each cell would have two NiOOH electrodes, each NiOOH electrode needed to be of one half the total required capacity. This led to the choice of Ni sheets with a loading of 0.055 g $Ni(OH)_2/cm^2$ (0.355 g $Ni(OH)_2/in^2$). Once the electrodes were cut to size, Ni tabs consisting of a 1- by 6-cm strip of 10-mil thick Ni was spot welded onto a corner of the electrode. The area covered by the tab was approximately 1 cm^2. For a given cell, the two NiOOH electrodes had the tabs spot welded on opposite sides so that the Ni tab connections would not be facing the Zinc

electrode (to prevent blocking of active Ni material by the tab).

3.3. Cell Assembly

To prevent dendritic growth on the zinc electrode and thus prevent shorting to the NiOOH electrodes, the Zinc electrode was wrapped with three layers of Celgard 3401 separator. Celgard 3401 is a microporous polypropylene sheet (0.02 μ effective pore size), with a wetting agent, and is produced by Celanese Fibers Corporation. Each layer was individually heat sealed as close as possible to the edges of the electrode. As a seal cannot be made on the tab, the separator was extended a minimum of 2 cm above the top of the electrode on the tab and sealed on the sides. The seal at the top of the electrode was close (within 3 mm) to the electrode for the 40% $Ca(OH)_2$ cells, one 100% Zn cell (Zn1) and one 10% $Ca(OH)_2$ special test cell (10Ca3). For all the other electrodes the seal was roughly 0.6 cm to 1.3 cm above the top of the electrode. As will be seen in the results and discussion section, the proximity of the seal to the electrode is very important. Care was taken to ensure that the separator experienced no rough handling, that there were no holes or weak seals present, and that no two layers had become heat sealed together.

Each NiOOH electrode was wrapped with a layer of Pellon 2502K4, produced by Pellon Corporation. The Pellon is used to keep the NiOOH electrode wet with electrolyte and is a nonwoven nylon wick.

The cell case was made of acrylic, as this polymer has good resistance to strong alkali solutions. On one face of the case, Ni rods, as leads for electrical connections, were inserted through holes in the acrylic and attached by epoxy. The case consists of three main parts, a face with the leads and hole for the reference electrode, a spacer, and

a back plate. All parts were sealed together by o-rings (carbon-filled ethylene propylene copolymer) which fitted into grooves in the face and back plates. The cell was assembled using nuts and bolts in the holes drilled outside of the o-ring area in each piece. The front and back faces were machined flat to within 0.03 mm and the spacer to within 0.05 mm. The spacer was a 6.60-mm thick frame with the void area in the center 1.5-mm wider than the electrode width (70 mm), and the height extending well above the top of the tabs. The void also extended 2 mm below the bottom of the electrode. The spacer included two holes drilled from the top down into the void. Nickel-plated stainless steel tubing was inserted into the holes and attached with epoxy. Swagelock fittings were attached to the outside to allow sealing and/or attachment to other tubing. These tubes were installed to allow the addition of electrolyte and other liquids and the addition or venting of gases. The cell case can be seen in Figure 5b. A more thorough description of the cell case can be obtained from Reference 5.

The cell was assembled so that the zinc electrode initially was under a pressure of 28 kN/m^2. To do this, the zinc electrode and the two NiOOH electrodes were subjected to this pressure (avoiding the tab areas), and their total thickness was measured. PTFE spacers were then added to the cell so that the total thickness of the compressed electrodes and spacers would equal the width of the space created by the 6.6-mm thick cell case spacer.

The cell was assembled with the zinc electrode sandwiched between the NiOOH electrodes (with the Ni tabs facing away from the zinc electrode) and the PTFE spacers between the back wall and a NiOOH electrode. This best simulates a typical battery where the zinc and NiOOH electrodes would be alternating, thus creating zinc electrode
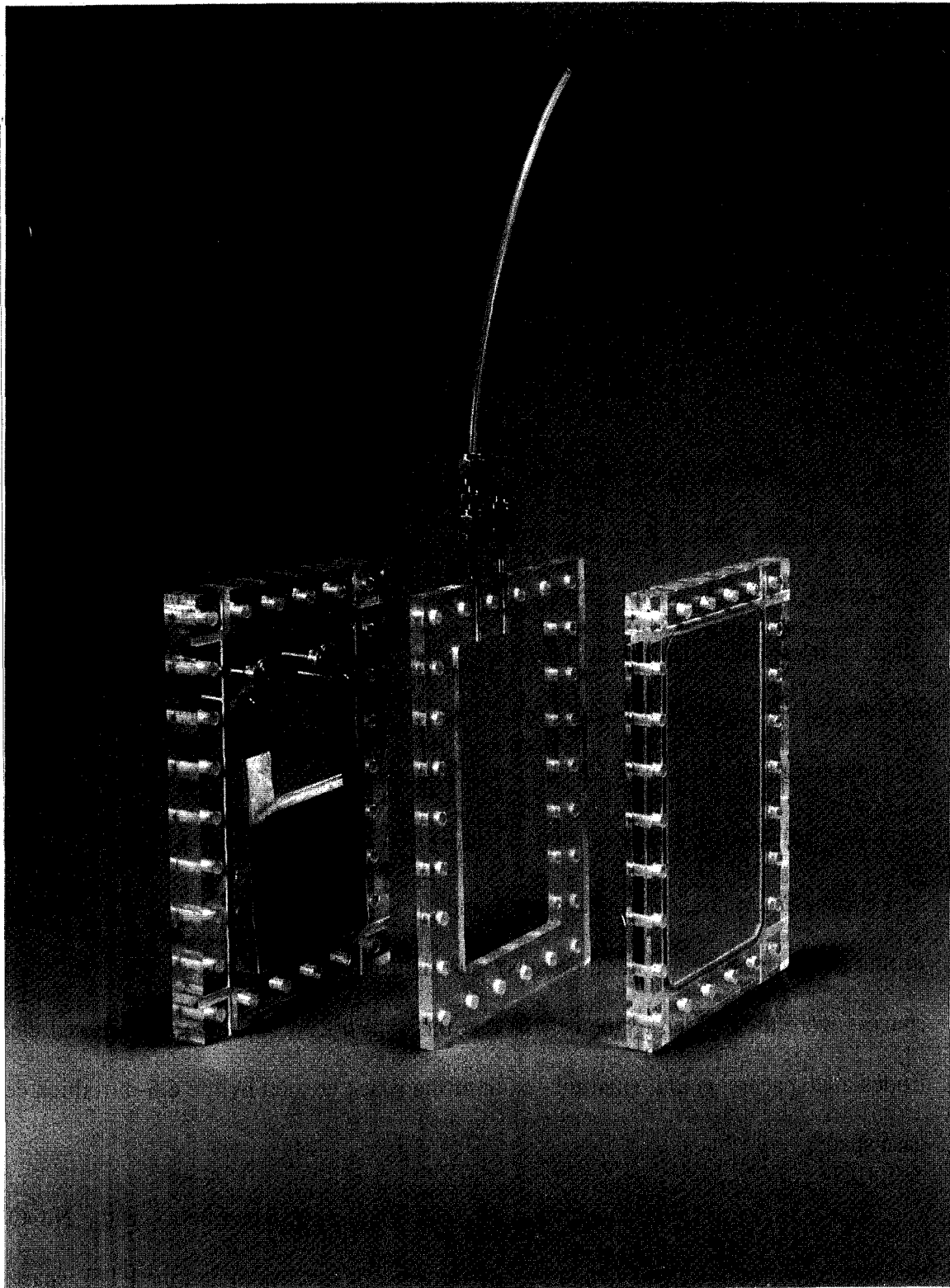
CBB 825-4772

Figure 5b. Components of the cell case with electrodes attached.

sandwiches.

Once the cell case was assembled, the reference electrode compartment was attached. The front face of the cell case has a 0.5-mm diameter capillary which opens adjacent to a NiOOH electrode. This provides an electrolyte contact from the NiOOH electrode to the reference electrode compartment. The reference electrodes were Hg/HgO with a Pt wire leading directly from the Hg to the outside of the reference electrode compartment, without running through the electrolyte. The Pt wire is used to provide a corrosion resistant, low resistance contact and path for measuring the reference electrode potential.

With the reference electrode attached, the cell was weighed. Then, a vacuum was applied to the cell to ensure there were no gross leaks. After this, a vacuum was again applied to the cell and under this vacuum the electrolyte was added, filling both the cell and the reference electrode compartment. The electrolyte was added to a level of ~0.6 cm above the top of the electrodes. The cell was then reweighed. The electrolyte consisted of 31% KOH, 1% LiOH by weight, and was saturated with ZnO. Carbon dioxide contamination was avoided and 15 Mohm or better deionized water was used. The KOH electrolyte was prepared from a J.T. Baker-analyzed 46% KOH reagent grade solution.

After addition of the electrolyte, one of the fill ports was sealed and an Askarite column was attached to the other to remove CO_2 from the air entering the cell. The cell was then connected to the cycling equipment and ~0.1 Ah of charge was applied to prevent corrosion of the Cu current collector in the zinc electrode. Three days were allowed for soaking to insure that the electrolyte would wick thoroughly into the elec-

trodes. The potential of the cell was monitored during this period to insure that no corrosion of the Cu current collector was occurring. The completed cell can be seen in Figure 5c.

3.4. Cell Cycling Computer and Equipment

The electrical connections to the cell included a power and ground connection to the zinc and NiOOH electrodes. The two NiOOH electrode tabs were internally connected together to maintain both at the same potential. To measure the potential of the electrodes, separate connections were made from the zinc electrode lead, the NiOOH electrode lead, and the Pt wire on the reference electrode to a voltage monitor. This arrangement allowed the measurement of the cell voltage (NiOOH electrode minus zinc electrode); Zinc electrode potential (zinc electrode minus the reference electrode); and the NiOOH potential (NiOOH electrode minus the reference electrode). The NiOOH and Zinc potentials given in this thesis are always referred to the Hg/HgO reference electrode in the same electrolyte. Potentials on the H_2 scale can be obtained by measuring the potential of the Hg/HgO electrode vs the reversible H_2 electrode for this electrolyte composition and then correcting for the difference in pH. However, this is not necessary as the important factor is the variance of the potentials with time, state of charge, and cycling.

The cycling equipment was designed and built by the Lawrence Berkeley Laboratory's Department of Instrument Science and Engineering, along with Marco Katz and James Nichols.[5,7] The equipment was specially designed for continuous computer control and monitoring of electrochemical cells with a failsafe shutdown mode in case of software or hardware crashes or power glitches. With improvements made by

XBC 858-6672

Figure 5c. Completed cell with external wiring (and author).

Thomas Adler, the system was capable of operating 24 h per day for months without failure - barring any power outage.[8] The cycling equipment consisted of a voltage monitor, current controllers, logic bin, and separate charge and discharge power supplies, along with the computer. The computer was a Digital Equipment Corporation LSI-11/23 with two 10-megabyte RL0-1 hard disk drives. There are eight current controllers which allow eight separate cells (or pairs of cells) to be cycled independently. In addition, the computer can monitor up to 16 cells, so each current controller can drive two cells in series. A request for a given current by the computer is sent to the logic bin which then sends it to the correct current controller. The current controllers can maintain a current to a digitally set level to within 0.25 mA and can be monitored by the computer to an accuracy of 1 mA. The voltages can be monitored by the computer using the voltage monitor to within 2 mV for a source resistance of < 5 Kohm. The logic bin also operates in a failsafe manner as the bin is driven by pulses from the computer. In case of a system crash for any reason, the pulses will cease. After 20 seconds of no pulses, the logic bin will place all current controllers under open circuit and computer disable. Once disabled, each current controller and the logic bin must be manually reset. Also, after a power outage, the logic bin remains disabled when the power returns to the system, until it is reset.

The software for the computer was written by Marco Katz and allows a variety of options.[7] The cells can be charged by constant current, constant voltage, or with an externally imposed current profile. Discharge can be either by constant current, constant power, externally imposed current profile, or even by a rapidly fluctuating power profile such as the EPA urban driving profile. The program controls the cells, continu-

exerting force against the restraining (but stretching) separator, thus implying that lack of restraint is probably not a factor.

Whatever the cause of enhanced shape change due to a high seal, it is definitely an undesired outcome. The closer the separator is sealed to the electrode, the better for reducing the Zinc redistribution rate. However, seals which are too close could be torn due to the expansion and contraction of the electrode during cycling. This is especially important with $Ca(OH)_2$ additions. For example, when the Zinc in a new 25% $Ca(OH)_2$ electrode is converted to complex, the volume occupied by the active material increases. The density of Zn is 7.14 g/cm^3, ZnO is 5.6, $Ca(OH)_2$ is 2.24 and for the complex it is 2.62. Even though the 40% $Ca(OH)_2$ cells were felt to have shorted due to the expansion of the electrodes ripping the separator, the 10 and 25% $Ca(OH)_2$ electrodes did not have to be sealed with as large a gap as they were. They could have been sealed much closer and thus their cycle lives might have been even longer.

4.3. Electrode X-ray Images and Photographs

Figure 21 shows an X-ray and photograph of an uncycled zinc electrode. All the zinc electrodes were X-rayed prior to cycling, and had similar appearances. As can be seen, the active material is distributed uniformly over the current collector. In examining the X-ray photographs, the darker areas are the areas containing more material. Unfortunately, the X-ray photographs do not clearly show any uniform material present. They tend to highlight the more dense, redistributed material. Thus when examining the following X-ray photographs of the cycled electrodes, the uniform material being refered to is not always obvious in the X-ray photograph (it is, however, easily seen in the original X-ray images).
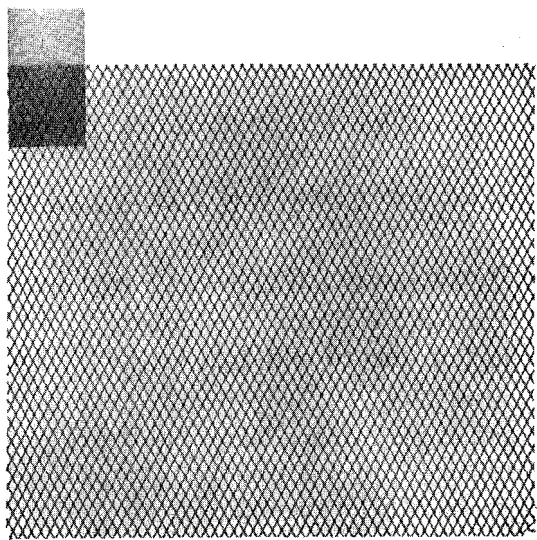
(a)
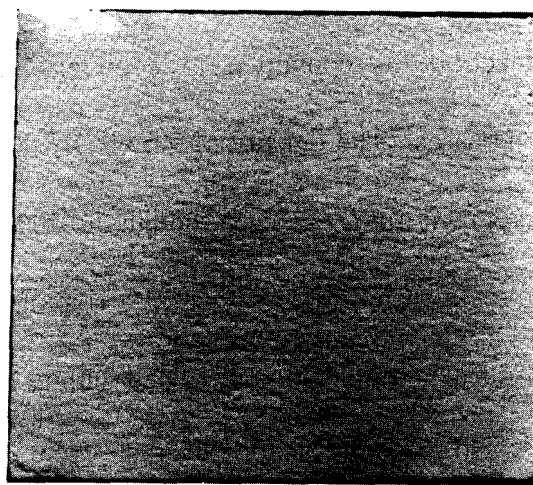
(b)

XBB 8910-8957

Figure 21. Typical uncycled zinc electrode.
(a) X-ray
(b) Photograph

ously records the data, and automatically switches from charge to open circuit to discharge and vise-versa. The program allows the setting of limits such as maximum or minimum voltages, maximum currents and/or coulombs charge or discharge. Programs were also written to facilitate the calibration of equipment and to insure that the proper values were recorded by the main program. The program also allows the use of excess charge factors. These factors are useful in accommodating the NiOOH electrode inefficiency during charge and dealing with other cell problems. For example, because the NiOOH electrode is normally only about 96% efficient, if the charge half-cycle following a discharge half-cycle is for the same number of coulombs as the discharge, the capacity of the cell will decrease by 4%. However, with the use of an excess charge, say 4% in the above case, the cell will maintain its capacity. This factor of 1.04 can be changed as cell properties change.

For cycling two cells in series, the program is designed to control the cells by using the poorer-performing of the two cells (i.e., whichever cell reaches the control limits first).

An interface program allows one to change the cycling parameters without having to halt cycling of any cells. Also, individual cells can be stopped or started without affecting the other cells.

Data analysis programs were written which plot cell cycles and capacities and also provide tabulation of major parameters. In addition to the stored data, continuous monitoring of all cell parameters is displayed on a slaved second CRT, and charge and discharge Ah are printed.

3.5. Cycling Procedure

After the new cells soaked for three days to assimilate the electrolyte, they underwent formation cycling. Formation cycles are required for preparing the NiOOH electrodes and permit the establishment of the desired Zn/ZnO ratio in the Zinc electrode. The charge for the first formation cycle is the sum of the cell design capacity plus one half of the theoretical capacity of the remaining ZnO. Thus cells with $Ca(OH)_2$ were charged less in the formation cycles than were the 100% Zn cells. The extended charge is required not only to develop the capacity of the NiOOH electrodes but also to establish a Zn and ZnO initial reserve ratio of 1:1. It is desired to have a Zn reserve to provide for low-resistance current paths during charge and discharge. A ZnO reserve is required to prevent excessive overpotentials at the end of charging half-cycles. Also, because the cell is not sealed, and the NiOOH electrode is less efficient than the zinc electrode, the excess charge needed to fully charge the NiOOH electrode causes an excess conversion of ZnO to Zn in every cycle. In sealed cells, the O_2 produced by the inefficiency of the NiOOH electrode would be used to react with the excess Zn produced to create ZnO, thus slowing or preventing the net conversion of ZnO to Zn in each full cycle. Since this does not happen in unsealed cells, as the ZnO reserve becomes depleted, extended discharges must be performed to reestablish the reserve. When the reserve is close to depletion, the overpotential of the zinc electrode increases during charge, and if the cell is allowed to continue cycling, it could short due to Zn dendritic growth.

The formation charges were performed at a 20 h rate, and the discharges were carried out at 0.526 A with a discharge limit on the Zinc potential of -1.0 V (vs Hg/HgO).

The discharge was then continued with the current being repeatedly decreased to discharge the zinc electrode as fully as possible, never discharging beyond -1 V for the zinc electrode. The lowest discharge current used was 0.01 A. At this point the total Ah removed in discharge is compared with the Ah of charge. Ideally these will be the same, but for the first formation cycles the ratio may be low. As some of the charge not recovered during the first formation cycle may be recovered on the second, usually the second charge is decreased slightly. Since the NiOOH electrode will be evolving O_2 when overcharged and H_2 when over discharged, the liquid level is monitored and deionized H_2O is added through the fill port, as needed, after a discharge. Occasionally, a vacuum is applied to the cell to remove gas bubbles from both the cell and the tubing connecting the cell to the reference electrode compartment. After the second or third formation cycle, the cell should be well behaved and the zinc electrode fairly efficient - above 90%. Typically, three or four formation cycles were performed. The last formation cycle consists of the same amount of charge as computed to charge the cell and create the Zn reserve. However, the discharge extends only to the cell design capacity so that the Zn reserve is established. Formation cycles are not included in the count of the number of cycles reported for a cell.

At this point the cells are now ready for normal cycling, performed at a 5-h charge rate of 0.263 A (5 h x 0.263 A = 1.315 Ah) and a 2.5 hour discharge rate of 0.526 A (2.5 h x 0.526 A = 1.315 Ah). For the 40% $Ca(OH)_2$ cells a high overpotential on the zinc electrode during charge caused the cell to short after only a few cycles - see Section 4.1.5. The 25% $Ca(OH)_2$ electrodes also exhibited above-average and erratic overpotentials at the 0.263-A rate, so the charge rate was decreased by 24% to 0.200 A.

The cells were cycled using the following procedure: first, they were charged at constant current until the computed number of Ah were passed, or until an upper voltage limit was reached. The computed amount of charge would be the quantity removed during the last discharge multiplied by the excess charge factor. The upper voltage limit was rarely reached. The cell would then be allowed to stand in open circuit for 10 min. A constant 0.526 A discharge would then begin and continue until either the cell voltage or the zinc electrode potential exceeded the specified values or until 1.32 Ah (the design capacity) were removed from the cell. The discharge limit voltage for the cell and the zinc electrode were usually 1 V and -1 V, respectively. After discharge the cell would again stand at open circuit for 10 min before beginning the next charge.

Pairs of cells were cycled in series, 10% with 10% and 25% with 25%, until performance differences caused them to be cycled separately. The charge excess factor was adjusted as necessary to retain cell capacity and was always maintained at the minimum value possible. The excess factor during normal cycles typically varied between 1.01 and 1.05. The zinc electrode potential was monitored, and if during the end of charge it increased (indicating the depletion of the ZnO reserve), either a reformation cycle or a slightly extended discharge would be performed. A slightly extended discharge was preferred because it would recreate the ZnO reserve without subjecting the electrode to the rigor of a reformation cycle. A reformation cycle would be performed when it was felt that there were other problems which may be alleviated if the cell was reformed. A reformation cycle would consist of discharging the cell to a Zn potential of -1 V at a final discharge rate of 0.01 A. A small Ah charge would then be performed to replenish the Zn reserve followed by the continuation of normal cycling

beginning with a charge. A reformation cycle was usually performed if there was a large decrease in capacity, indicating a short.

Whenever a short was suspected, a formation cycle was attempted in order to save the cell. If this was inadequate in eliminating the short, the cell would be made to stand fully discharged for a few days and perhaps a vacuum would be applied on the cell. If both of these procedures failed, no other options were available except to dismantle the cell. Notes and data were taken as if the cell cycling experiment had finished. Then, the electrolyte would be removed and saved and the cell disassembled. The outermost two layers of the separator on the zinc electrode would be replaced (saving and labeling the used material). Also, if the NiOOH electrodes in the cell had been causing problems, they too would be replaced, again saving the old. The cell was then reassembled with fresh electrolyte and reformed. However, all attempts at cycling cells after reassembly resulted in shorts after only a few cycles - see Sections 4.1.3 and 4.1.4.

Cycling continued until either the cell shorted, the cell capacity dropped and remained below 70% of the original capacity, or when 150 cycles were reached.

Cells were cycled on the basis that studying the migration of Zinc was the important consideration, along with observing problems and performance. Thus, it was not attempted to imitate any future commercial cycling where adjusting excess factors, doing extended discharges etc. may not be practical. Cells were normally observed at least once in every 24-h period during cycling.

3.6. Cell Disassembly

After cycling was completed, the cells were weighed and then disassembled. In disassembling the cell, care was taken to avoid the loss of any material and to

quantitatively determine the amount of material in a given portion of the cell. This includes, for example, the distinction between the Zinc in the bulk electrolyte, the Zinc in the electrolyte in the NiOOH electrode, and the Zinc deposited in the NiOOH electrode.

To do this, first the bulk electrolyte was poured into a weighed bottle. Then, using weighed absorbent paper tissues (Kimwipes) and plastic bags, the cell was disassembled, absorbing excess electrolyte into the tissues. The NiOOH and Zinc electrodes were placed between tissues to extract the electrolyte from the electrode pores (after first removing the bulk electrolyte from their outer surface). The nylon wicks, two outer layers of separator, spacers, and cell case were wiped or placed within tissues and saved. This included the electrolyte in the reference electrode. All individual pieces were weighed.

The zinc electrode was then X-rayed followed by the removal of the final layer of separator. Photographs were taken of the electrodes during disassembly, and also of the dried Zinc electrode.

3.7. Analysis Techniques

The zinc electrodes and NiOOH electrodes had scrapings and portions removed for SEM and powder X-ray diffraction analyses. In addition the zinc electrodes had weighed portions removed over the body of the electrode. These were dissolved and analyzed to observe material migration over the electrode. To perform a mass and chemical balance on the cell, a single cell was selected and detailed analyses were performed. All the material removed from the cell, including the zinc electrode, NiOOH electrode, nylon wick, separator, tissues, etc. were placed in 70% HNO_3 to dissolve any

metals (except perhaps some Pb). The solutions were then chemically analyzed.

Chemical analysis was mainly performed by the University of California, College of Chemistry Analytical Laboratory using an atomic absorption spectrometer (AAS) for all the metals. Results for AAS are usually accurate to within 2% for the equipment being used. The amount of H_2 was measured by a combustion analysis. X-ray fluorescence analysis was attempted, however, due to the expense and inconsistent results, it was rarely used. X-ray fluorescence should yield results accurate to within 5%, when properly calibrated for the samples of interest.

The electrodes were X-rayed at the medical facility in the Lawrence Berkeley Laboratory. The energy of the X-ray was 60 KeV and the exposure was 100 mAs.

Powder X-ray diffraction was performed using the Siemens Kristalloflex Diffraktometer at the Lawrence Berkeley Laboratory. The International Centre for Diffraction Data powder X-ray diffraction handbook was used to compare spectra of known compounds with those of the samples investigated. The samples were pulverized with a mortar and pestle and mounted on polymethylmethacrylate with petroleum jelly. Typical slit widths of 1.0, 1.0 ,1.0 , 0.15, and 0.15 mm were used. The spectrum from 10 to 80 degrees was examined at a rate of 1 second per 0.1 degree.

Scanning electron micrographs were taken using the AMR 1000 model SEM also at the Lawrence Berkeley Laboratory. Samples were mounted using double-sided tape and then were coated with Au. X-ray analysis was performed using a KEVEX series 7000 EDS (Kevex Instruments, San Carlos, CA). The machine provided chemical identification and semi-quantitative analysis, along with elemental mapping. The energy used was 20 KeV, and polaroid film was used for obtaining the

micrographs/photographs.

X-ray crystallography was attempted but the size of the crystals was below the resolution capability of the equipment available.

Chapter 4
Results and Discussion

4.1. Performance of Cells

4.1.1. Cell Zn1

The first cell investigated had a 100% Zn electrode. This cell will be identified as Zn1 and it underwent 150 cycles. The capacity of the cell versus cycle number can be seen in Figure 6, and representative cycles are shown in Figure 7. All capacity plots are based on 1.32 Ah for 100% capacity, regardless of the cell's initial capacity. Most of the formation cycles performed during cycling, along with a few troubled cycles, are not shown in Figure 6. The capacity at the end of cycling was roughly 1.1 Ah which is ~92% of the initial capacity. The estimated total Ah passed during charge was 176 Ah and on discharge 171 Ah. This leads to an overall coulombic efficiency of 97%, but it must be noted that some (~5) of the low efficiency cycles were removed (because of computer problems).

To compare the performance of the various cells, special note will be made of the total charge the cell received vs the grams of excess ZnO present. As excess Zinc is required to accommodate Zinc redistribution, an increase in the value for Ah passed vs excess Zinc would mean that the rate of Zinc redistribution had probably decreased. The excess ZnO for this cell was 4 g (based on the design capacity of 1.32 Ah). This corresponds to the electrode receiving 176/4 = 44 Ah/g of excess ZnO. The above calculation when based on its actual initial capacity of ~1.2 Ah, yields 42 Ah/g excess ZnO. As cycling of the electrode was only stopped because it had reached 150 cycles, the Ah/g excess ZnO do not reflect the limit of this electrode.
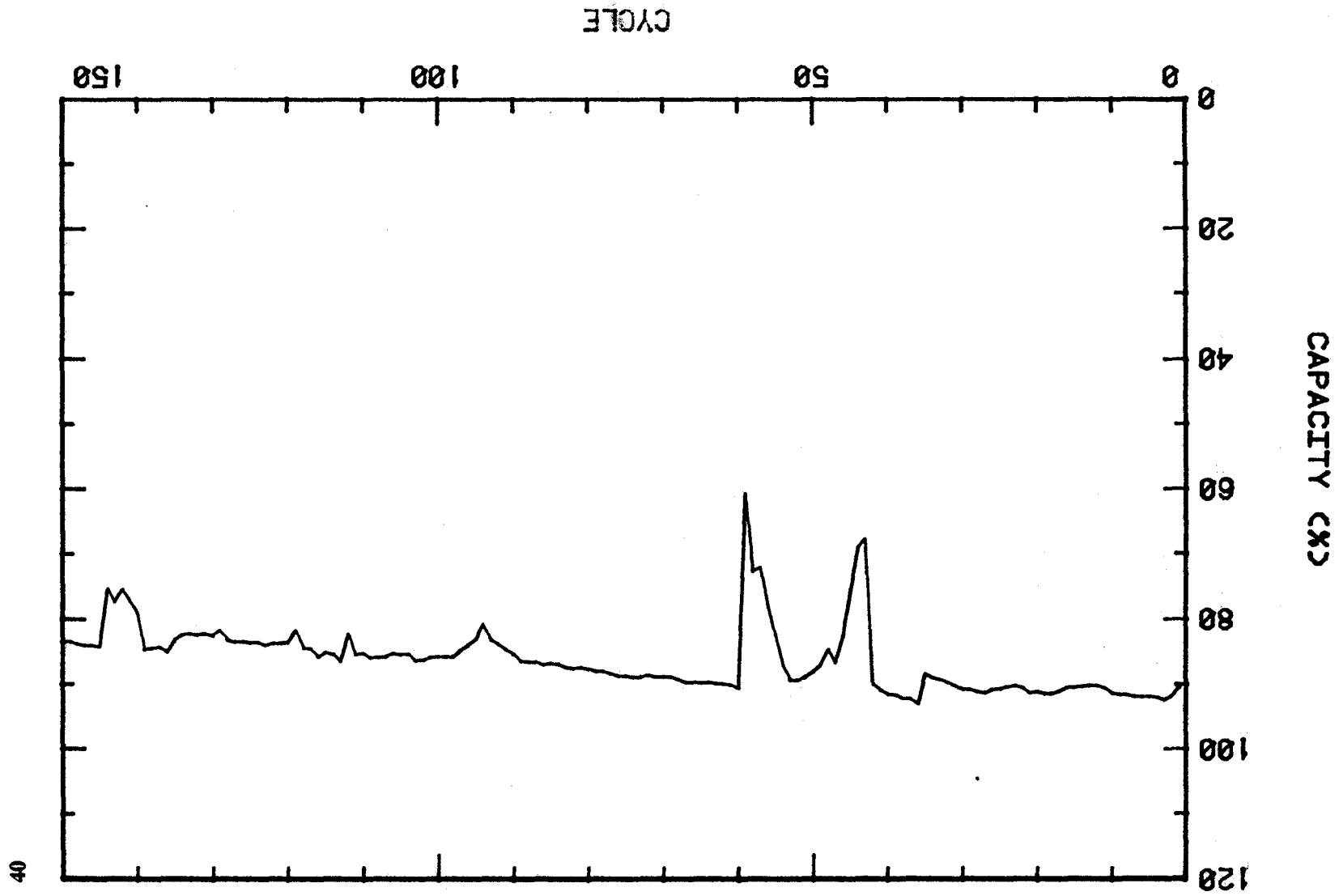
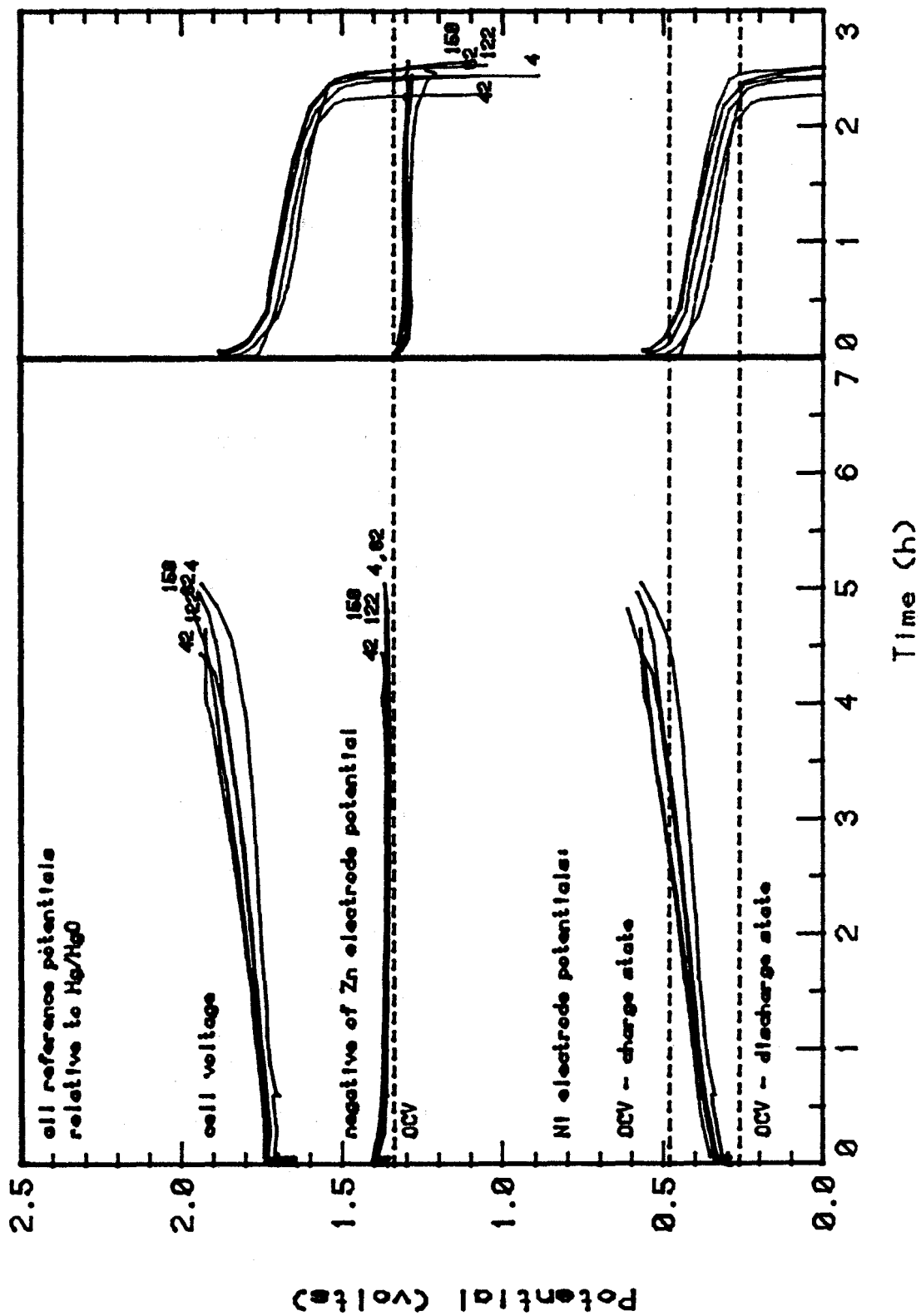Figure 6. Capacity vs cycle number for Cell Zn1 (100% Zn).

Figure 7. Voltage vs state of charge curves for representative cycles of Cell Zn1 (100% Zn).

The excess charge factor varied for this cell from 1.02 to 1.03 initially, to 1.04 for the last 50 cycles. This cell experienced a variety of cycling conditions due to various tests, but all conditions were within limits which should not have affected the shape change results. This electrode had a close seal of the separator at the top (within 3 mm of the electrode).

4.1.2. Cell Zn2

The second 100% Zn electrode, Zn2, had a high seal (from 0.6-1.3 cm above the electrode). The cell was cycled for 64 cycles, and the capacity plot can be seen in Figure 8. Representative cycles are shown in Figure 9. The capacity at the end of cycling was ~0.8 Ah which is 65% of its initial capacity. The electrode received ~79 Ah in charges and delivered 71 Ah in discharges. This leads to an average coulombic efficiency of 90%.

Again based on 4 g of excess ZnO, 20 Ah/g excess ZnO were obtained from the electrode before failure. Based on the actual initial capacity of 1.21 Ah, this is 19 Ah/g excess ZnO. As is seen in Figure 8, the cell began to lose capacity by cycle 40 and by cycle 55 was losing capacity very rapidly. Cell cycling was halted because of loss of capacity. There were indications of possible shorts but all methods to recover the capacity failed. The excess charge factor varied from 1.02 initially to 1.1-1.2 for the last 20 cycles. Again, this electrode only differed from Zn1 in the closeness of the upper seal to the electrode.

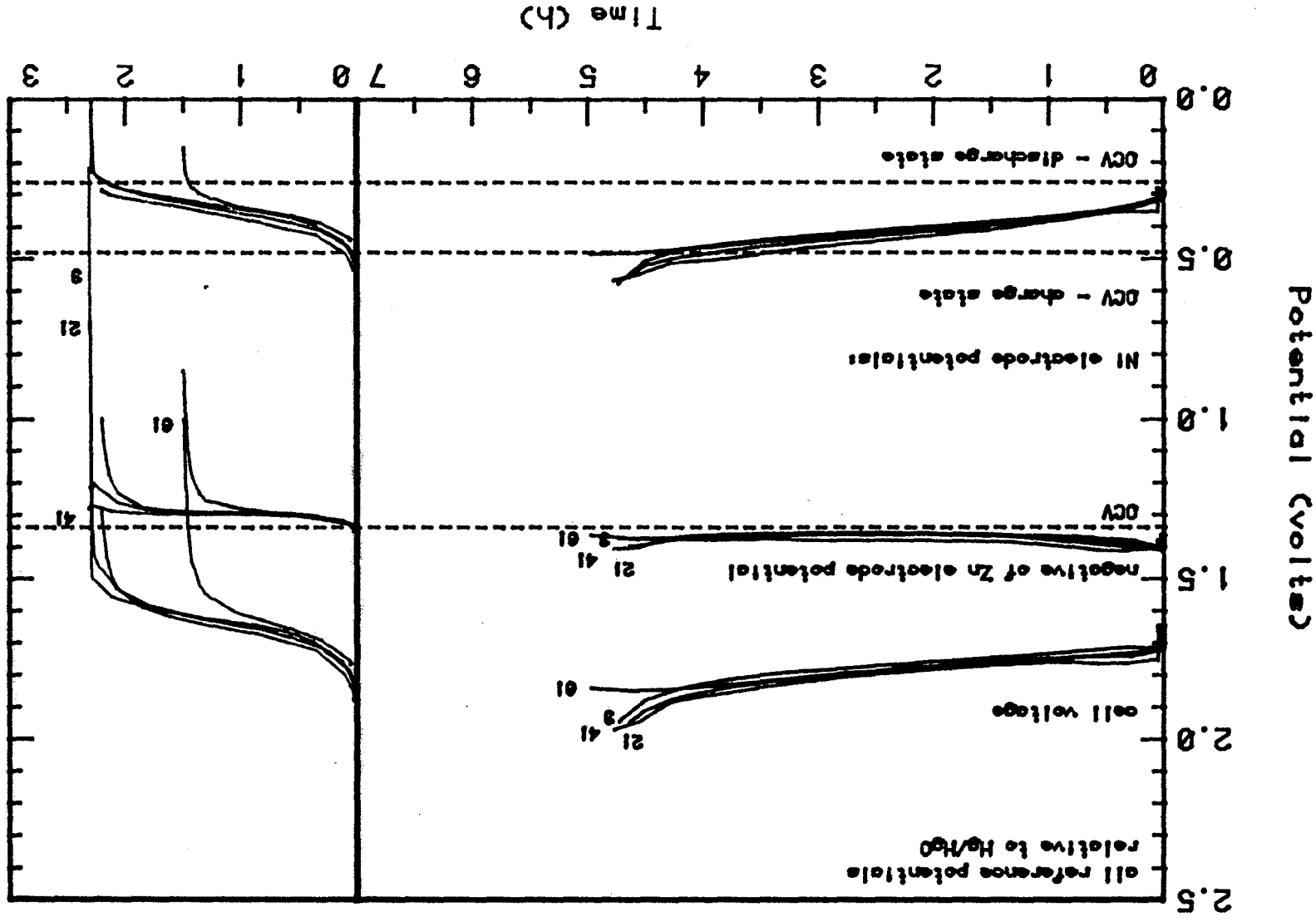Figure 8. Capacity vs cycle number for Cell Zn2 (100% Zn).
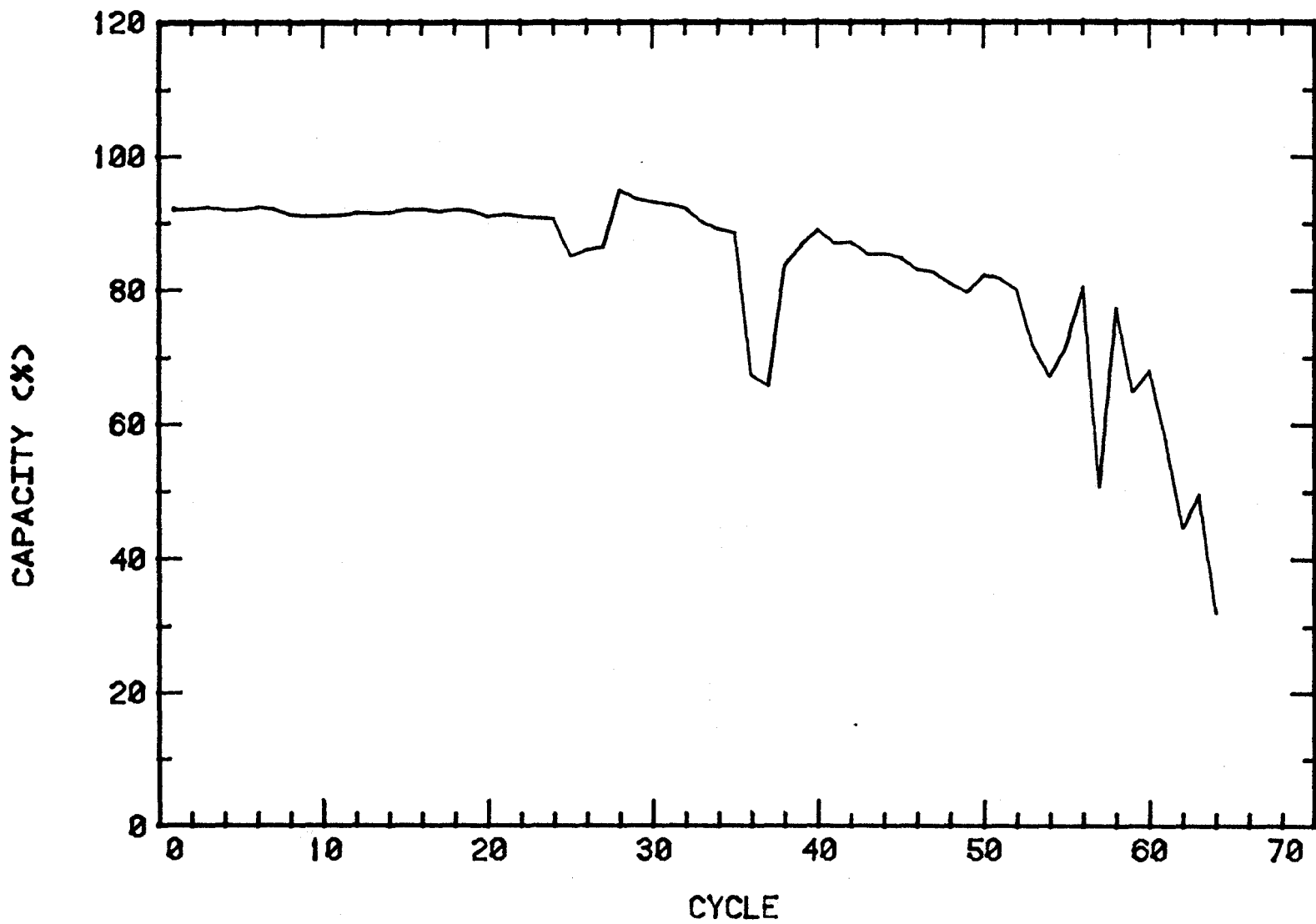
Figure 9. Voltage vs state of charge curves for representative cycles of Cell Zn2 (100% Zn).

4.1.3. Cells 10Ca1 and 10Ca 2

The two cells with zinc electrodes containing 10 mol% $Ca(OH)_2$, 10Ca1 and 10Ca2, were cycled in series until cycle 46 when their characteristics differed sufficiently to warrant their separation. Both cells had a high top seal and thus should be compared with Zn2. The NiOOH electrodes in these cells were not well behaved. They exhibited very high overpotentials from time to time. The overpotential problems did not appear to affect the performance of the zinc electrode, however.

Operation of cell 10Ca1 was discontinued after 64 cycles. The capacity plot can be seen in Figure 10 and representative cycles are shown in Figure 11. The capacity at the end of cycling was roughly 0.87 Ah which is 71% of the initial capacity. The electrode accepted a total of ~74 Ah in charge and delivered 68 Ah in discharge. Thus, the coulombic efficiency was 92%.

The excess ZnO present for a 10% $Ca(OH)_2$ electrode is only 3.4 g based on design capacity. This corresponds to the electrode receiving 22 Ah/g excess ZnO. Based on the initial capacity of 1.22 Ah, this value is 21 Ah/g excess ZnO. The excess charge factor varied from 1.02 initially to 1.1-1.2 for the last 10 cycles. The capacity declined gradually throughout cycling. Operation of the cell was discontinued because of loss of capacity. It was believed that a short may have been the cause, so the cell was dismantled and the top two layers of separator were replaced. After reassembly with new NiOOH electrodes, the cell continued to exhibit low capacity and operation was ceased. The new NiOOH electrodes, however, seemed well-behaved.

When comparing this cell to Zn2 it must be remembered that this cell had less excess Zinc. It has been observed that as the amount of excess Zinc is decreased for
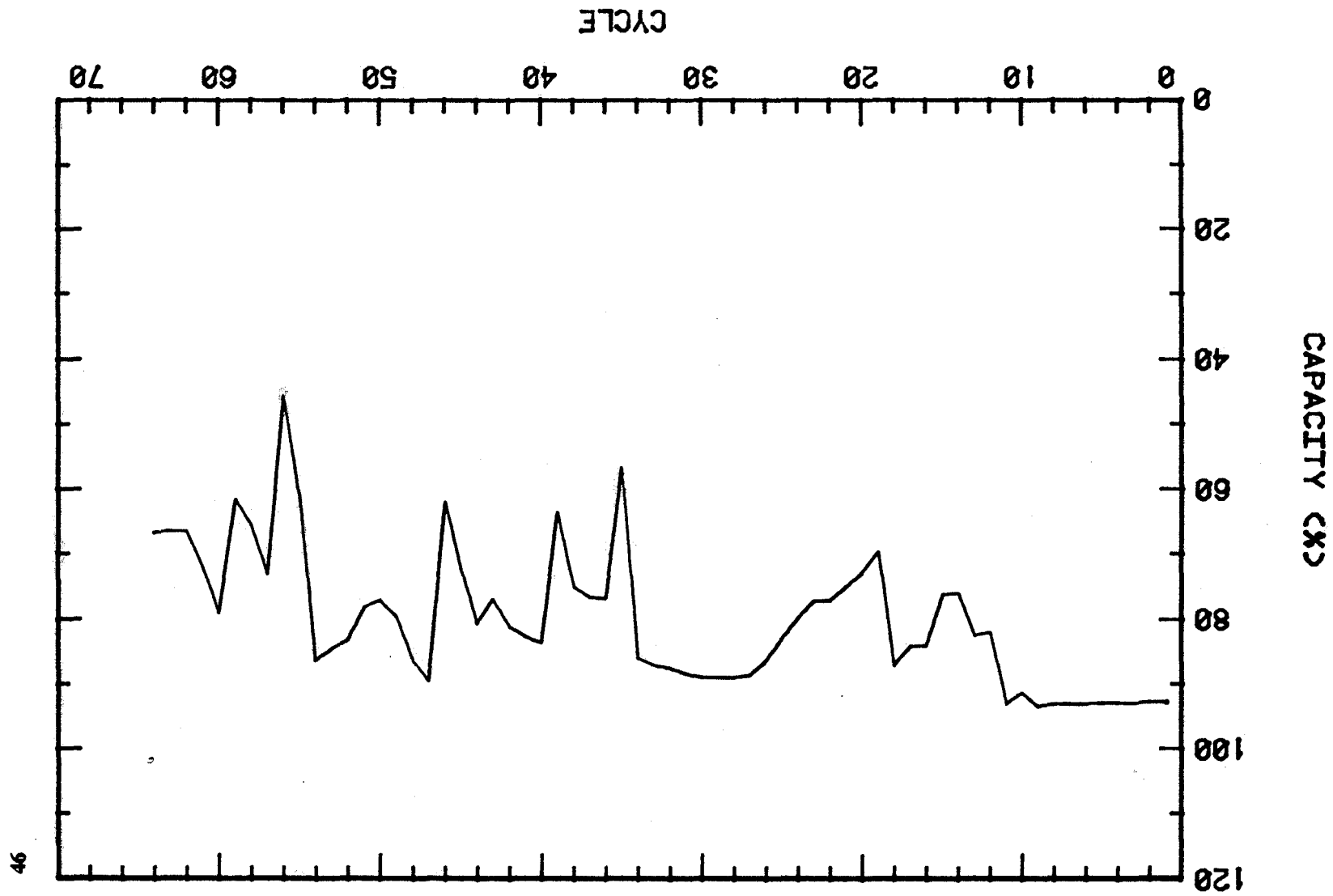
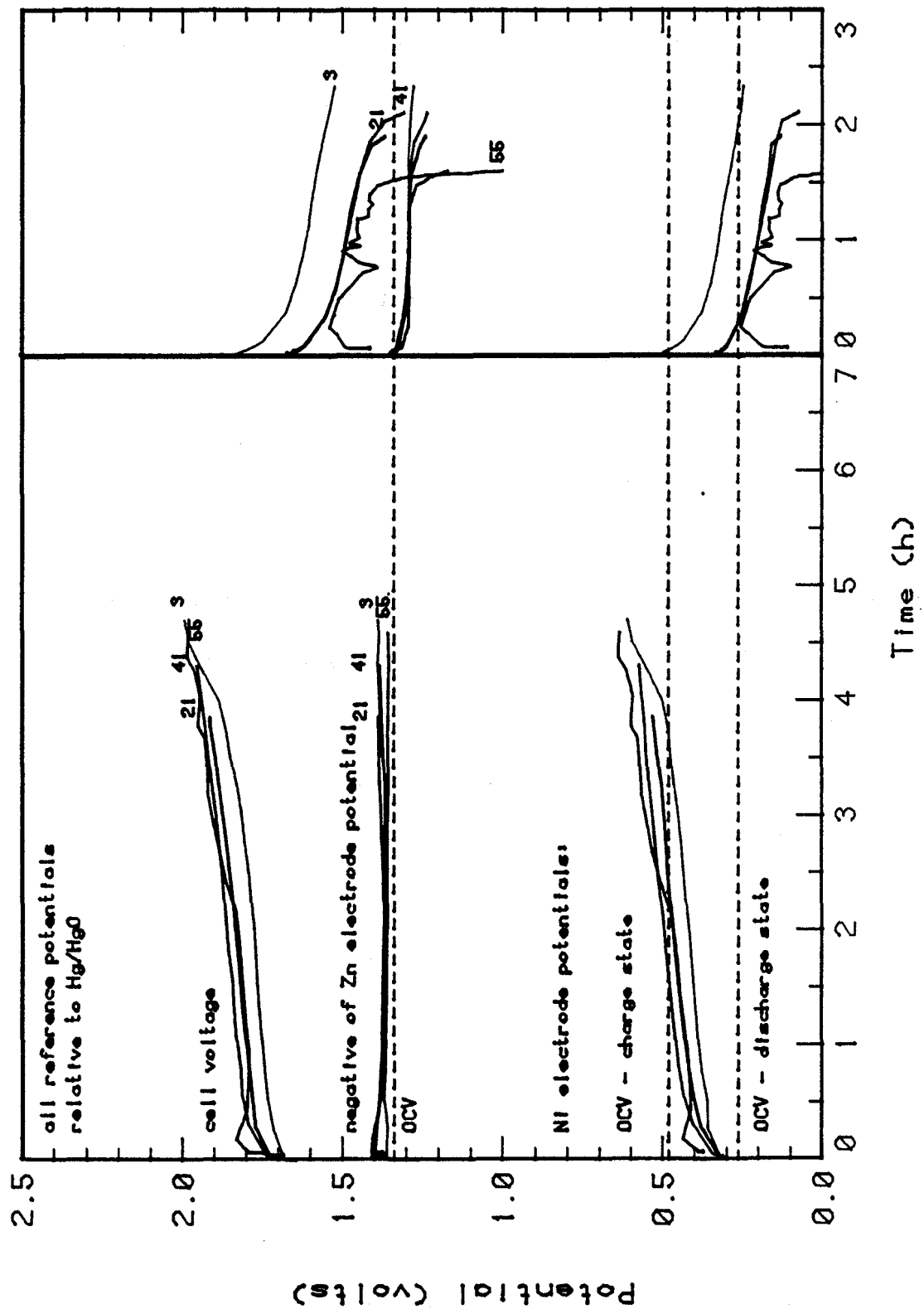Figure 10. Capacity vs cycle number for Cell 10Ca1 (10 mol% Ca(OH)$_2$).

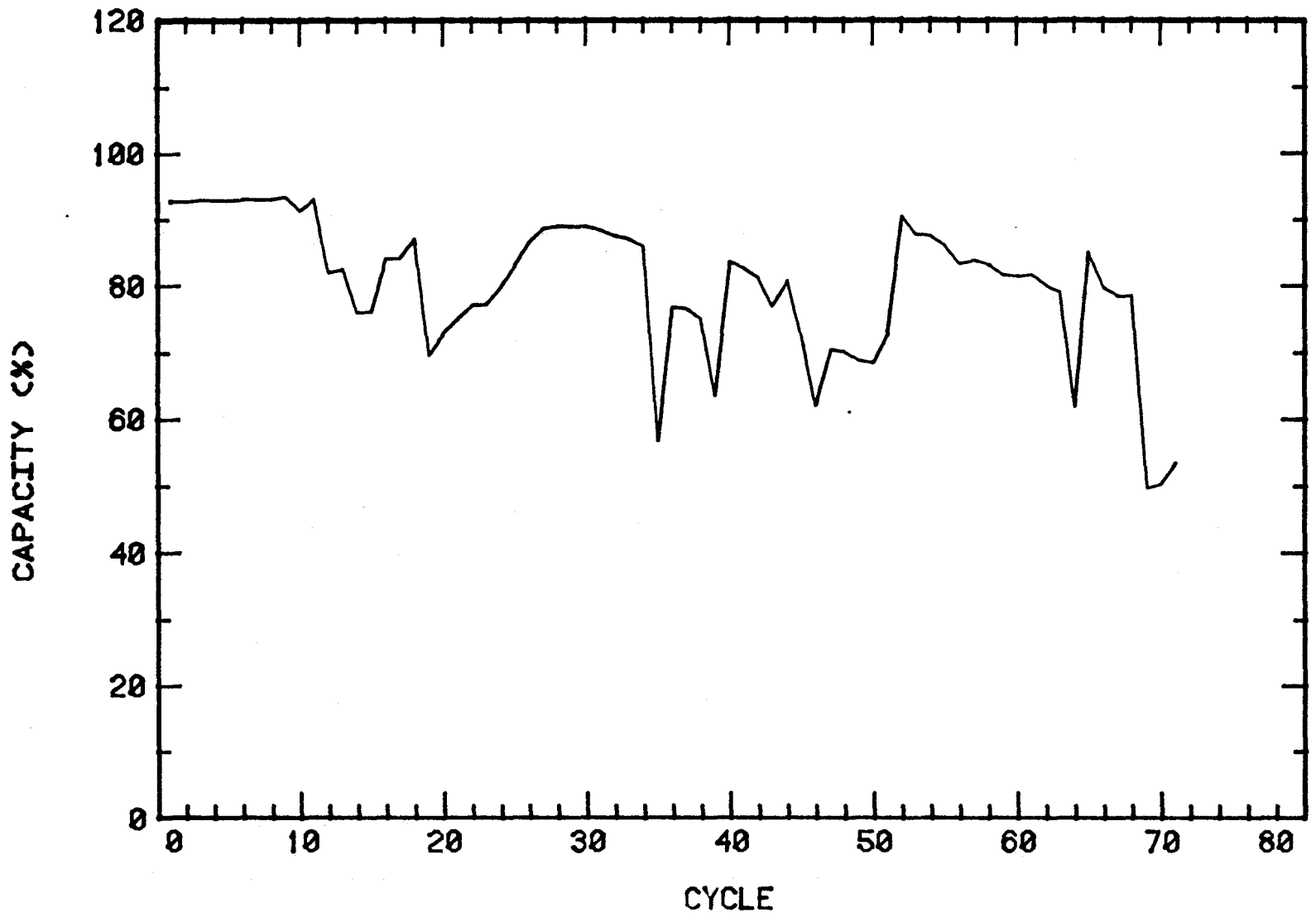Figure 11. Voltage vs state of charge curves for representative cycles of Cell 10Ca1 (10 mol% Ca(OH)$_2$).

all-Zn electrodes, the cell life decreases. Thus, if the $Ca(OH)_2$ had no effect on the cell, the decrease in excess ZnO should have lowered the cycle life. So, even though 10Ca1 and Zn2 reached the same number of cycles, this is taken as an indication that $Ca(OH)_2$ did have a positive effect on the remaining Zinc.

Operation of cell 10Ca2 was discontinued after 71 cycles. The capacity vs cycle number plot is shown in Figure 12, and voltage vs state of charge curves for representative cycles are shown in Figure 13. The capacity near the end of life decreased rapidly from 1.03 to 0.70 Ah, which is 57% of the initial capacity. Approximately 82 Ah in charge and 75 Ah in discharge were received and delivered, respectively, for a coulombic efficiency of 91%. This amounts to 24 Ah/g excess ZnO based on design capacity and 23 Ah/g excess ZnO based on the initial capacity of 1.22 Ah. The excess charge factor varied from 1.02 initial to 1.08 near the end of cycling. Operation of this cell was also discontinued due to loss of capacity. Using the same procedure as for 10Ca1 the cell was disassembled and reassembled. Similar to 10Ca1, this cell also continued to perform poorly and cycling was stopped. Again, as this cell had less excess ZnO, the fact that it performed better than the pure Zn cell Zn2 shows that $Ca(OH)_2$ improved the performance of the cell.

4.1.4. Cells 25Ca1 and 25Ca2

The two cells containing zinc electrodes with 25 mol% $Ca(OH)_2$, 25Ca1 and 25Ca2, were also cycled in series, until cycle 66. The NiOOH electrodes in these cells also performed poorly and exhibited high overpotentials, however the problem was not so severe as with the 10% cells. In addition, after cycle 16 the charge current was decreased from 0.26 to 0.20 A, in order to avoid erratic cell potentials. These

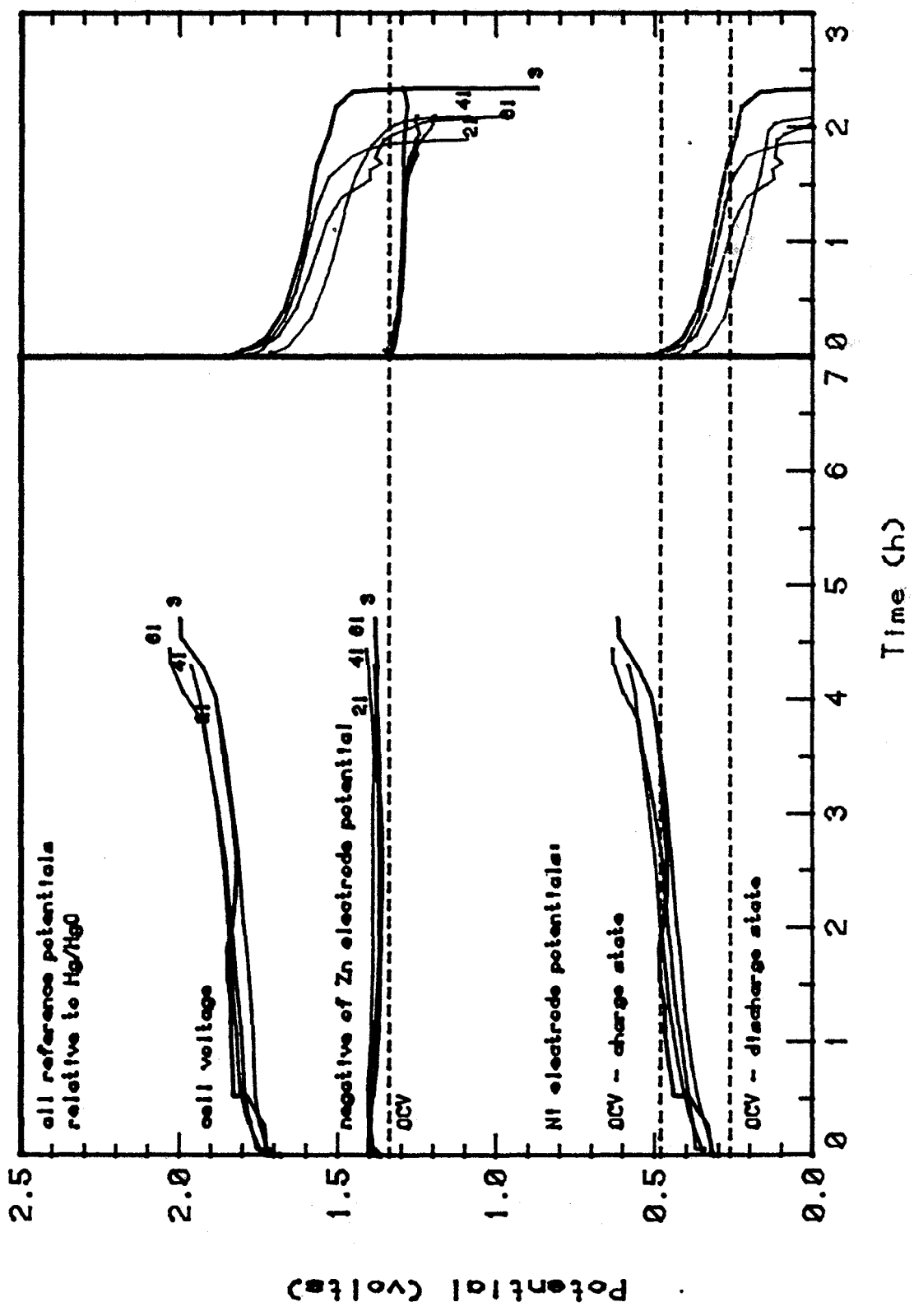Figure 12. Capacity vs cycle number for Cell 10Ca2 (10 mol% Ca(OH)$_2$).

Figure 13. Voltage vs state of charge curves for representative cycles of Cell 10Ca2 (10 mol% Ca(OH)$_2$).

electrodes were also constructed with a high seal and should be compared with Zn2 as the base case.

Operation of cell 25Ca1 was discontinued after 151 cycles. Its capacity behavior is plotted in Figure 14, and representative cycles can be seen in Figure 15. At the end of cycling the capacity was 1.24 Ah which is 94% of initial capacity. Here the initial capacity was indeed the design capacity of 1.32 Ah. About 194 Ah were passed on charges and 185 Ah on discharges leading to an average coulombic efficiency of 95%.

The excess ZnO for the 25% $Ca(OH)_2$ electrode is 2.6 g which results in 75 Ah/g excess ZnO. The excess charge varied from 1.02 initially to 1.05 near the end of cycling. The capacity was fairly stable overall, with occasional dips due to soft shorts (shorts which disappear by themselves) or other factors. It should be noted that capacities greater than 100% are due to the performance of extended discharges to replenish the ZnO reserve. Operation of the cell was discontinued because it reached 150 cycles. The zinc electrode was limiting in this cell for the final 50 cycles, but because of the problems with the NiOOH electrodes it is not easy to rationalize this behavior. If the zinc electrode was shorted to the NiOOH electrodes, then the NiOOH electrodes should also have been running out of capacity at the same time (since the NiOOH electrode would also have been unable to charge completely). It is possible that the zinc electrode had become inefficient (evolving gas) but there was no indication of this. It is expected that this Zn-25 mol% $Ca(OH)_2$ electrode could have continued to cycle for many more cycles.

When comparing this cell with Zn2, the dramatic improvement achieved by adding $Ca(OH)_2$ can be seen. Zn2 has 1.5 times more excess Zinc than 25Ca1, yet the
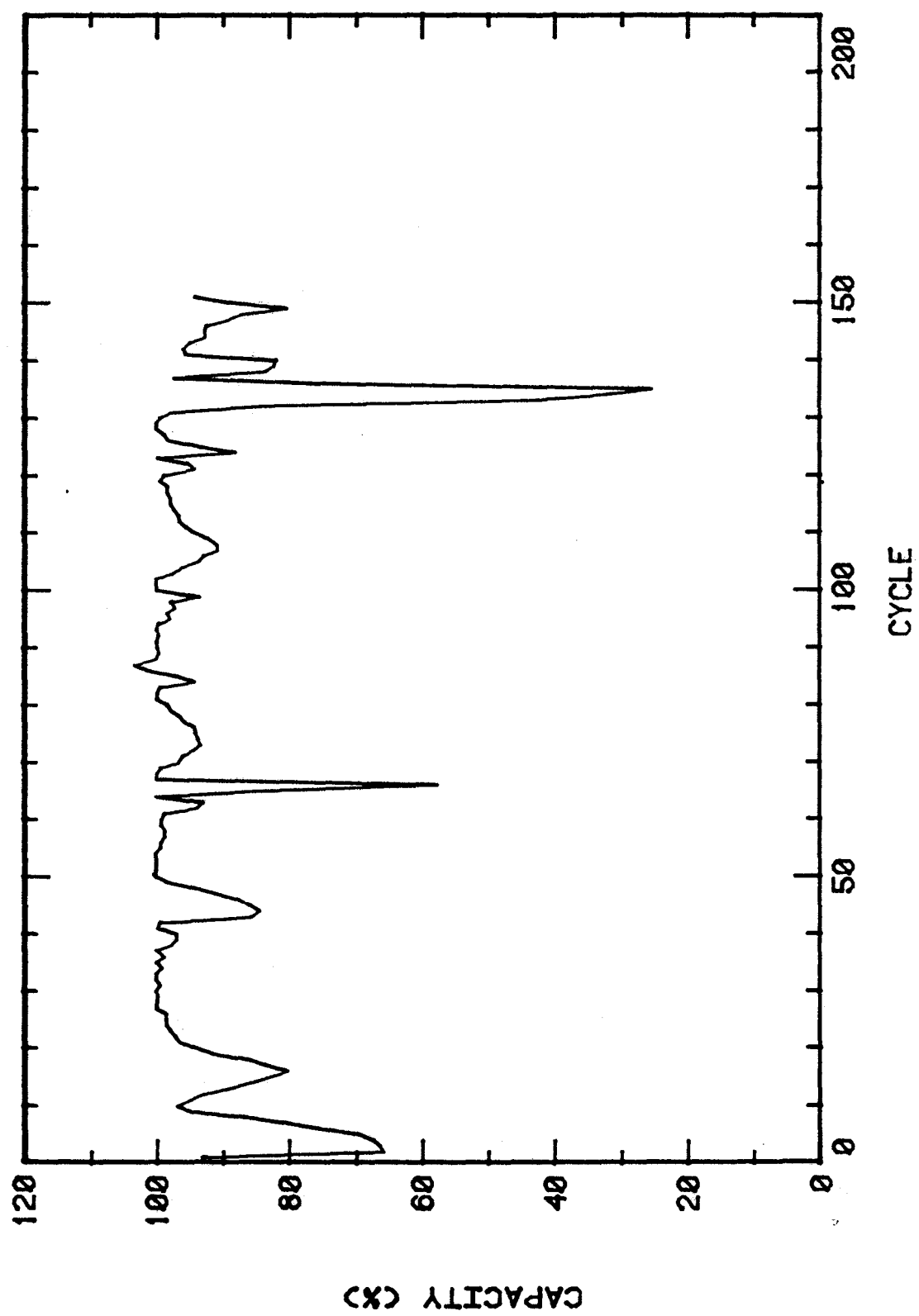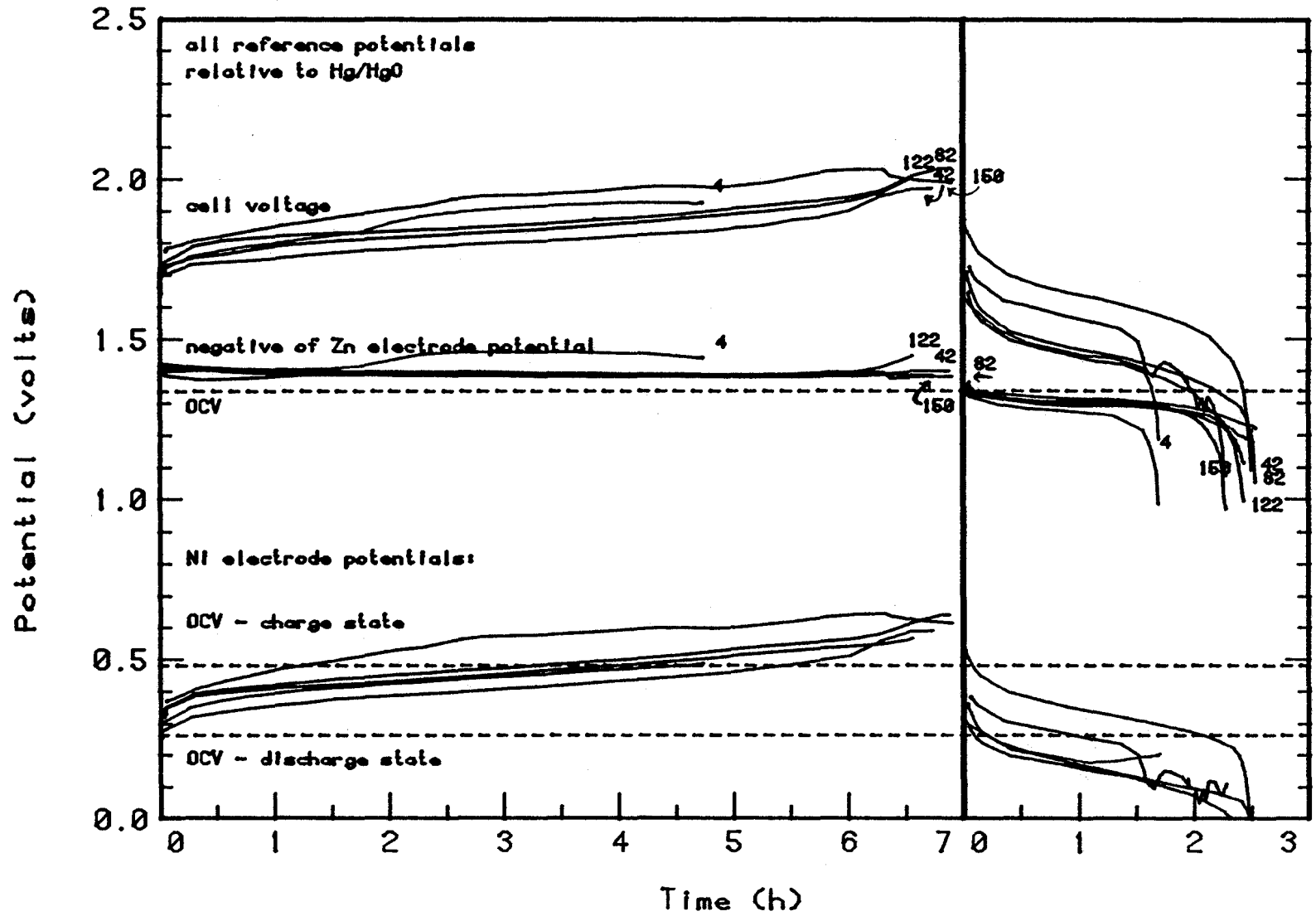
Figure 14. Capacity vs cycle number for Cell 25Ca1 (25 mol% $Ca(OH)_2$).

Figure 15. Voltage vs state of charge curves for representative cycles of Cell 25Ca1 (25 mol% Ca(OH)₂).

latter cycled more than twice as many cycles. When the excess Zinc is decreased to the level in 25Ca1 and 25Ca2 (125% excess) a dramatic loss in cycle life is normally the case for all Zn electrodes.[19] Cell Zn2 cycled 19 Ah/g excess ZnO and only 13 Ah/g total ZnO. Cell 25Ca1, on the other hand, cycled 75 Ah/g excess ZnO and 42 Ah/g total ZnO. Even the tight seal cell Zn1 only cycled 44 Ah/g excess ZnO and 29 Ah/g ZnO.

Operation of the second 25% $Ca(OH)_2$ cell, 25Ca2, was discontinued after 106 cycles. Its capacity vs cycle number plot can be seen in Figure 16 and representative voltage vs state of charge cycles are shown in Figure 17. The capacity at the end of cycling was ~1.0 Ah corresponding 76% of the initial capacity. The capacity, however, decreased rapidly from 100% of design capacity at cycle 97 due to a short. During charges ~135 Ah were passed and 128 Ah were delivered during discharges, for an average coulombic efficiency of 95%. This amounts to 52 Ah/g excess ZnO. The excess charge factor varied from 1.00 at times to an average of around 1.03.

This cell was performing very well until the short. The short could be seen in the assembled cell as material protruding from the edge of the zinc electrode. An attempt to dismantle the cell and reassemble was unsuccessful resulting in the loss of the cell. As there was no capacity decline occurring before the short, the cell should have completed many more cycles if it were not for the short. Even with the short, however, this cell performed better than both Zn1 and Zn2 on a cycled Ah/g excess ZnO basis. Again, the zinc electrode is seen to be limiting at the end of discharge.

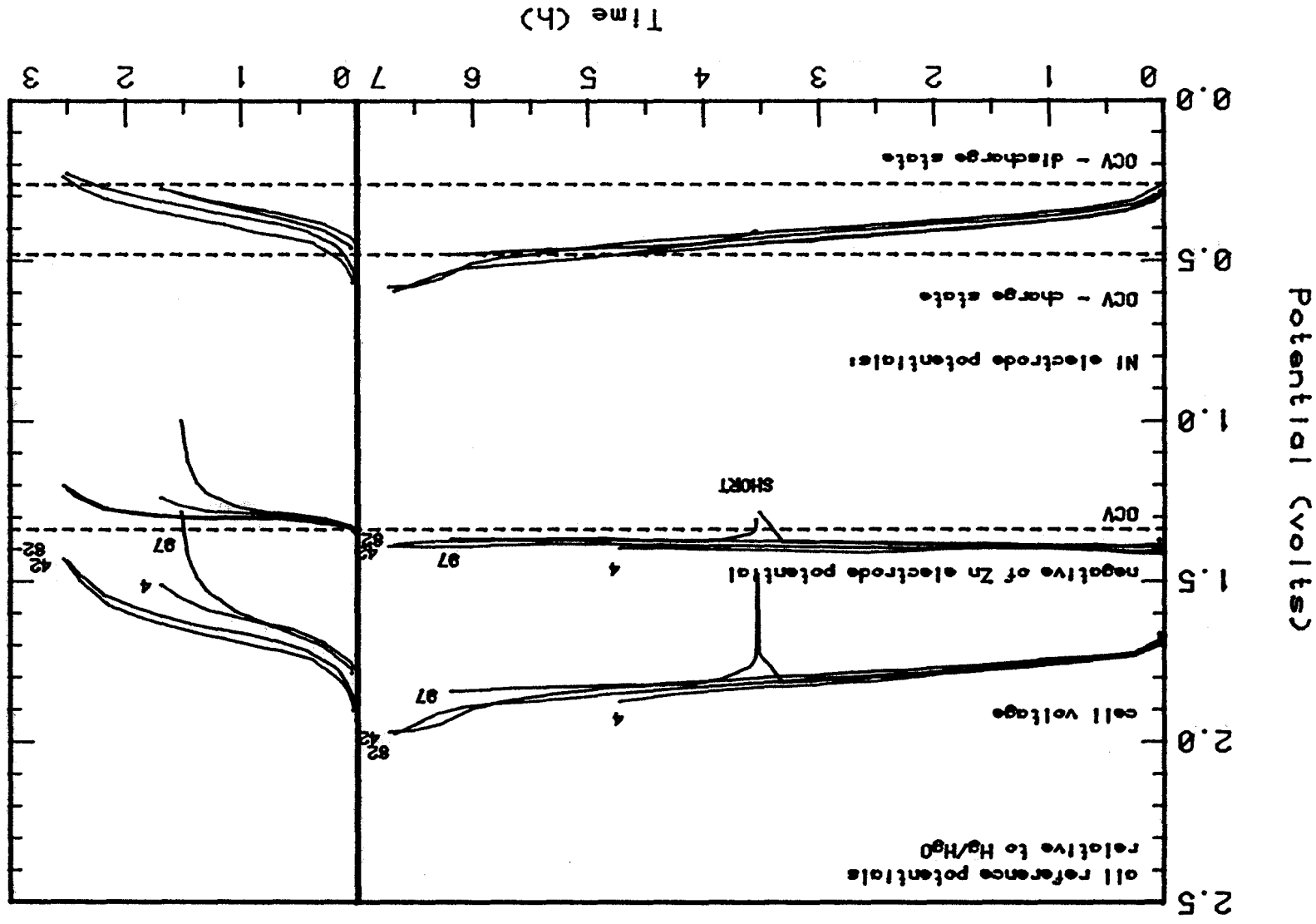Figure 16. Capacity vs cycle number for Cell 25Ca2 (25 mol% $Ca(OH)_2$).
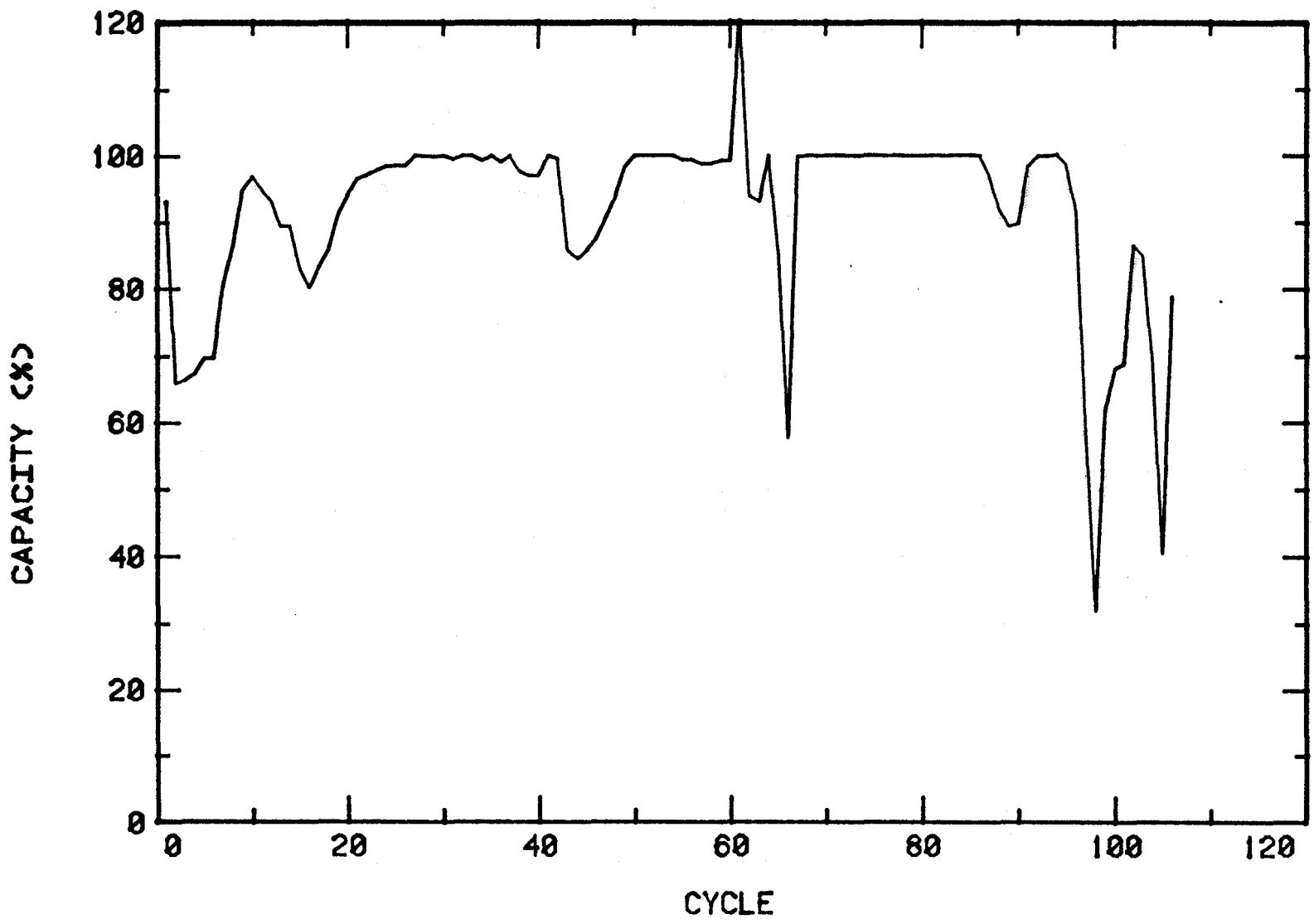
Figure 17. Voltage vs state of charge curves for representative cycles of Cell 25Ca2 (25 mol% Ca(OH)₂).

4.1.5. Cells 40Ca1 and 40Ca2

The two 40% Ca(OH)$_2$ cells both shorted within the first few cycles, apparently because they could not accept the charge current of 0.263 A. For the 25% cells the current on charge was lowered to 0.200 A because of this. It was felt that for the 40% cells, a charge current lower than 0.200 A would be required, which corresponds to a charge time too long to be practical. Another cause for their failure was that they were tightly sealed, and when the electrode expanded due to the Ca(OH)$_2$ and ZnO forming the complex, the separator ripped at the seams, facilitating dendritic growth and shorts. This was the reason why the other Ca(OH)$_2$ cells (10% and 25%) were sealed with a less tight separator. No further cycling experiments were performed on 40% Ca(OH)$_2$ cells.

The high overpotential for the 40% electrodes during charge is clearly seen in Figure 18. Also, the increasing overpotential on the zinc electrode due to Ca(OH)$_2$ addition is clearly evident. This overpotential results in some energy inefficiency but mainly increases the chance of shorting. The overpotential can be decreased by lowering the charge current, however, this raises the time it takes to charge the cell.

It is believed that the zinc electrode charging mechanism involves electrodeposition of Zn from zincate in solution, where the zincate is continually replenished by dissolving ZnO. With Ca(OH)$_2$ addition, however, there is an added rate limitation of decomposing the complex to form ZnO or zincate. The time and/or driving force required to form zincate with complex present, in addition to the fact that Ca(OH)$_2$ removes supersaturated zincate, probably results in a lower concentration of zincate
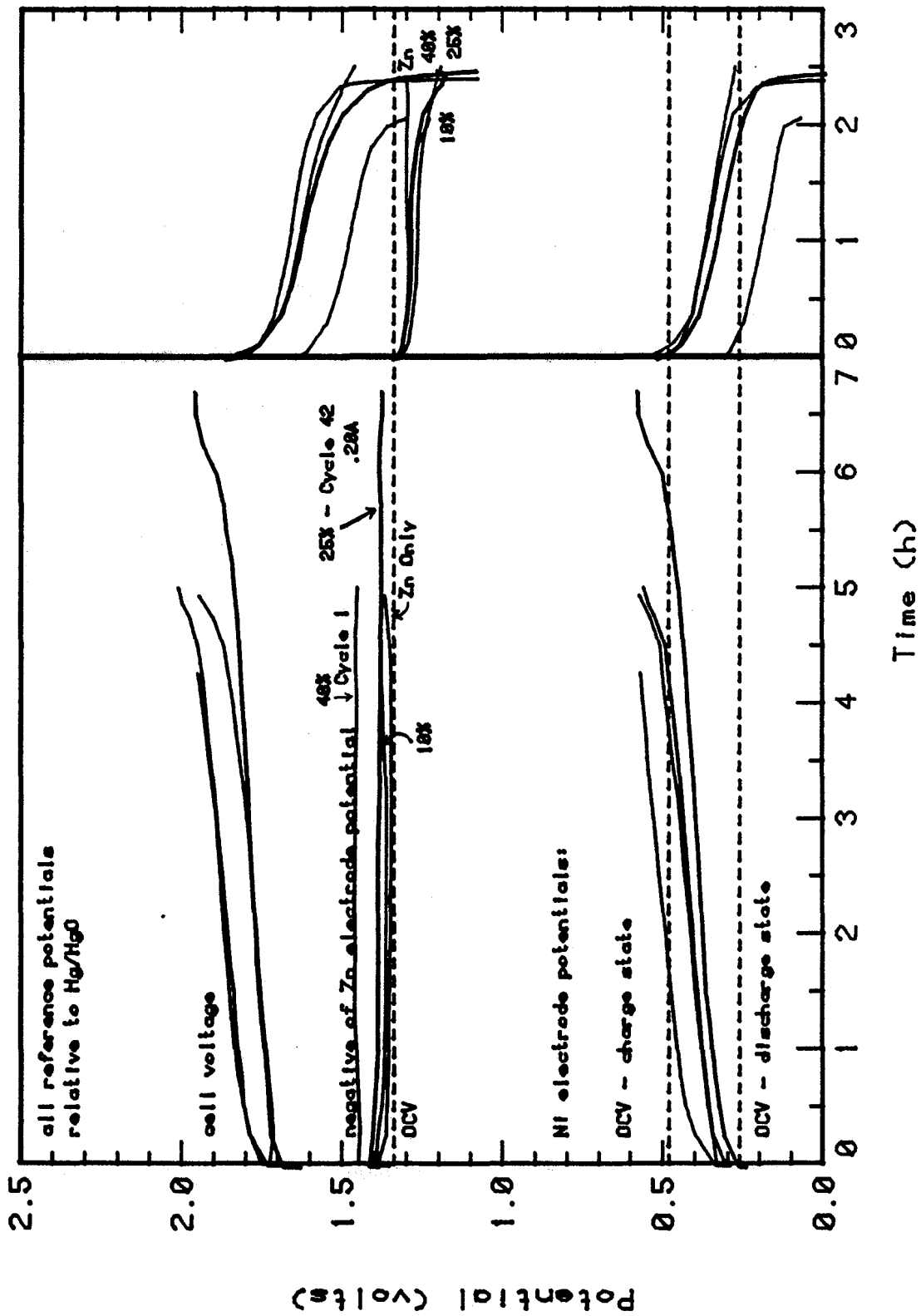
58

Figure 18. Increasing zinc electrode overpotential during charge due to Ca(OH)$_2$ addition.

during charge causing the higher overpotentials. A summary of the performance of the various cells is listed in Table 4.

4.2. High and Low Seal Effects

The difference between the high-seal zinc electrode and the low-seal zinc electrode was very evident in comparing Zn1 and Zn2. A further experiment was performed using a 10% $Ca(OH)_2$ electrode.

A 10% $Ca(OH)_2$ electrode was constructed with a low seal (as compared to all the other $Ca(OH)_2$ cells which were high sealed). The electrode was used for a separate type of experiment and thus was positioned within the cell in a manner which was different than that for the other zinc cells. The zinc electrode was between the PTFE spacer on one side and the NiOOH electrodes on the other, so that only one face of the

TABLE 4 Cell Performance				
Cell Name	Cycles Completed	Reason for Termination	Seal Type	Ah/g Excess ZnO
Zn1	150	Reached 150 cycles	Low	42
Zn2	64	Low capacity	High	19
10Ca1	64	Low capacity	High	21
10Ca2	71	Low capacity	High	23
10Ca3	103	Finished experiment	Low	39
25Ca1	150	Reached 150 cycles	High	75
25Ca2	106	Shorted	High	52
40Ca1	2	Shorted	Low	—
40Ca2	2	Shorted	Low	—

zinc electrode faced the NiOOH electrodes. This arrangement, however, is not considered to have been as large a factor as the low seal, in the results for this cell. Operation of this electrode was discontinued after 103 cycles. The capacity of the cell can be seen in Figure 19 and typical cycles are shown in Figure 20. The capacity at the end of cycling was 1.16 Ah which is 88% of the initial capacity of 1.32 Ah. Approximately 134 Ah passed in charge and 129 in discharge, giving an average coulombic efficiency of 96%. This corresponds to 39 Ah/g excess ZnO. The excess factor was close to 1.05 throughout, and the cell was very well behaved. Operation was discontinued only because further cycling would provide little new information. The cell was performing similar to Zn1, which was also low sealed. With 10% $Ca(OH)_2$ this cell would be expected to show a slightly longer life than the 100%-Zn Zn1 cell.

As will be seen in the X-ray images in Section 4.3, high seal electrodes allow the movement of Zinc material into the gap between the top of the electrode and the seal. This can amount to a significant amount of Zinc. The separator in low-seal electrodes appears to slow the rate of Zinc redistribution. This implies that convection may be an important factor in shape change. This agrees with the results of Gunther and Bendert.[3] In addition, the convective movement of the electrolyte might entrain small particles of material so that material transport may not be only through dissolution. This material transport may be further enhanced by the pressure of the electrode against the restraining separator (the very top and edges of the electrode are not under restraint). However, this transported material is mainly Zinc, and if the transport was just the bulk movement of material due to the lack of restraint, a stoichiometric amount of $Ca(OH)_2$ would also be expected to move. In addition, the corners of the separator often have dendrites

CAPACITY FOR CELL
10CA3

Figure 19. Capacity vs cycle number for Cell 10Ca3 (10 mol% Ca(OH)$_2$).
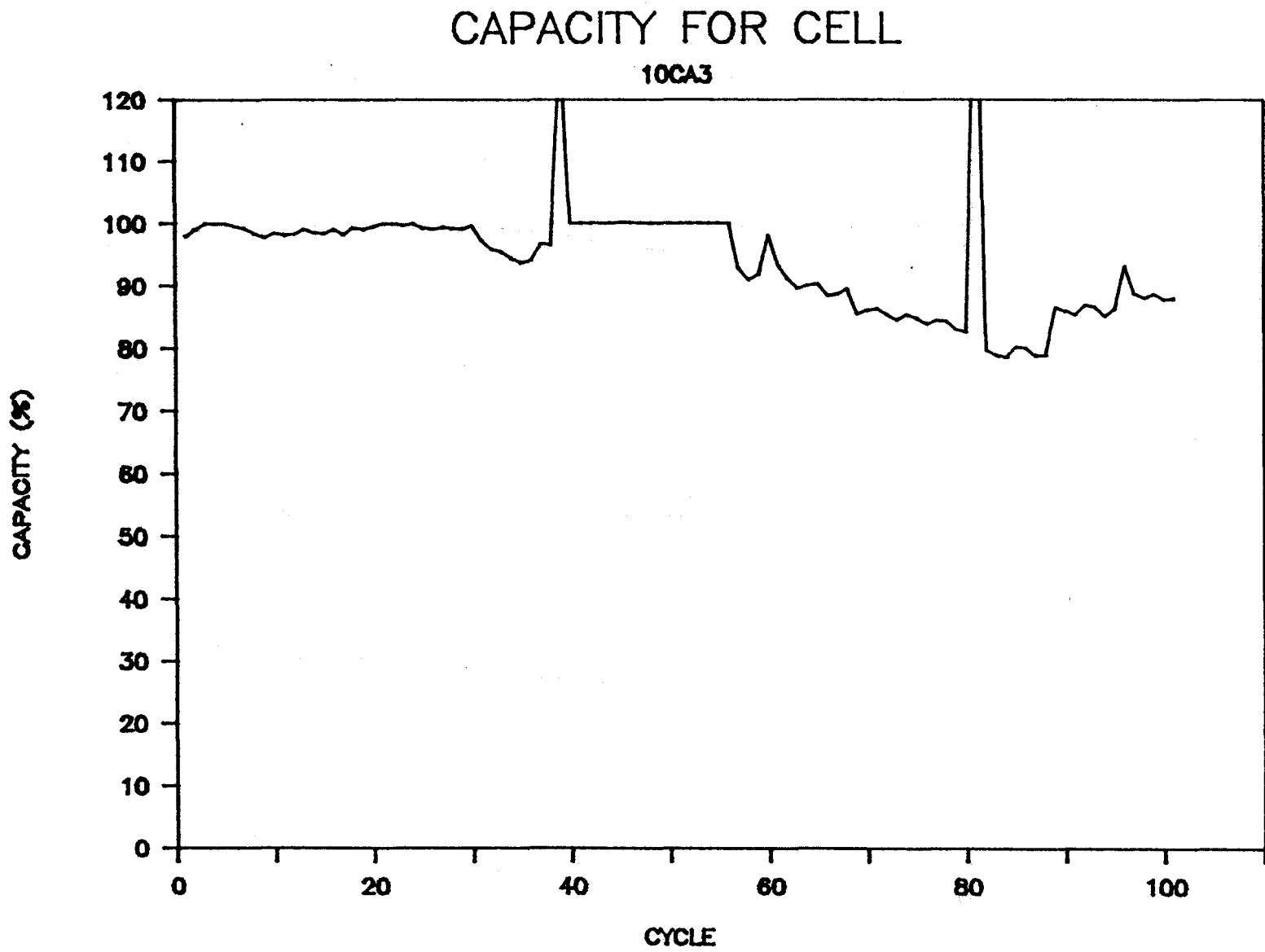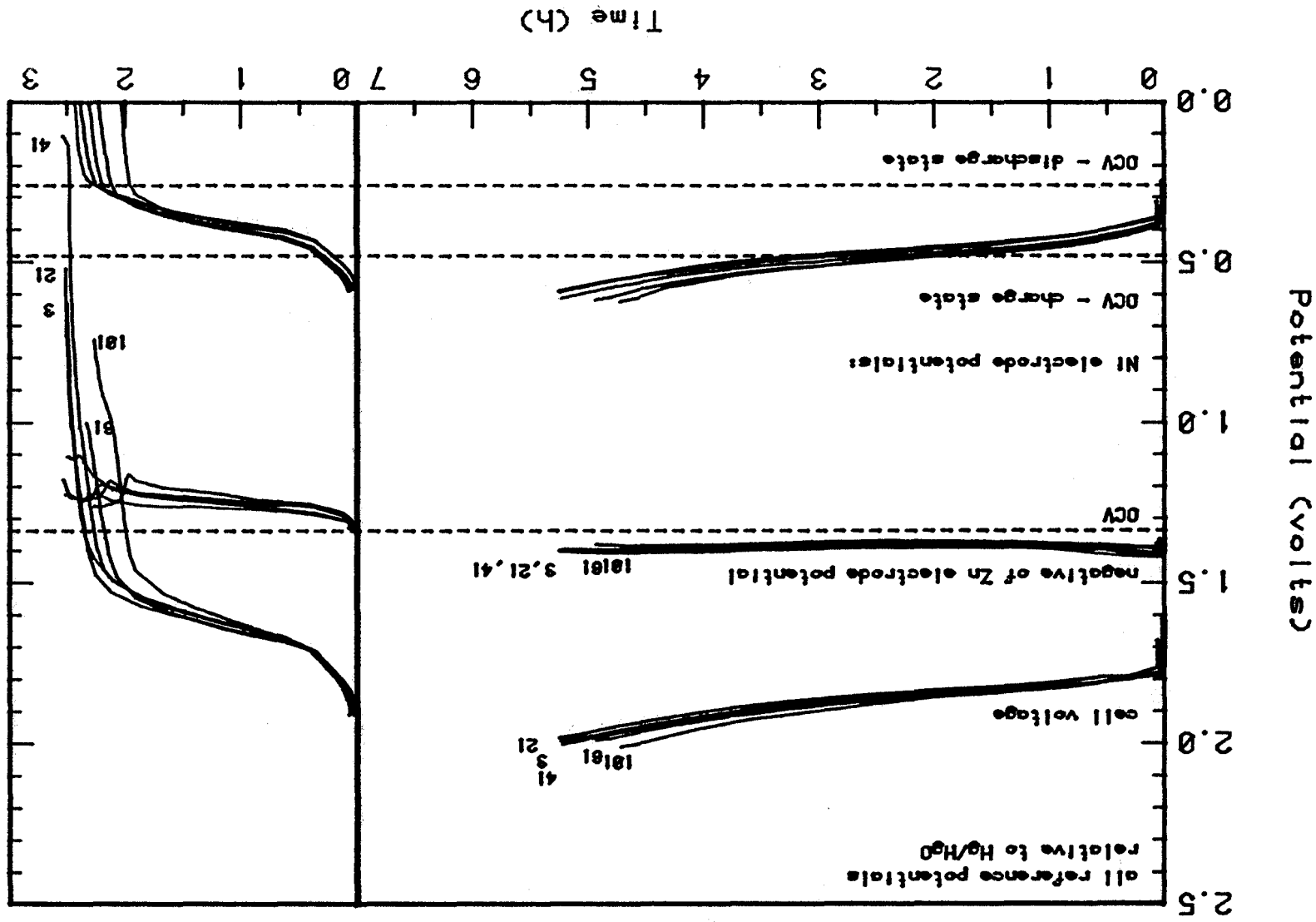
Figure 20. Voltage vs state of charge curves for representative cycles of Cell 10Ca3 (10 mol% Ca(OH)₂).

Figures 22 through 31 show X-ray images and photographs of the zinc electrodes after cycling.

The X-ray of Zn1 can be seen in Figure 22. This electrode operated for 150 cycles and was low sealed. Migration of the Zinc is toward the edges, with significant migration toward the tab side. The reason for the migration toward the tab side is not clearly understood and occurs to this extent only in this electrode. The X-ray also shows that there are many islands of Zinc in the regions being depleted of Zinc. This observation indicates that Zinc migration does not occur uniformly, but that in addition to the general migration (toward the edges in this case), Zinc tends to locally cluster, leaving areas of bare current collector. These islands then slowly move towards the edges or disappear as the Zinc migrates toward the edges. This phenomenon will be better illustrated later in this section and will also be presented in Section 4.6. Also in Figure 22, a small amount of Zinc growth can be seen heading up the tab. This is possible because the separator is not sealed at the tab. No significant growth occurs at the top of the electrode in the other areas because of the low seal. The fact that there is Zinc growth only on the unsealed tab area provides an additional illustration of the significant role of the separator seal location in preventing Zinc migration to this area.

Electrode Zn2, on the other hand, has significant Zinc growth along the top, as seen in Figure 23. This electrode underwent 64 cycles and was high sealed. The high seal allowed the Zinc to migrate away from the current collector. This Zinc had very poor contact with the rest of the electrode and does not appear to contribute to cell capacity. The loose seal seems to have enhanced the rate of Zinc redistribution and almost completely depleted Zinc from the center of the electrode, leaving very dense
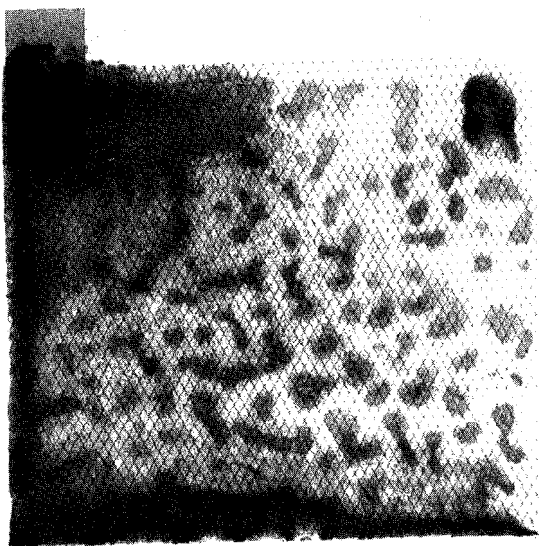
(a)
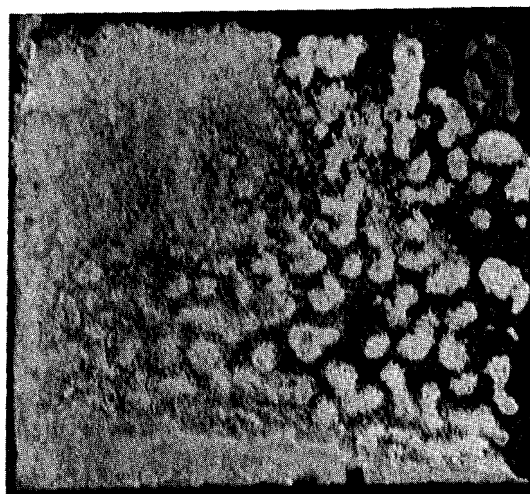
(b)

XBB 8910-8958

Figure 22. Electrode Zn1 (100% Zn) after 150 cycles.
(a) X-ray
(b) Photograph

deposits of Zinc at the edges. Again, island regions of Zinc are also seen.

Figure 24 is the X-ray of the zinc electrode from 10Ca1 when the cell was temporarily stopped and disassembled at 59 cycles. Examination of this X-ray reveals that there is significant movement of material toward the edge of the electrode. Comparing this X-ray with that of Zn2, however, shows a major difference. Unlike the Zn2 electrode, there are no bare current collector areas in the 10Ca1 electrode. The center region of the 10Ca1 electrode, while still having islands, has a fairly uniform background of material. The composition of the islands and background material will be discussed in the next section. Again, significant growth is seen at the top of the electrode.

This cell was reassembled after replacing the two outer layers of separator (to eliminate a short). The NiOOH electrodes were also replaced. Figure 25 is the X-ray of the electrode after operation was finally terminated at 64 cycles due to low capacity. Comparing this X-ray with the earlier X-ray illustrates the continuing movement of material toward the electrode edges. The island regions of Zinc have disappeared from the center area of the electrode, but there still is a uniform background material. Overall, the X-ray appears to show less material on the electrode than was seen in the previous X-ray. The movement of material away from the electrode is quantified and discussed in the following sections and is the topic of Section 4.7.

Figure 26 is the X-ray of cell 10Ca2 after operation was interrupted at cycle 68. This X-ray is very similar to that of 10Ca1. Figure 27 is the X-ray of 10Ca2 after its termination at cycle 71. This cell was reassembled in the same manner as 10Ca1. Again this X-ray is similar to that of 10Ca1 after testing was terminated (Figure 25).
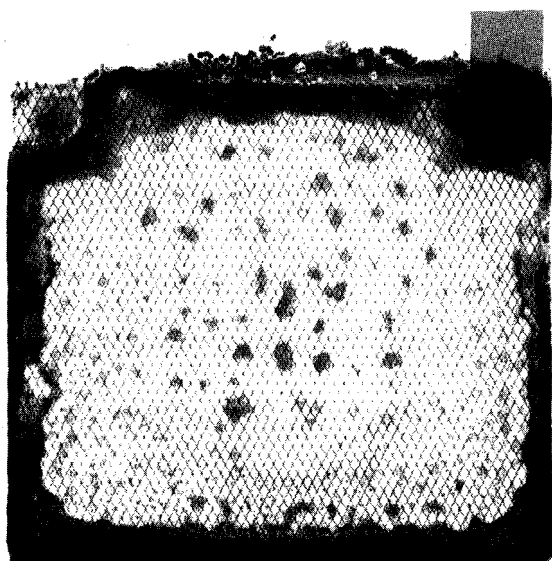
(a)
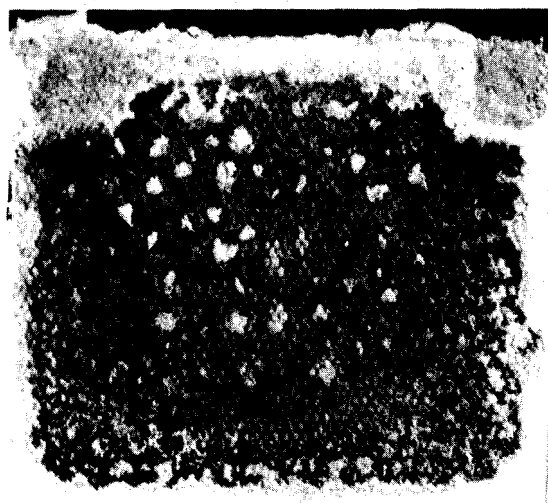
(b)

XBB 8910-8959

Figure 23. Electrode Zn2 (100% Zn) after 64 cycles.
(a) X-ray
(b) Photograph

XBB 8910-8954

Figure 24. X-ray of electrode 10Ca1 (10 mol% $Ca(OH)_2$) after it was temporarily stopped at 59 cycles.

(a)

(b)

XBB 8910-8960

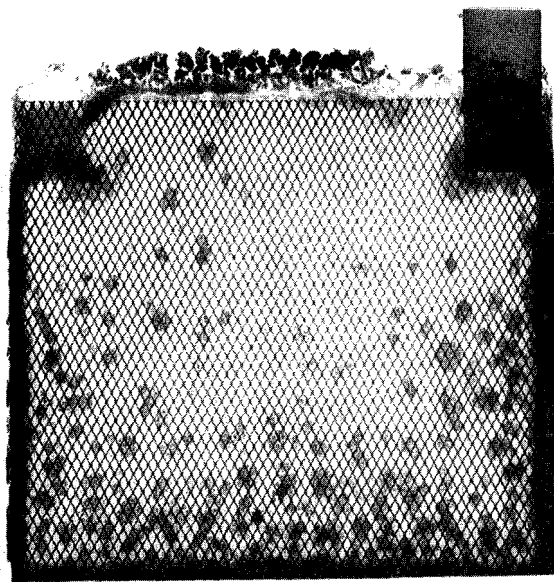Figure 25. Electrode 10Ca1 (10 mol% $Ca(OH)_2$) after it was discontinued at 64 cycles.
(a) X-ray
(b) Photograph

The growth at the top of the electrode in cell 10Ca2 was removed prior to the taking of the X-ray in Figure 27.

The X-ray of cell 25Ca2 after 97 cycles is seen in Figure 28, and it also shows a very uniform background material. It is also evident that there is more of this material than in the 10% $Ca(OH)_2$ cells. Again, material migration toward the edges is seen, but not as much as in the 10% $Ca(OH)_2$ cells.

This cell had been disassembled to remove a suspected short. The cell was reassembled with the original NiOOH electrodes after replacing the outer two layers of separator. The short quickly reappeared and operation of the cell was terminated at cycle 106. The X-ray of the electrode after cycle 106 is seen in Figure 29. It is apparent when comparing the two X-ray images of this cell, that there are no major differences. The ten extra cycles did not increase the growth at the edges significantly, nor did they deplete the background material in the center. As this cell was reassembled with its original NiOOH electrodes, no further material loss from the zinc electrode was expected.

Figure 30 is the X-ray of cell 25Ca1 when testing was terminated after 151 cycles. This X-ray is very similar to the X-ray of 25Ca2 taken when 25Ca2 had only received 97 cycles. This observation indicates that the electrode's active material is migrating at a very slow rate and that further cycling would not cause a significant loss of capacity due to shape change. Uniform distribution of active material was the desired outcome from the use of $Ca(OH)_2$, and that appears to be the case. This is apparent because as is seen in the X-ray, the uniform section is such a large portion of the total electrode that it would have been impossible to maintain cell capacity if this material was not active.

XBB 8910-8955

Figure 26. X-ray of electrode 10Ca2 (10 mol% Ca(OH)$_2$) after it was temporarily stopped at 68 cycles.

(a)

(b)
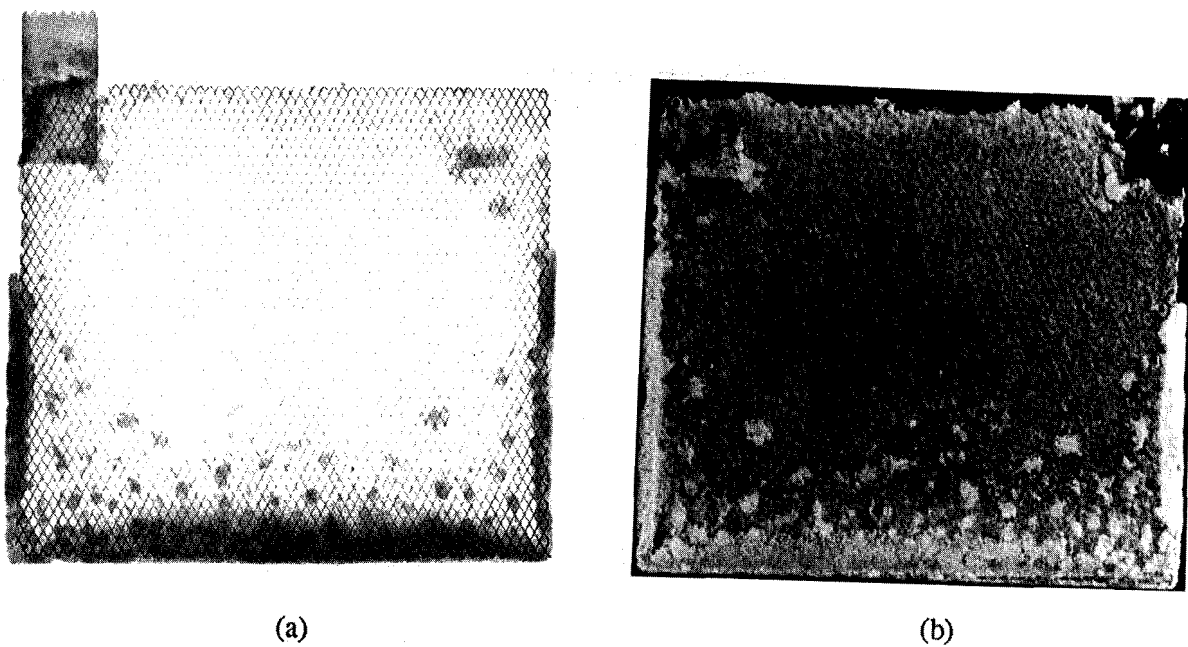
XBB 8910-8961

Figure 27. Electrode 10Ca2 (10 mol% Ca(OH)$_2$) after it was discontinued at 71 cycles.
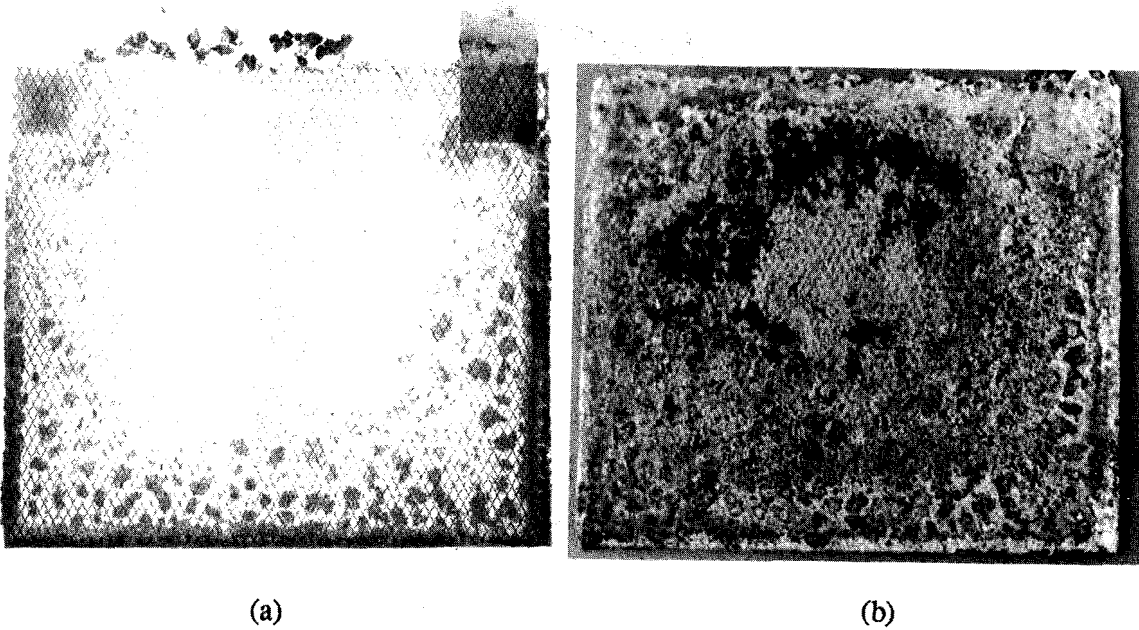(a) X-ray
(b) Photograph
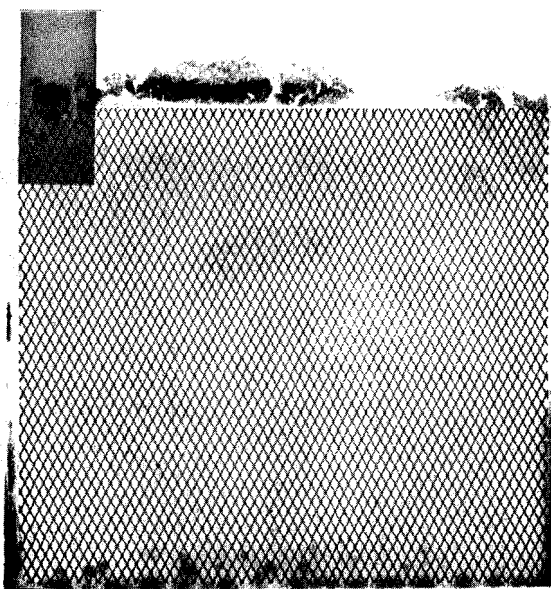
XBB 8910-8953

Figure 28. X-ray of electrode 25Ca2 (25 mol% $Ca(OH)_2$) after it was temporarily stopped at 96 cycles.

(a)

(b)
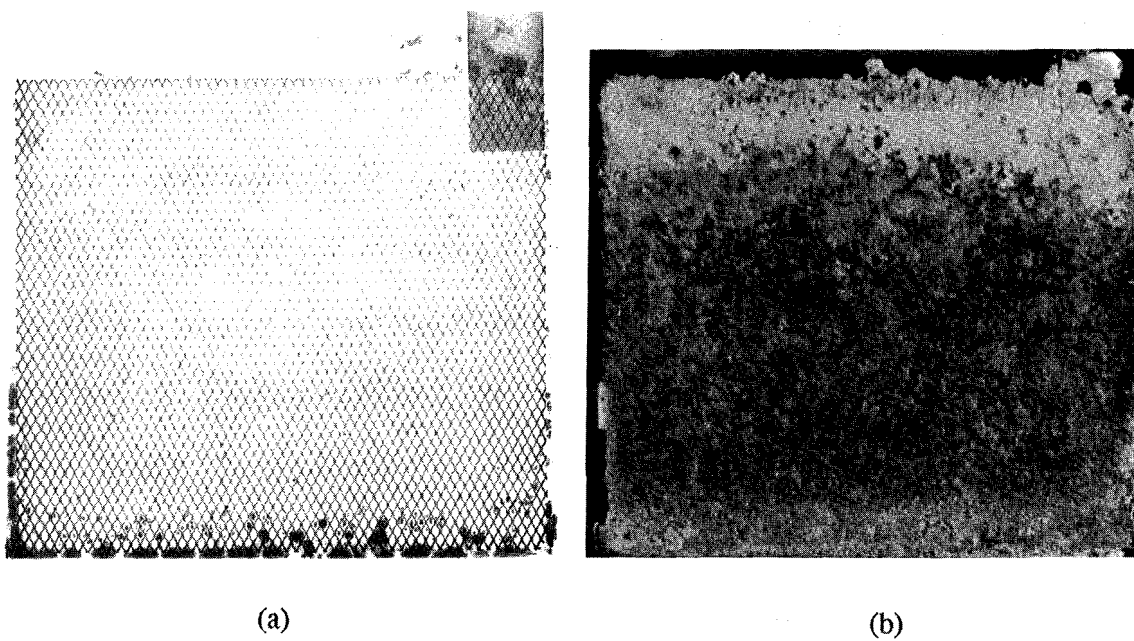
XBB 8910-8962

Figure 29. Electrode 25Ca2 (25 mol% Ca(OH)$_2$) after it was discontinued at 106 cycles.
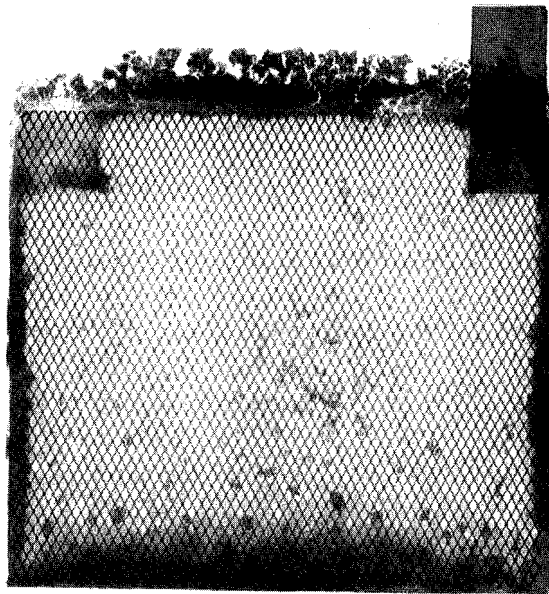(a) X-ray
(b) Photograph

The uniformity of the elements over the electrode will be discussed in Section 4.5.

The final X-ray (Figure 31) is that of 10Ca3 which was disassembled in the charged state after 103 cycles. This is the zinc electrode which was cycled in the NiOOH electrode test and thus had only one surface facing the two NiOOH electrodes. In addition, this cell was close sealed. Comparing this X-ray with those of the other 10% $Ca(OH)_2$ cells (Figures 24-27), reveals significant differences. First, it is noticed that the direction of shape change is toward the center of the electrode. This could have occurred because of the higher current density on this electrode, compared to the other cells (same total current but only one side faces the NiOOH electrodes). The second and most important difference is that there is much less shape change in this cell compared to the others (as will be seen in the next section, shape change is only due to Zinc migration). The decrease in the rate of shape change for this close-sealed 10% $Ca(OH)_2$ cell vs the high-sealed 10% $Ca(OH)_2$ cells is taken as an indication that close sealing decreases the rate of shape change. However, it is recognized that the difference in cycling condition and in the direction of shape change would have had a major influence.

In addition to the visible differences when comparing this cell to the others, disassembling it in the charged state also led to differences in chemical composition. This is discussed within Section 4.4.

4.4. SEM, EDS, and X-ray Diffraction Results

All zinc electrodes were examined microscopically using a SEM. EDS was also used for qualitative determination of chemical composition. This allowed the determination of chemical variations over microscopic areas of the electrode, including the

(a)

(b)
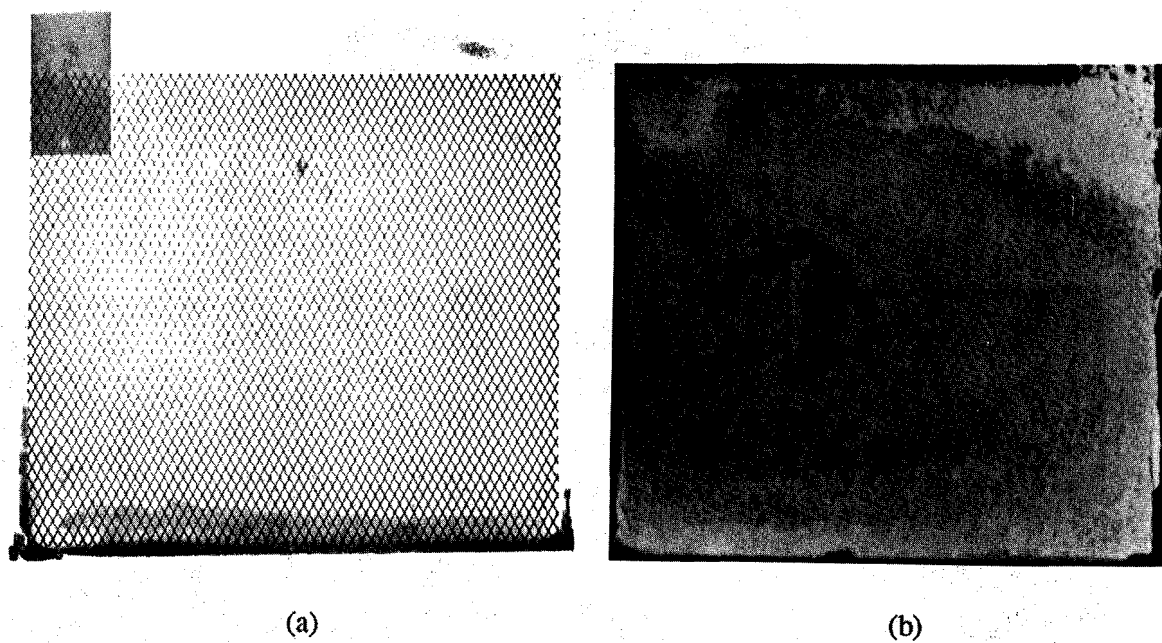
XBB 8910-8963

Figure 30. Electrode 25Ca2 (25 mol% Ca(OH)$_2$) after testing was terminated at cycle 151.
(a) X-ray
(b) Photograph
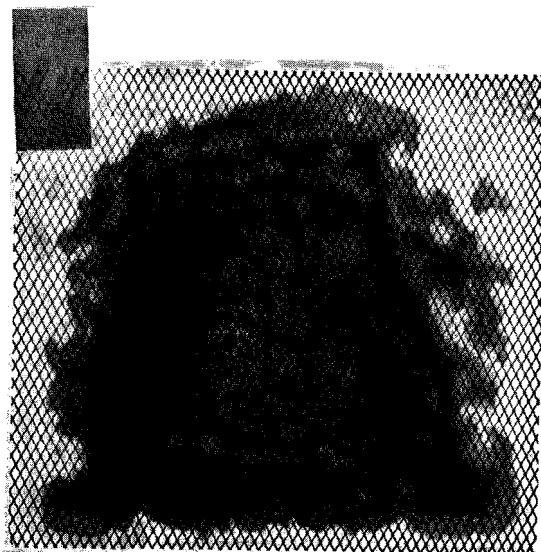
(a)
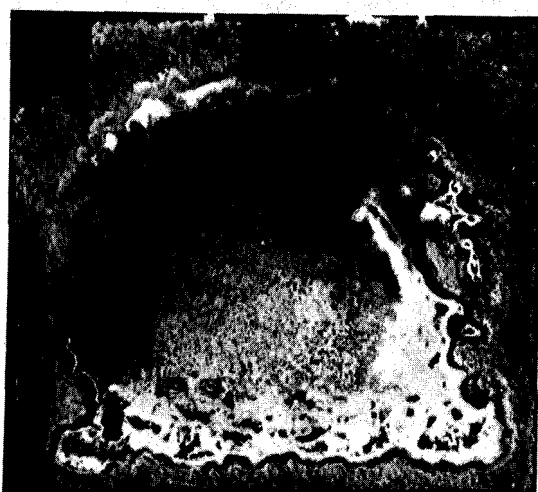
(b)
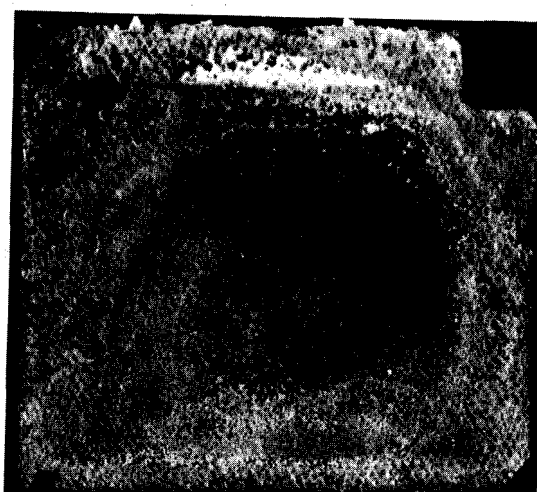
(b)

XBB 8910-8964

Figure 31. Electrode 10Ca3 (10 mol% $Ca(OH)_2$) after testing was terminated at 103 cycles. Note that the Zn is moving toward the center in this electrode.
(a) X-ray
(b) Photograph

identification of whether an individual crystal or spot of powder was Zinc, Calcium, Potassium, or a mixture of these elements. Further analysis was carried out by X-ray powder diffraction. This method allowed determination of the chemical state of the elements, i.e., whether they were present as elements or compounds. For example, one could determine whether Zinc was as metallic Zn or as ZnO, or whether the calcium zincate complex in one area or electrode was the same as that in another.

Figure 32 is a map of a typical cycled zinc electrode. The micromorphology will be discussed in reference to the numbered areas on the map. The placement of the numbers on the map indicates the type of area being examined and not necessarily that the area under discussion is in exactly the same spot as the number. For example, area 4 represents typical islands and not just one island at that location. Area 1 is the growth off the current collector at the upper edge of the electrode. Area 2 is the semi-uniform region approaching the edges, between the center island regions and the growth at the edges. This area has more material than the center regions as was seen in the X-ray photographs. Area 3 is the center region between or away from the islands, and area 4 represents the islands. Area 5 is the dense growths (semi-dendritic) off the sides (not top) of the current collector.

For the pure Zn electrodes (Zn1 + Zn2), only the high-sealed electrode had any area 1 (growth off the top). This growth appeared to be clumps of Zinc powder with no crystalline structure or smooth surfaces. It was white in color indicating that it was ZnO and not grayish-black metallic Zn. Area 2 was again mostly powdered ZnO with varying porosity as seen in Figure 33, photographs A and B. The crystalline Zinc structure seen in photograph C was rarely found. Zinc does not appear to form crystals
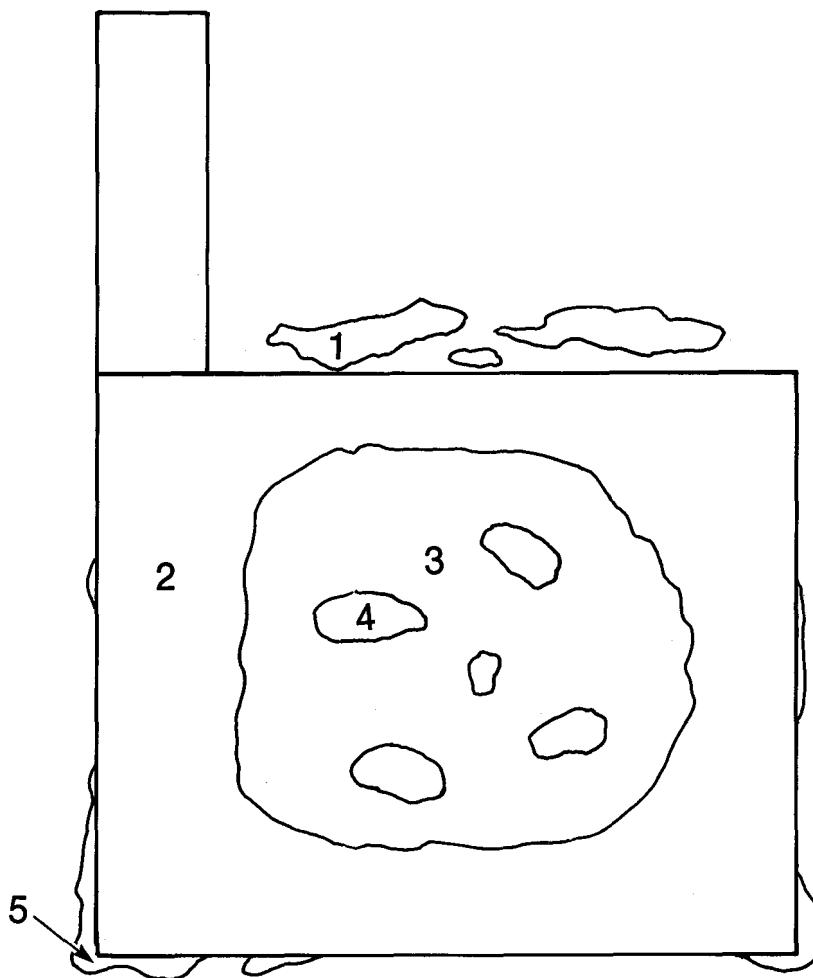
XBL 882-9530

Figure 32. Map of a typical cycled Zn electrode. The numbers identify various types of regions.

(1) Growth off the current collector at the upper edge of the electrode.

(2) Semi-uniform region near the edges - between island regions and the growth at the edges.

(3) Center region between islands.

(4) Island areas.

(5) Dense growth off the sides (not the top) of the current collector.

readily in the electrodes. Area 3 was mainly bare current collector with slight residual Zinc. Area 4 was stiffer than areas 1 and 2 and separated from the electrode in one piece. This area was overall very dense as can be seen in Figure 34 photograph A, but still had areas with porosity similar to that of area 2 - photograph B. Again, crystals were found, photograph C, but these were not very common and were only found at a small portion of the edge of the island. Area 5 was very hard and difficult to break into smaller pieces. The color was more grayish, indicating that some metallic Zn may be present, however, the oxide itself seemed to be bonded tightly. Figure 35, photograph A illustrates the typical structure. Here solid Zinc structures were also found, photograph B, but mainly (> 95%) the structure was closely-packed particles.

For the electrodes with 10 and 25% $Ca(OH)_2$, very interesting morphology was observed (10Ca3 will be discussed later in this section). As all these cells are similar in structure, they will be discussed as a group, pointing out differences between the 10 and 25% when appropriate. Area 1 was mainly ZnO powder as can be seen in Figure 36 photographs A and B. This indicates that the movement of material to the top is not caused by pressure forcing the material up. If this was the case, the material at the top should be representative of the electrode composition instead of being almost completely Zn/ZnO. However, in the portions of this growth closer to the electrode, see photograph C, some crystals were found. These crystals were found to contain both Calcium and Zinc by EDS, and by powder X-ray it was found that the crystals were indeed the calcium zincate complex. The fact that these crystals are larger than the crystals typically found in the body of the electrode (shown in the following figures) further indicates that the surface pressure on the electrodes alone cannot be the cause of the movement. It seems more likely that occasionally small particles of $Ca(OH)_2$ or
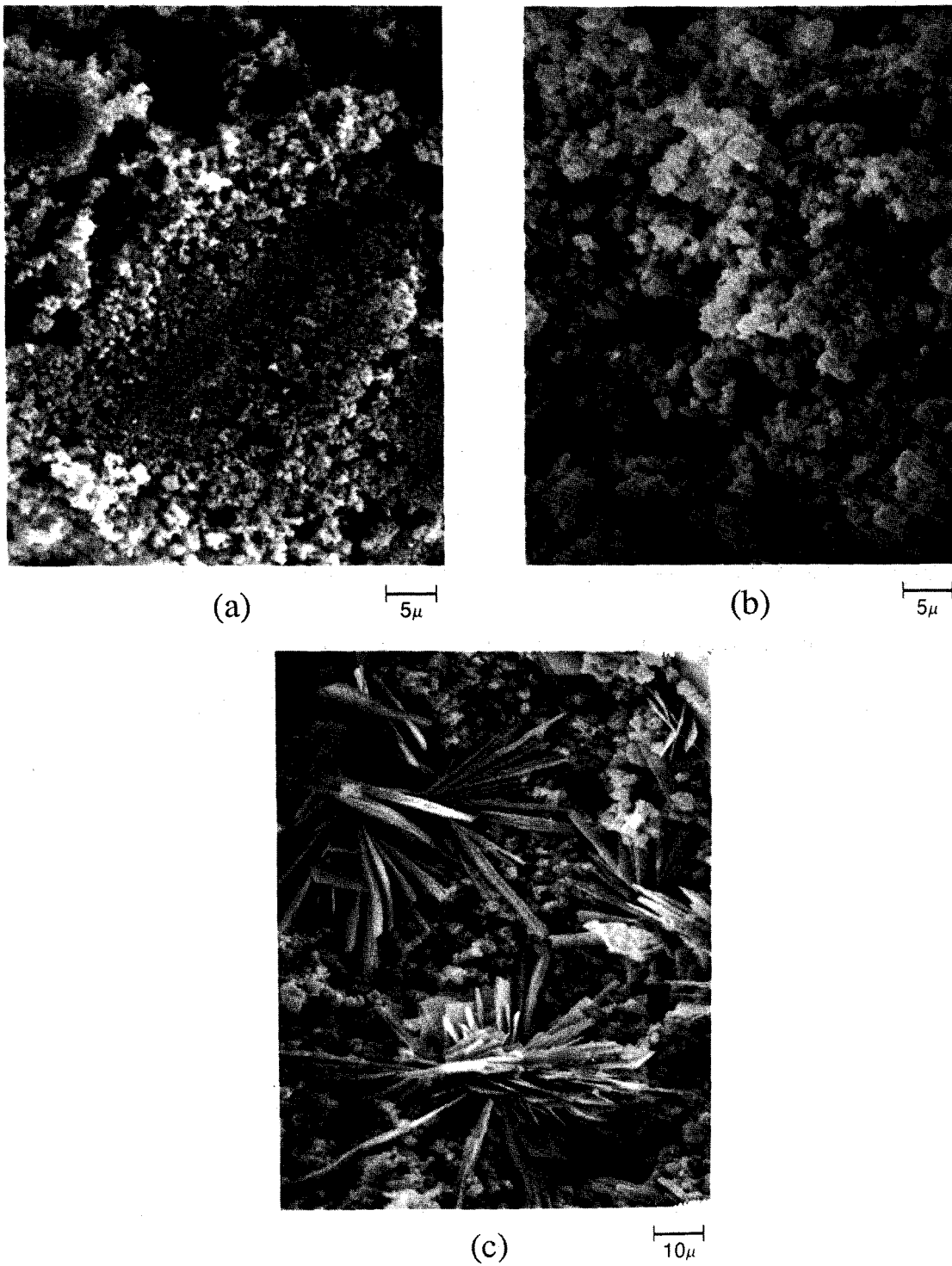
XBB 8910-8985

Figure 33. Morphology of area 2 in 100% Zn electrodes.
(a & b) Typical structure - porous powder.
(c) Zinc crystalline structure (rarely seen).

(a)

10μ

(b)

5μ

(c)

7μ
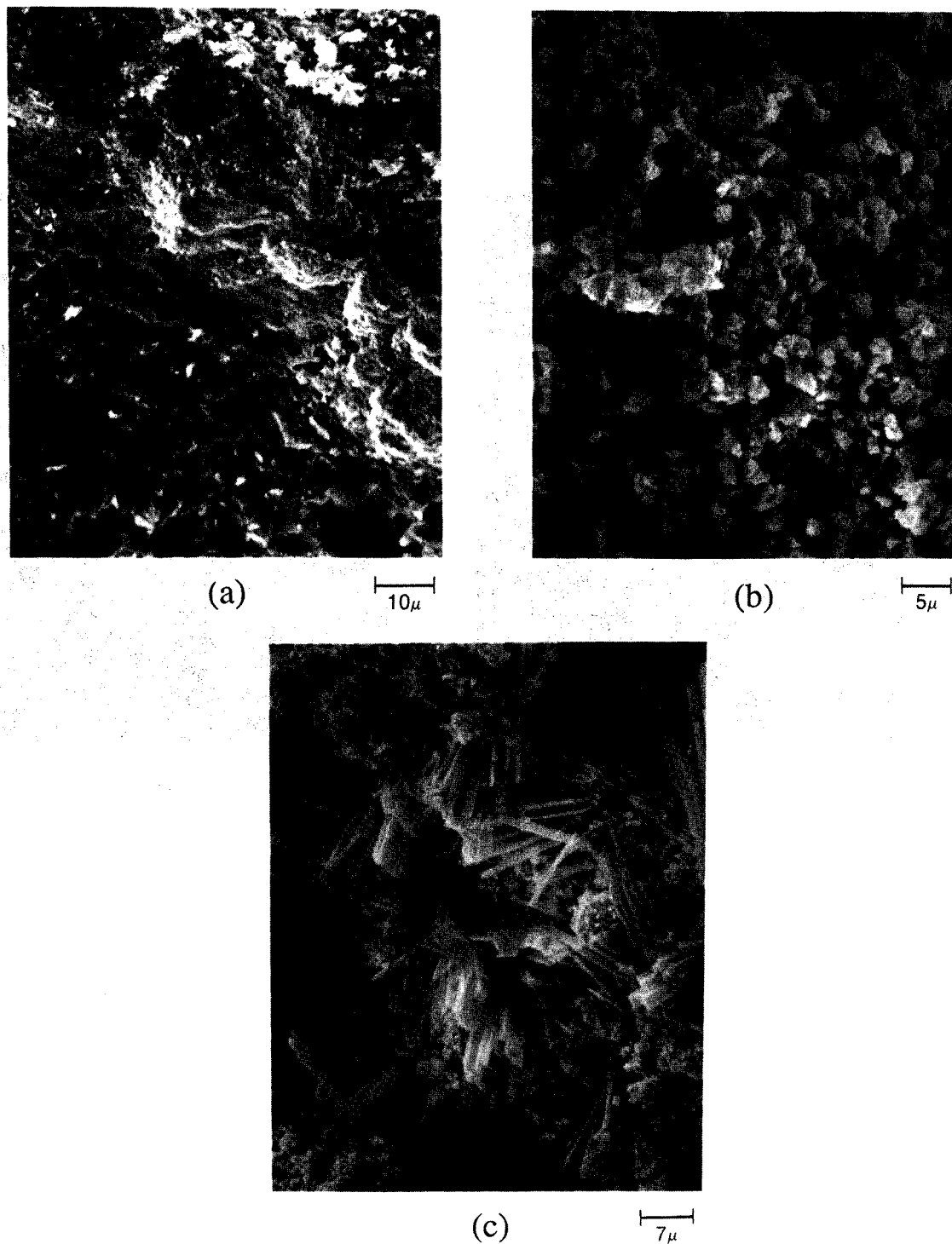
XBB 8910-8986

Figure 34. Morphology of area 4 in 100% Zn electrodes.
(a) Dense region of island.
(b) Powdery porous region.
(c) Zinc crystalline structure (uncommon).

(a) 5μ

(b) 10μ
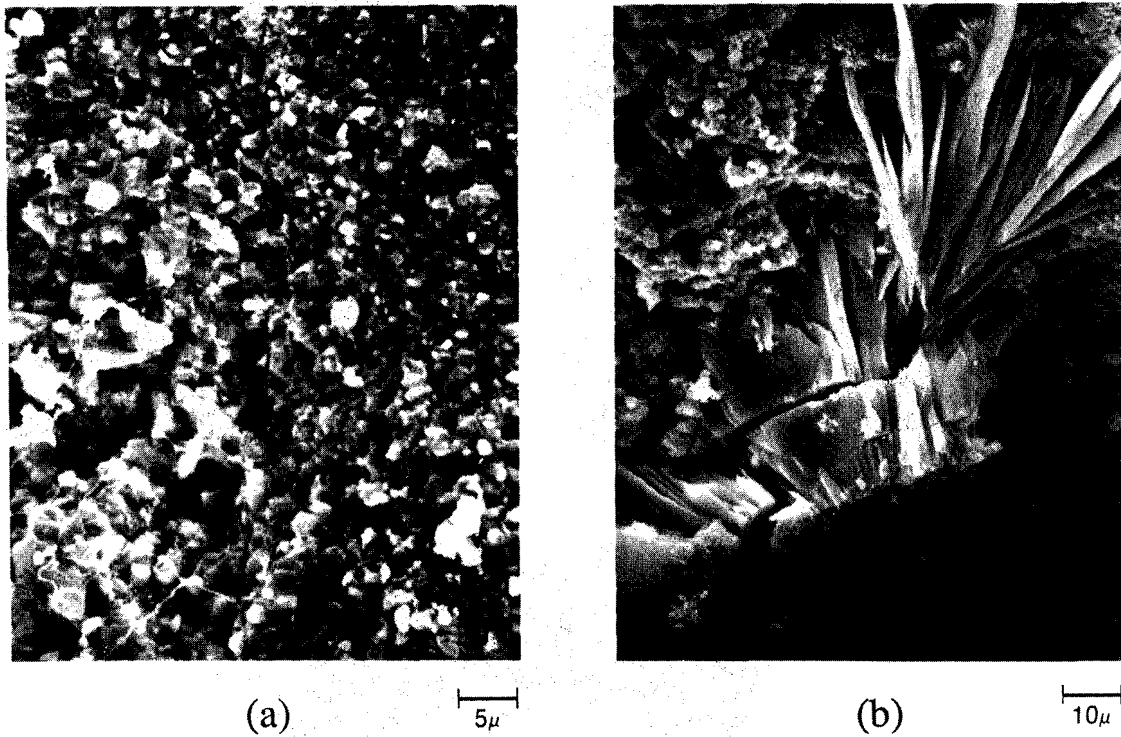
XBB 8910-8993

Figure 35. Morphology of area 5 in 100% Zn electrodes.
(a) Closely packed particles.
(b) Solid Zinc structures (uncommon).

calcium zincate are swept up by the convective flow and combine with the nodules leading to the larger crystals. On these cells, a vacuum was occasionally applied to remove air, and this may also have caused the movement of some Ca-containing material. Also, even though $Ca(OH)_2$ is only very slightly soluble in KOH, some $Ca(OH)_2$ may have diffused to area 1.

Area 2 mainly consists of crystalline calcium zincate with varying amounts of Zinc packed around the crystals. This can be seen in photographs A-C in Figure 37. The amount of Zinc increases from the center of the electrode toward its edges. All of the Calcium was found to be as calcium zincate and was almost always in a crystalline or solid form. The 25% $Ca(OH)_2$ electrodes contained very little of area 2 compared to that of the 10% electrodes. However, even the 10% cells also did not have much of area 2, as most of the uncomplexed Zinc had moved to the edges.

Area 3 was almost all crystalline as can be seen in Figure 38. Very little excess Zinc was found, and all of the Calcium was present as complex. In photograph B, the PTFE which binds the electrode together can easily be seen. For the 25% $Ca(OH)_2$ electrodes, area 3 made up the majority of the surface. This structure was found every-where in the working area of all the Calcium electrodes, with no bare current collector spots anywhere. The morphology seen in photograph C is typical of this region, but the other structures are common also. In photograph D, the diamond-type structure of the crystals is apparent. Very few hexagonal crystals were seen in the electrodes.

Area 4, the islands, consisted of a calcium zincate layer of the normal thickness attached to the current collector. On top of this was an island of Zinc. The two areas are very distinct and separate as can be seen in Figure 39. There were no real islands on

(a)

10μ

(b)

5μ

(c)

20μ
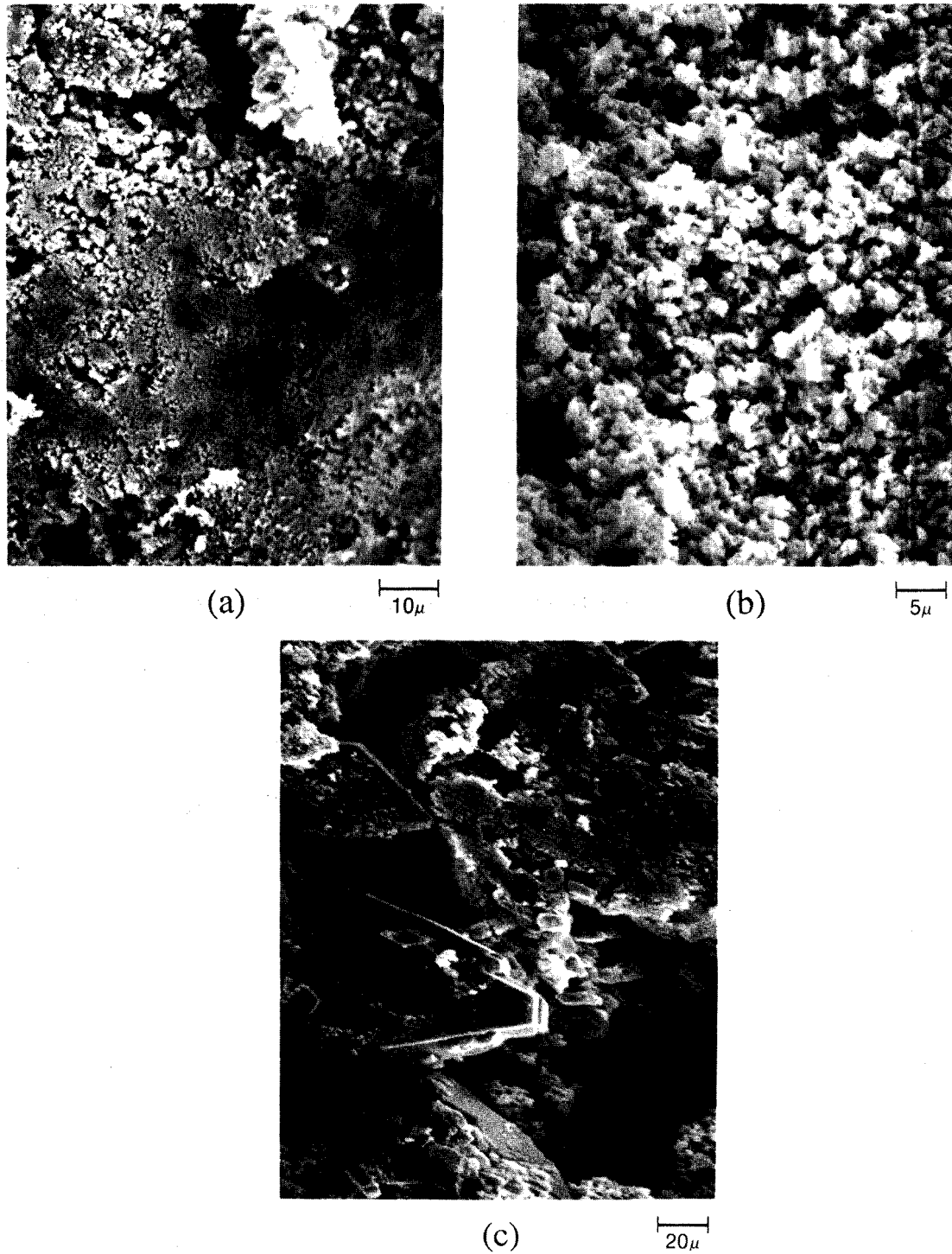
XBB 8910-8988

Figure 36. Morphology of area 1 in zinc electrodes with $Ca(OH)_2$.

(a) Dense Zn/ZnO powder.

(b) Zn/ZnO powder.

(c) Calcium zincate crystals - found closer to the zinc electrode.

(a) 40μ

(b) 17μ

(c) 17μ
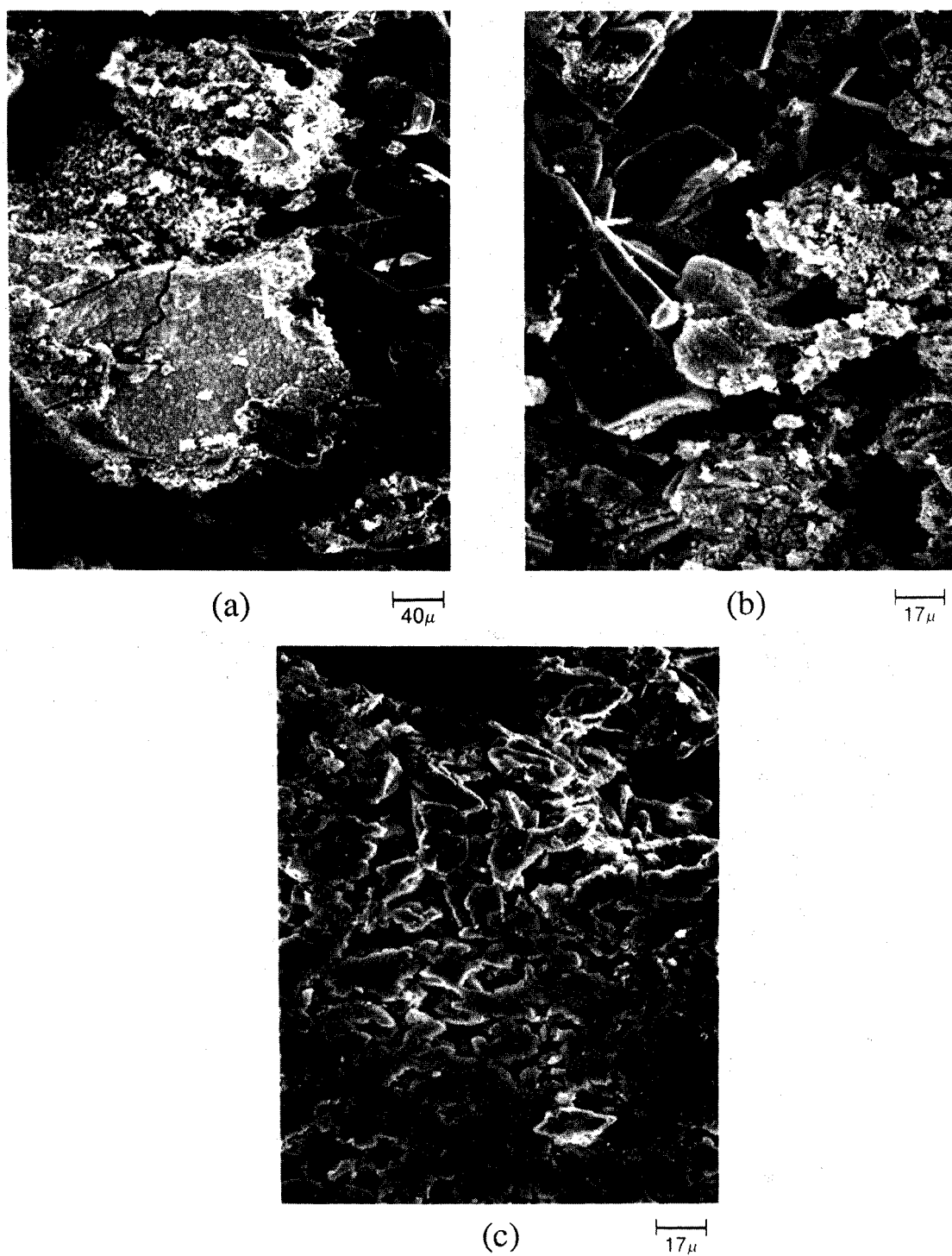
Figure 37. Morphology of area 2 in zinc electrodes with $Ca(OH)_2$.
(a - c) Calcium zincate crystals surrounded by Zinc powder.

(a)   13μ

(b)   20μ

(c)   17μ

(d)   5μ
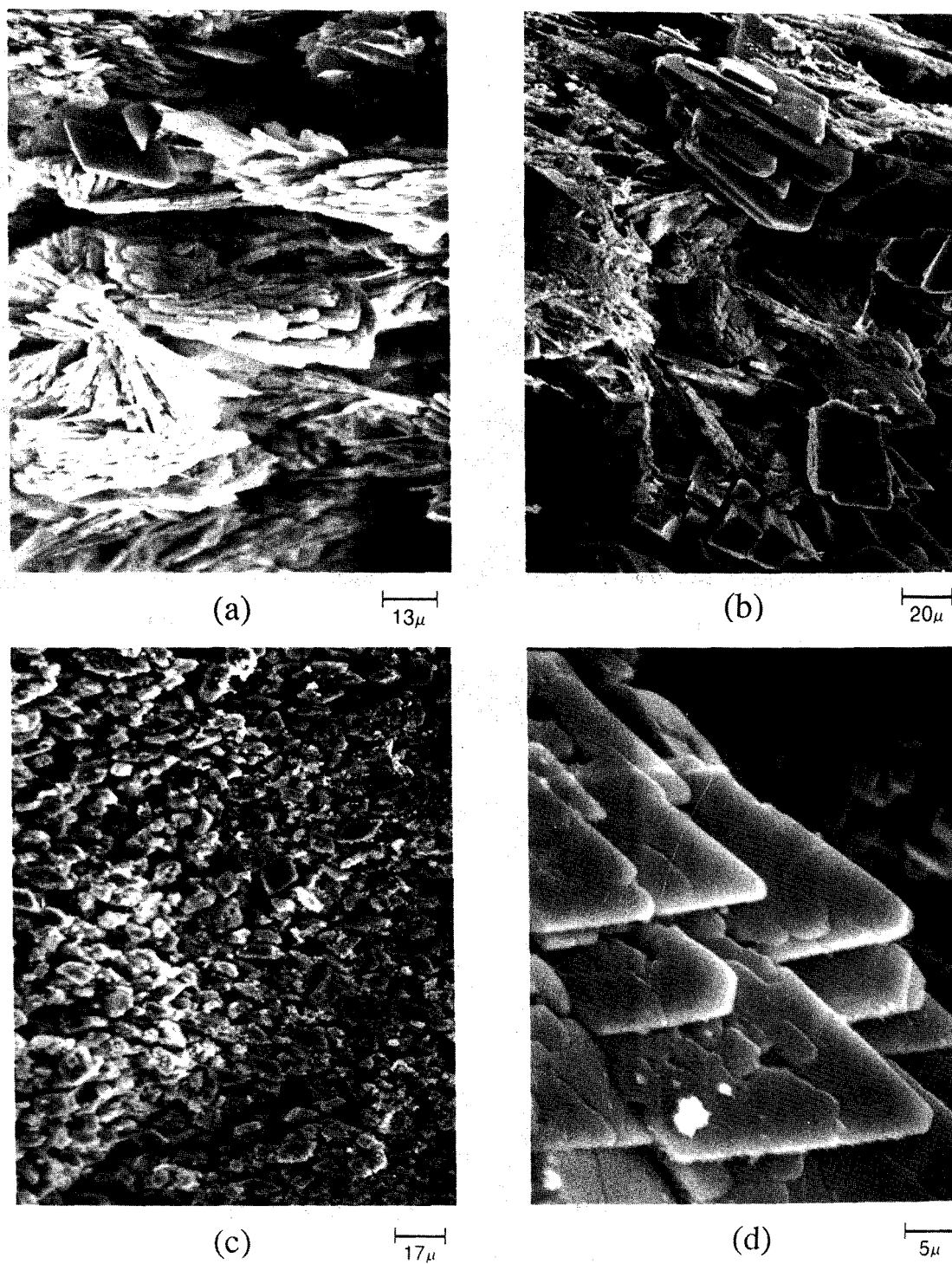
XBB-8910-8989

Figure 38. Morphology of area 3 in zinc electrodes with $Ca(OH)_2$.
(a, c & d) Calcium zincate crystals are found everywhere with very little powder present.
(b) PTFE filaments can be seen binding the crystals together.

the 25% $Ca(OH)_2$ cells and thus the area 4 discussion only pertains to the 10% cells. The island-type region at the bottom of 25Ca2 is taken to be edge growth and was not considered to represent islands. In photograph A, one area is crystalline complex, while the other area is dense ZnO powder. The gap between the two was introduced when preparing the sample. In photograph B the large triangle shaped area is dense powdered Zn/ZnO. On one side of the Zinc area are large complex crystals and on the other side are small complex crystals. The ledge area separating the complex from the Zinc appeared to be PTFE as EDS was unable to identify any elements. Photograph C of Figure 39 shows the typical Zinc area. As can be seen, this area is much more dense than the normal ZnO powder seen elsewhere. The islands differ from area 2 in that in area 2 there was still excess Zinc (excess in the amount required to make the complex - not in the amount required for cycling) with the crystals. In area 2 not all the excess Zinc had moved away to the edges, so there was still Zinc interdispersed with the crystals. In the islands, however, there is no excess Zinc mixed in with the crystals. The Zinc for some reason coagulated at the surface and formed islands, while the surrounding excess Zinc migrated away. With further cycling these islands would become smaller or slowly drift toward the edges. The migrating Zinc then may create new islands closer to the edge. This process was illustrated in Section 4.3 with the X-ray photos (Figures 24-27). The island regions will also be discussed in Section 4.6.

Area 5 of the 10 and 25% $Ca(OH)_2$ electrodes consisted of dense Zn/ZnO powder. Only where there was current collector was any calcium zincate found. Otherwise, this region consisted only of the migrated Zinc which had become very dense and occasionally produced dendrites. The pressure of this growing Zinc at the edges of the electrode

(a)

50μ

(b)

50μ

(c)

17μ
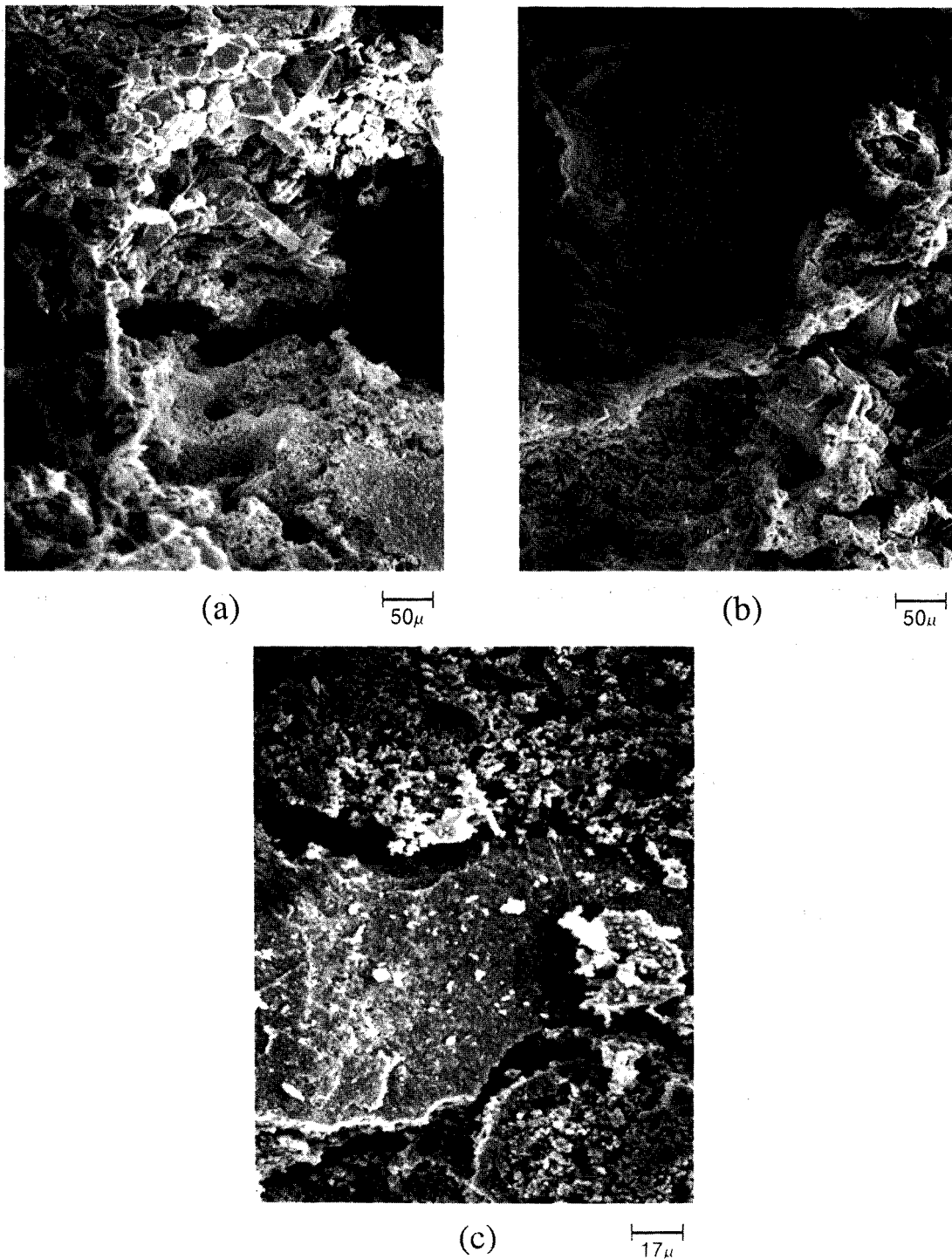
XBB 8910-8990

Figure 39. Morphology of area 4 (islands) in zinc electrodes with $Ca(OH)_2$.

(a - b) Clear distinction between the zinc and calcium zincate areas is seen. Area with crystals is where calcium zincate is found.

(c) Typical Zinc area of island - dense.

against the separator may have caused the tight packing of the Zinc particles. Photographs A-C in Figure 40 show this area. Photograph A shows a sample of this edge growth that was pried away from the electrode. As can be seen the Zinc is very tightly packed and because this area is darker than the rest of the electrode, it probably contains a significant amount of metallic Zn. Photographs B and C show closeup views of various regions in area 5, whereas photograph B represents a more typical appearance. The smoothness of the surface in photograph C probably means that the region being examined is metallic Zn. There was much more growth at the edges of the 10% $Ca(OH)_2$ cells than in the 25% cells. This also follows from the fact that there was more Zinc available for migration in the 10% $Ca(OH)_2$ cells.

Other areas of the cell investigated included the separator, the nylon wicks, and NiOOH electrodes. Both the separator and the nylon wicks had large crystals of the complex adhering to them. The photograph in Figure 41 shows some of the crystals on the nylon wick. These crystals are very large compared to those found in the electrode. Also, some of these crystals exhibit a more hexagonal shape than those found in the electrode. Only Calcium and Zinc are found in the crystals in the nylon wick and an analysis of the noncrystalline area of the wicks reveals only potassium from the electrolyte. In addition, no calcium zincate crystals were found on the NiOOH electrodes by SEM, while EDS analysis indicated that there was significant Zinc (15-25 at%) in the electrode but no Calcium. Chemical analysis showed there was 0.015 g $Ca(OH)_2$ (0.2 wt%). This seems to indicate that the Calcium must have migrated both as larger particles, either of $Ca(OH)_2$ or calcium zincate, and as either very tiny particles or dissolved in solution. The solubility of $Ca(OH)_2$ was found to be roughly 7 micrograms/ml in the

(a)   200µ

(b)   5µ

(c)   2µ
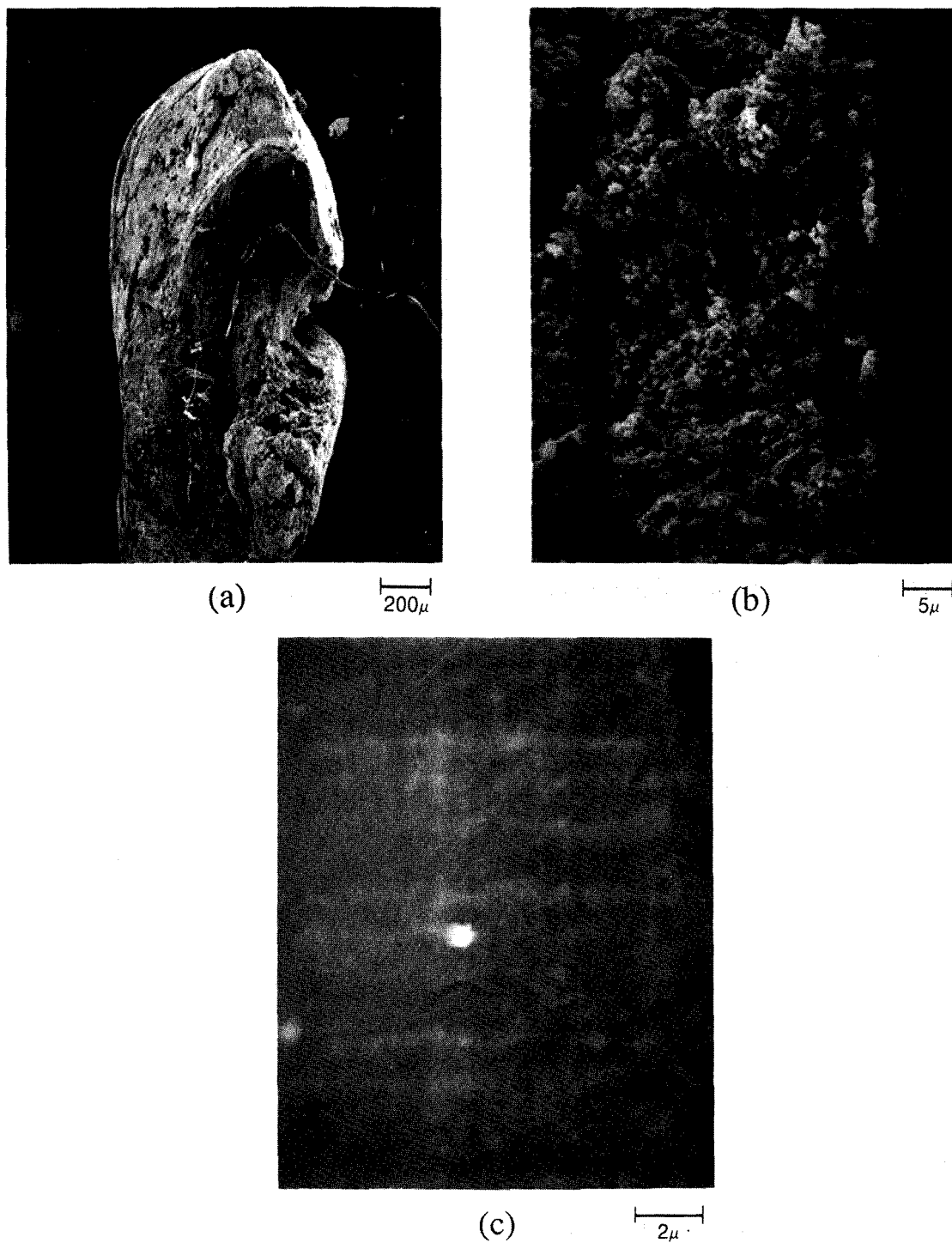
XBB 8910-8991

Figure 40. Morphology of area 5 in zinc electrodes with $Ca(OH)_2$.

(a) A sample of edge growth - all Zinc.

(b) Typical dense Zinc structure.

(c) Area with very dense Zinc.

electrolyte. The migration of Calcium would most likely have been caused by electrolyte convection, with the particles escaping through the top unsealed tab area of the electrode and then being filtered by the nylon wick before reaching the NiOOH electrode. As there is normally no electrolyte at the level of the opening of the separator, the particles could have been entrained in gas bubbles rising to the liquid surface and then followed the bubbles out through the separator opening when a vacuum was applied. Extremely tiny particles could have traveled through the microporous holes in the separator, but this route is unlikely.

Once the particles were near the nylon wick, they were no longer in a solution as highly supersaturated as that which is expected to occur at the zinc electrode during discharge. As was discussed in the chapter on synthesis of the complex, the diamond-shaped crystals were prevalent when created from supersaturated solution and the hexagonal crystals only appeared after prolonged time in a saturated or slightly supersaturated solution. Thus, perhaps the migrating crystals were diamond shaped and then slowly transformed to hexagonal-shaped ones. The large size of the crystals could be the result of growth made possible by lack of contact with the cycling electrode. As these crystals are no longer in contact with the electrode, they are not subject to being destroyed and recreated every cycle. Thus, they were able to grow by combining with the tiny crystals or the minute amount of dissolved $Ca(OH)_2$. The small amount of Calcium in the NiOOH electrode must have resulted from either these tiny crystals becoming trapped in the NiOOH electrode, $Ca(OH)_2$ combining with ZnO in the NiOOH electrode, or $Ca(OH)_2$ precipitation. The Zinc in the NiOOH electrode will be discussed in the following sections and will be the topic of Section 4.7.

400μ
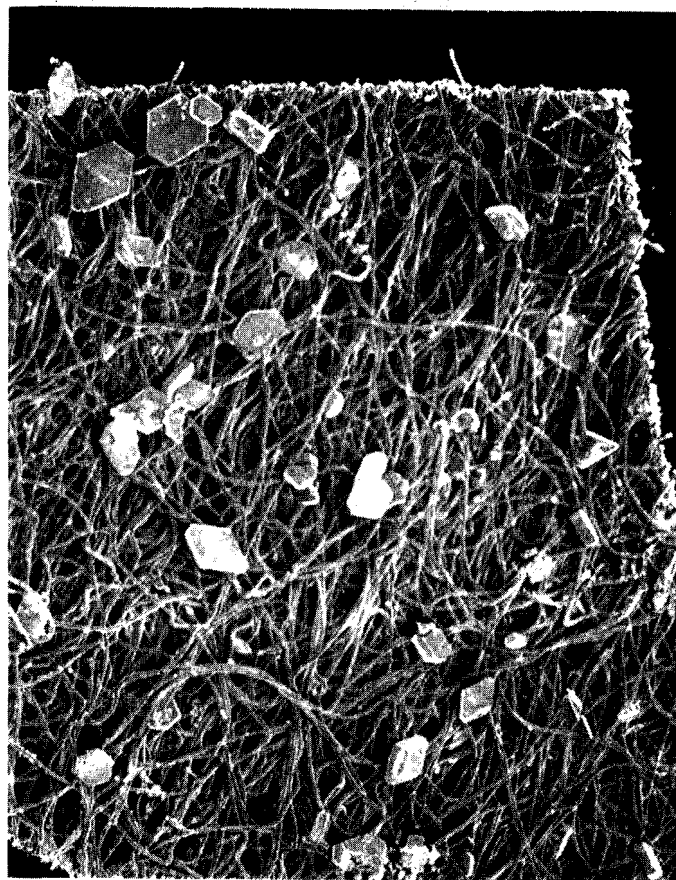
XBB 8910-8965

Figure 41. Crystals of calcium zincate adhering to a nylon wick.

The two 40% Ca(OH)$_2$ electrodes which shorted after only three or four cycles (including formation cycles), were also examined. These electrodes had more Calcium than that required to form a complex with all the Zinc present. Figure 42 shows photographs of the resulting morphology. Throughout the electrode complex and excess Ca(OH)$_2$ are present. In one electrode, the excess Calcium tended to form ball-shaped structures as seen in photograph B. This electrode was discharged to 0.1 V (vs Hg/HgO) and allowed to stand for more than a week before disassembly. Photograph C is typical of the second 40% electrode. There is no uncomplexed Zinc except in areas where the Zinc was present as metallic Zn. Photograph A shows an area where the Calcium concentration is changing from just enough to make the complex to having a considerable excess of Ca(OH)$_2$. In the one 40% Ca(OH)$_2$ electrode, complex is almost always present underneath the excess Ca(OH)$_2$ and not vice-versa. Also, as the excess Ca(OH)$_2$ in this electrode often appears in a fluffy to crystalline ball shape, it further indicated that Ca(OH)$_2$ itself will dissolve to make these shapes. These ball shapes may also be the result of the Zinc leaving a particular crystal and moving to adjacent areas of excess Ca(OH)$_2$ during a cycle. All cells described so far were disassembled in a completely discharged state, and except for the two 40% Ca(OH)$_2$ cells, they had no excess Ca(OH)$_2$. Thus, this ball shape could be common in a charged 10% or 25% cell also, as in a charged cell uncomplexed Ca(OH)$_2$ should be present.

To investigate electrode morphology in the charged state, the 10% Ca(OH)$_2$ electrode, 10Ca3, which was also used to test the NiOOH electrodes, was dismantled in the charged state. The X-ray of this electrode is shown in Section 4.3, Figure 31. Due to the cycling conditions, the Zinc migrated from the edges toward the center of the

(a)   20μ

(b)   5μ

(c)   17μ

(d)   14μ
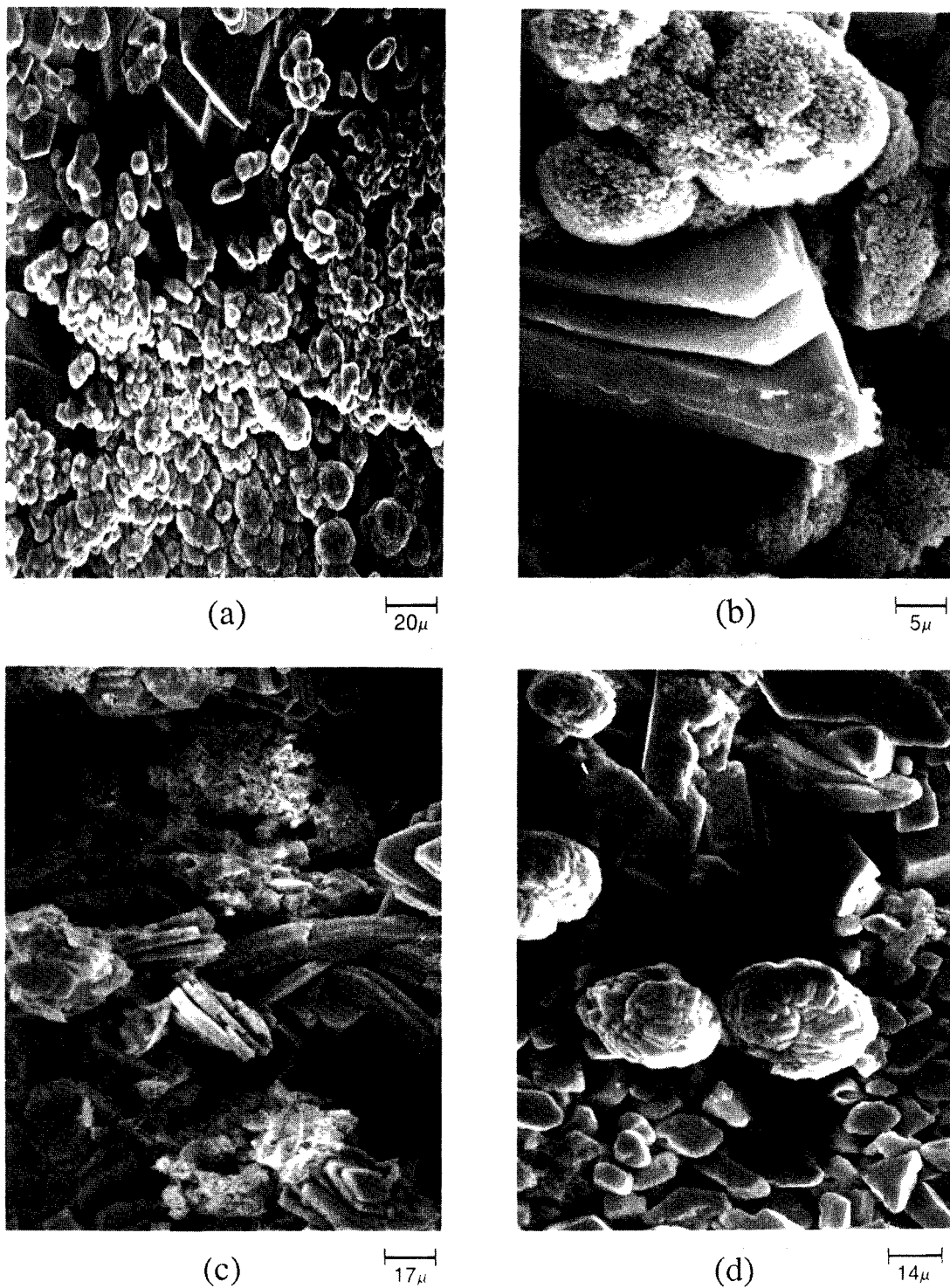
XBB 8910-8992

Figure 42. Morphology found in 40% Ca(OH)$_2$ electrodes after a few cycles.
(a - d) Crystals are calcium zincate whereas powders and ball-shaped structures are calcium hydroxide.

electrode. However, the direction of the migration is not significant when discussing the differences between this cell and the ones disassembled in the fully discharged state. Unlike the other cells, in this electrode there was a considerable amount of uncomplexed $Ca(OH)_2$. In the areas near the edges, very little Zinc was left. The main material found was Calcium, along with some lead. This can be seen in Figure 43, photograph A, which is typical of the area. EDS analysis showed that this area is almost all Calcium and powder X-ray diffraction indicated that the Calcium is present mainly as $Ca(OH)_2$. It also showed that no complex and very little Zn and ZnO were present. Photograph B is also of the same type area, but it shows a region where there was some Zinc. The powder is the Zinc, and the crystal is Calcium (probably $Ca(OH)_2$) with no complex visible. The observed lack of complex is probably a result of the Zinc being present as metallic Zn, at least up to the point of disassembly of the cell, and thus it could not combine with the Calcium to form the complex. The isolation of the $Ca(OH)_2$ from the Zinc at the edges of this cell implies that considerable Zinc migration must occur during single charge and discharge half-cycles (as Calcium is only seen as complex in the discharged cells). This will be discussed further in Section 4.6. Although many of the $Ca(OH)_2$ crystals appear hexagonal in shape, they are found by chemical analysis and by powder X-ray diffraction to be very different from the hexagonal complex crystals.

The center region of the electrode, however, is quite different. The material here is very darkly colored on the surface, indicating metallic Zn. Also, the material was very hard and difficult to scrape. Microanalysis found that the top layer of the electrode was indeed all Zinc and densely packed. Powder X-ray analysis showed that the Zinc was
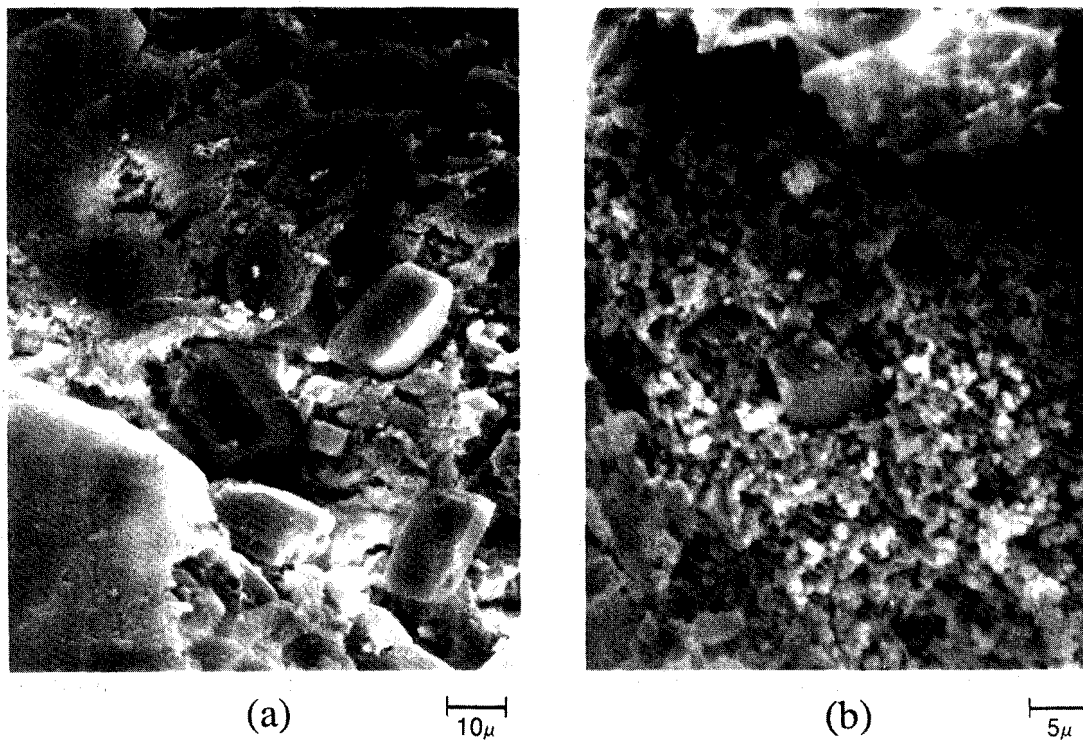
XBB 8910-8994

Figure 43. Morphology near the edge of the 10Ca3 (10 mol% $Ca(OH)_2$) electrode when disassembled in the charged state.

(a) $Ca(OH)_2$ crystals and powder - no Zinc.

(b) Calcium crystal surrounded by Zinc powder - no complex (very little of this is found).

almost all metallic and that no $Ca(OH)_2$ or complex was present. This can be seen in photograph A in Figure 44. However, close to the current collector the morphology is like that shown in photograph B. In this area there is a significant amount of complex and metallic Zn. Powder X-ray studies show little or no $Ca(OH)_2$ and some ZnO. So, the area to which the Zinc migrated consists of a layer of calcium zincate crystals with a top layer of metallic Zn. A discussion of the consequences of this structure as related to complex formation and cycling will be presented in Section 4.6.

In comparing this electrode to the 40% $Ca(OH)_2$ electrodes, the ball-type Calcium structures seen in the 40% electrodes (Figure 42 photograph B) are not observed here. This implies that the particular ball shapes may indeed have been the result of the lower voltage the 40% cells were allowed to reach in their last discharge half-cycle or the extended time before their disassembly. The ball-shaped structures may also only be present in the 40% $Ca(OH)_2$ cells because these cells had excess $Ca(OH)_2$ present at all states of charge, while this was not the case in the other $Ca(OH)_2$ cells.

A few of the powder X-ray diffraction patterns are seen in Figure 45. While comparing relative peak height is useful, it must be noted that different height ratios can result from variable particle sizes or partial aligning of the crystals during sample preparation.

4.5. Chemical Analysis

4.5.1. Analysis Technique

Whereas the EDS on the SEM was able to give some quantitative chemical compositions, the uncertainties when using EDS on a powdery material are large. Also,

(a)   5μ

(b)   30μ
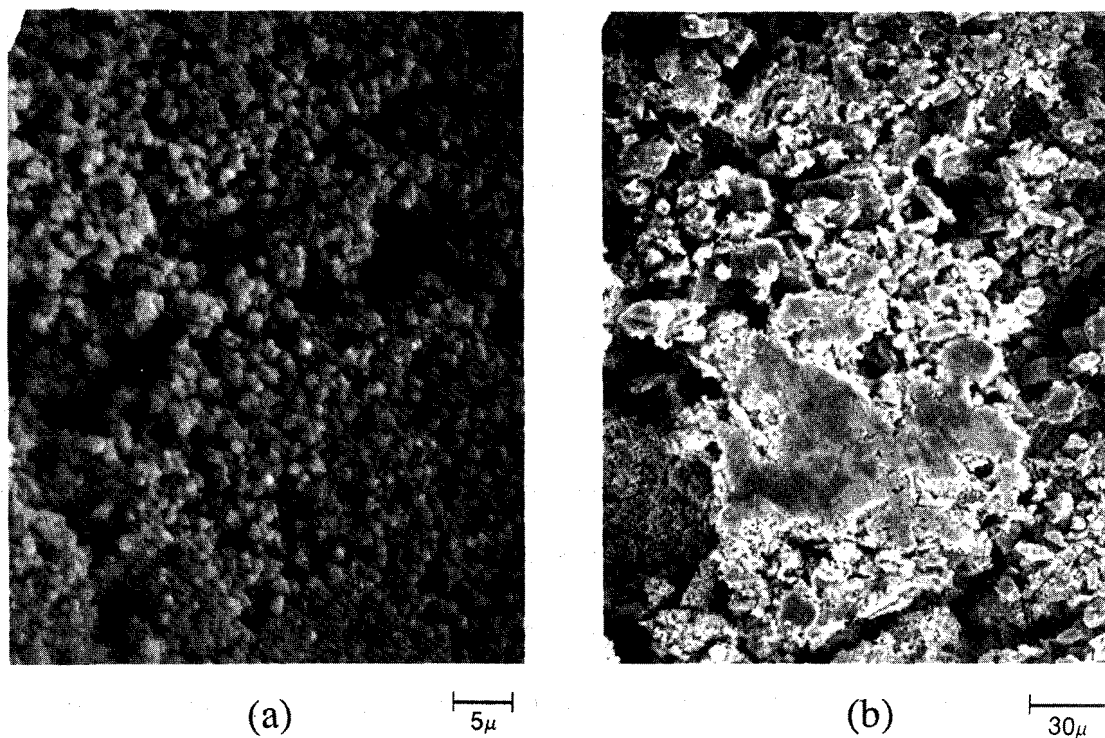
XBB 8910-8995

Figure 44. Morphology in the center region of 10Ca3 (10 mol% Ca(OH)$_2$) in the charged state.
(a) Typical of this region near the surface - densely packed Zinc particles with no Calcium.
(b) Close to the current collector, complex is found with metallic Zn.
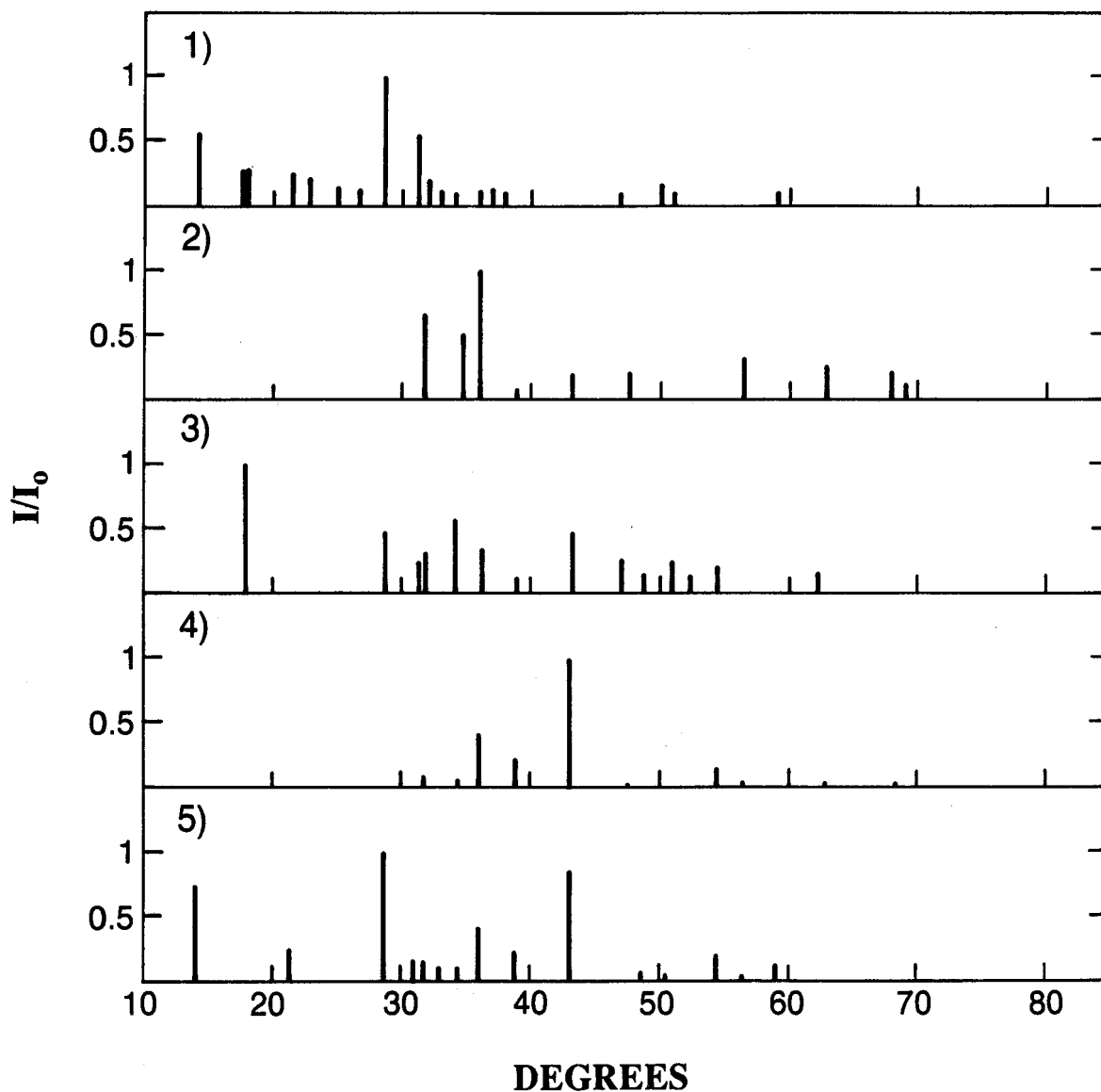
Figure 45. Powder X-ray diffraction patterns of various areas in the electrodes.

(1) Taken from Cell 25Ca2, area 3. Shows mainly calcium zincate.

(2) Taken from Cell 25Ca2, area 5. Shows no calcium zincate. Mainly ZnO.

(3) Taken from Cell 10Ca3, near the sides. Shows $Ca(OH)_2$ and Zn metal, but no calcium zincate.

(4) Taken from Cell 10Ca3, near the center but at the surface. Shows metallic Zn.

(5) Taken from Cell 10Ca3, near the center but in the interior near the current collector. Shows calcium zincate and metallic Zn.

XBL 882-9531

although the SEM was able to tell us that there was a complex layer present over the entire electrode, it is not capable of determining the uniformity by weight of that layer. For these reasons and the desire to perform a chemical balance from the virgin to the final cycled electrode, detailed elemental chemical analyses were performed.

The two elemental analysis techniques investigated included atomic absorption spectroscopy (AAS) and X-ray fluorescence. As mentioned in Section 3.7, technical problems, as well as the expense, of the X-ray fluorescence equipment prevented its intensive use. Thus all the chemical analysis results were obtained by AAS. Normally AAS results can be expected to be accurate within 2% for the equipment being used. Analysis of the same sample over a period of a month found the repeatability to be within 5%. However, due to some unexpected interference between Ca and Zn, the Ca results are only accurate to within 10%. Usually when Zinc was present the Calcium results were artificially low.

4.5.2. Uniformity of Calcium Zincate

The uniformity of the complex layer is important to investigate in order to insure that the Calcium itself is not slowly migrating. Also, it was desirable to help confirm that all the Calcium was complexed in each area of the electrode. While elemental analysis cannot confirm the presence of complex, it can confirm whether or not there was enough Zinc to complex with all the Calcium present.

To determine the degree of uniformity, samples of 39.5 mm^2 area were punched from various parts of the electrodes. A representative electrode is shown in Figure 46. The area of the punch was found to be consistent to within 2% on metal sheets, and it was estimated to be at worst within 10% on actual electrodes. Each punched sample

was also weighed, and at least 2 representative samples from each Ca-containing electrode were chemically analyzed. The primary investigation of uniformity was performed on electrode 25Ca1, with eight punched samples being analyzed.

The analysis showed that the amount of Calcium varied less than 8% over the face of the electrode, and that any weight differences between regions were due to variations in the amount of Zinc. While the variation in the Calcium content is within the experimental error, if the variation is real, it may only be due to a slightly nonuniform mass distribution in the initial electrode. The punches taken near the center were found to have (within 8%) the expected ratio of Zn to Ca for the complex, and thus verified that this area most likely contained only the complex. The samples near the edges had the same amount of Calcium but had more Zinc, which was also expected. In addition, the composition found in the center regions of this cell agree with the amount found in the other 25% cell (only the center was investigated in 25Ca2). The same result was found with the two 10% cells. All of these results agree with the results from the X-ray, SEM, EDS, and powder X-ray analyses described earlier.

There is a small disagreement, however, when the amount of $Ca(OH)_2$ complexed is determined. By the other techniques, no uncomplexed Calcium was observed, but, by chemical analysis there is some indication that the center areas may be up to 8% low in Zinc. Also, if uniformity over the electrode is assumed for PTFE, Cu, and Pb, the weight of the punches from the central regions are up to 10% low, assuming all the Calcium was complexed. While this is within the uncertainty in the measurements and assumptions, the fact that both results point to a slight amount of uncomplexed Calcium in the center of the electrode, leads to the possibility that it may be true. In addition, the
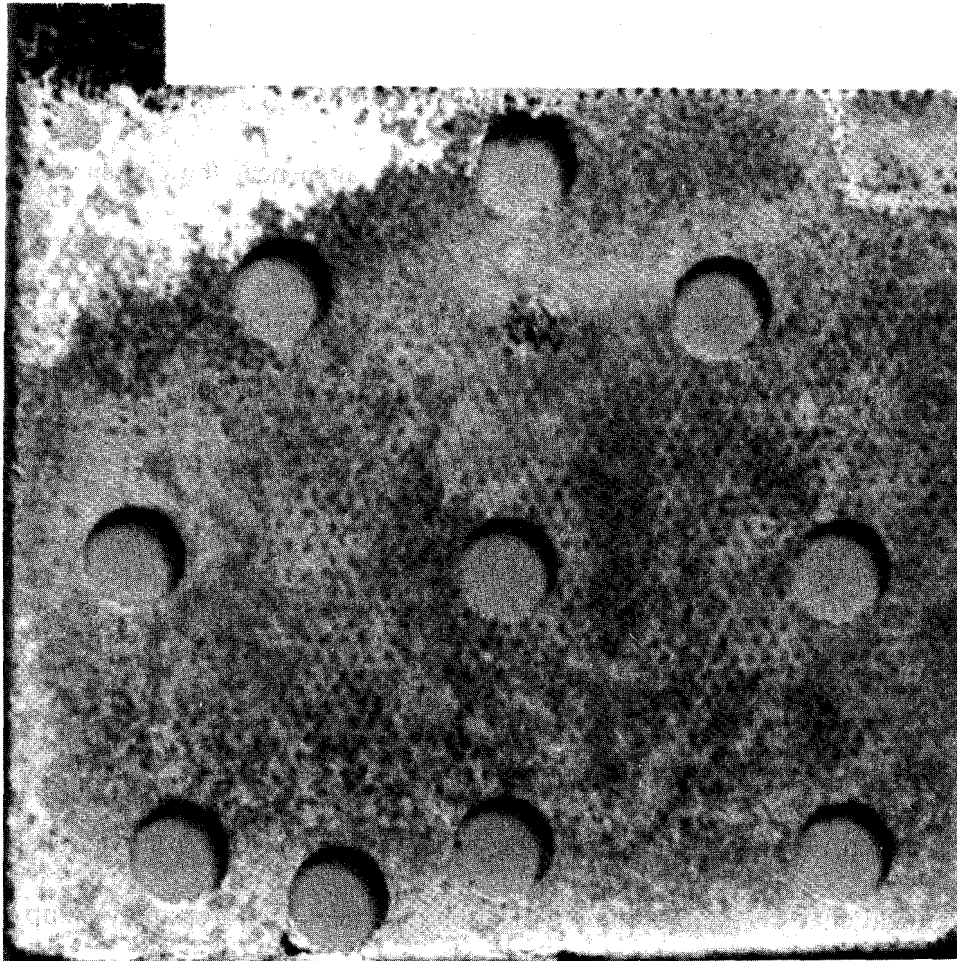
XBB 8910-8952

Figure 46. Photograph of a representative electrode showing the areas where samples were removed for examining uniformity.

analysis of the overall composition of the body of the electrode (after trimming the side growth and an additional 1 mm from each side), shows that there is barely enough Zinc left to complex with the Calcium in the electrode. Yet it was found by both EDS and chemical analysis that there was excess Zinc toward the edges. This also indicates that the center may be slightly depleted in Zinc. It must be remembered, however, that the SEM observation and EDS analysis never found any uncomplexed Calcium, and that the missing 5 to 8% Zinc is within the uncertainty of the AAS, even without allowance for any sample preparation error. Furthermore, any conclusions drawn from observing weights assume that the complex is indeed of the exact stoichiometry (including waters of hydration) obtained from literature ($CaZn_2(OH)_6 \cdot 2H_2O$).[16-18] The consequences of this (possible) depletion of Zinc are discussed in Section 4.6.

4.5.3. Material Balances

In addition to the uniformity of the electrode, it was desired to perform a full material balance on the cell. A material balance would show if the electrode had lost or gained any material and from or to where this material was transported. A material balance was felt to be especially necessary because the results of James Nichols indicate that the zinc electrode loses from 0.8 to almost 2 g of Zn during cycling.[5] Also, it was desired to see if any Calcium had migrated to the other areas of the cell or into the electrolyte.

Due to the number of analyses required for a complete balance, a full investigation was performed only on cell 25Ca1. For sample preparation the electrolyte was poured into a bottle and then the cell was disassembled with tissues being used to absorb the liquids from the electrodes, nylon wick, separator, and also to absorb any remaining

electrolyte. The tissues used to absorb the electrolyte from the zinc electrode, and the ones used for the two NiOOH electrodes were kept separate and the others were combined. Then, all materials were immersed in individual containers of 70% HNO_3 for a time sufficient to insure that all the non-organic material was dissolved. One NiOOH electrode, and its nylon wick and tissue were saved for future reference. It was assumed that the two NiOOH electrodes would have the same amount of material so the values obtained from the one were just doubled.

Table 5 shows the results of the analyses. The values for the initial ZnO and $Ca(OH)_2$ are also based on chemical analyses. As can be seen, the Zn balance closed to within 2%, which is well within experimental error. Since there are many approximations involved, along with the uncertainty in the measurements, the experimental error is expected to be up to 10%. For Zinc, the main possibility of error is introduced in assuming that the two NiOOH electrodes are identical. For Calcium the main error would be the AAS uncertainty. The Ca balance also closed to within 2%. However, the expected initial amount of $Ca(OH)_2$ was 1.4 g while by analysis it was found to be only 1.25 g. This means that either the analysis was inaccurate by 12%, or that the 25% $Ca(OH)_2$ electrodes are only 23% $Ca(OH)_2$. Most likely it was a combination of the two. The initial Zn analytical and expected values agree to within 1%. The lower than expected value for $Ca(OH)_2$ in the initial electrode could be because of a higher loss factor for the smaller $Ca(OH)_2$ particles when the electrode is fabricated (compared to ZnO particles) or perhaps some moisture in the source $Ca(OH)_2$. A quantitative examination for H_2O in the $Ca(OH)_2$ was performed well before electrode fabrication, but no moisture was found at the time.

TABLE 5 Mass Balance for Cell 25Ca1							
	Initial (g)				Final (g)		
	ZnO	Ca(OH)$_2$	KOH		ZnO	Ca(OH)$_2$	KOH
Liquid Electrolyte	.899	0	5.07		.233	.0003	1.144
Electrolyte Tissue	0	0	0		.395	.0262	1.571
Zinc Electrode Tissue	0	0	0		.204	.0184	.771
Ni Electrode Tissue (doubled)	0	0	0		.042	—	.551
Total Electrolyte	(.899)	(0)	(5.07)		(.874)	(.0449)	(4.037)
Separator	0	0	0		.117	.0177	.126
Nylon Wick (doubled)	0	0	0		.090	.0229	.109
Ni Electrode (doubled)	0	0	0		1.519	.0292	.356
Total	(0)	(0)	(0)		(1.726)	(.0698)	(.591)
Zinc Electrode Body	4.631	1.252	0		2.309	1.051	.036
Zinc Electrode Edges & Tops	0	0	0		.710	.058	.012
Total in Zinc Electrode	(4.631)	(1.252)	(0)		(3.019)	(1.109)	(.048)
Grand Total	5.530	1.252	5.07		5.619	1.224	4.68
% Increase - Initial to Final	—	—	—		1.6%	-2.2%	-7.7%

ZnO 5.530 - 5.619 = -.089 $\quad \frac{.089}{5.53} \times 100 = 1.6\%$ increase in ZnO

Ca(OH)$_2$ 1.252 - 1.224 = .028 $\quad \frac{.028}{1.252} \times 100 = 2.2\%$ loss of Ca(OH)$_2$

KOH 5.07 - 4.68 = .39 $\quad \frac{.39}{5.07} \times 100 = 7.7\%$ loss of KOH

The amount of Zinc in the overall electrolyte remained constant to within 3%. However, in post cycling analysis it is somewhat arbitrary as to what constitutes the

electrolyte. The value which is listed in Table 5 for the amount of ZnO in the electrolyte (0.874 g) only considers the electrolyte to consist of the bulk electrolyte and any liquid extracted from the cell constituents. However, if all the KOH in the cell is considered to be as "electrolyte" then the amount of ZnO in the electrolyte would be 0.96 g. This value is obtained by assuming that the zincate concentration of the electrolyte remaining in the cell constituents (mainly in the nylon wick, zinc and NiOOH electrodes) is the same as that in the electrolyte extracted from each, respectively. Using the value of 0.96 g, there is found to be 7% more Zinc in the final electrolyte than in the initial electrolyte. In addition, as 8% less KOH was found in the final electrolyte, the overall final electrolyte is thus 15% higher in Zinc than the initial electrolyte. This means that the final electrolyte was supersaturated with zincate.

What is even more interesting about the electrolyte, however, is the value for the dissolved ZnO in the tissue used to absorb electrolyte from the NiOOH electrode vs the amount of KOH found. There is only about 40% of the amount of Zinc that is expected if the electrolyte was Zinc saturated. This is what would be expected if the NiOOH electrode was acting as a Zinc "sink". The large amount of Zinc in the NiOOH electrode shows that it is indeed a Zinc "sink". Over 95% of the Zinc which left the zinc electrode wound up inside the NiOOH electrodes. This migration will be discussed in more detail in Section 4.7. While the NiOOH electrode produces OH⁻ during discharge (the last half-cycle performed), thus diluting the zincate, some of the Zinc in the NiOOH electrode would have been expected to dissolve over the period that the cell was standing before disassembly. This should have brought the zincate concentration close to saturation. The fact that this did not occur further indicates that the $Ni(OH)_2$

and/or NiOOH binds with the ZnO. Also, it can be seen that the zinc electrode tissue is ~30% more supersaturated compared to the overall electrolyte and about 50% supersaturated compared to the initial electrolyte. It is expected that the electrolyte near the zinc electrode would become supersaturated during a discharge, but it was unexpected that such a large concentration gradient from supersaturation to undersaturation would still exist by the time the cell was disassembled (~ three days). All of these calculations assume that the KOH concentration is uniform throughout the cell (31%) as the analysis found very little gradient in KOH concentration.

While only about 65% of the Zinc initially present in the negative electrode remained, over 85% of the Calcium was still present. The small amount of Calcium which migrated may have traveled by convection as small complex particles. The amount of Calcium in the electrolyte itself was very small (~9 micrograms/ml), so it is not expected that a Calcium concentration gradient could have caused the migration.

A mass balance on the current collector showed that 0.25 g (10%) was missing. The missing material was Cu, but again the missing amount falls within experimental error. Only 0.0002 g of Cu were found in the NiOOH electrodes. A PTFE balance was not performed. The LiOH concentration in the final electrolyte was approximately one third of the original value.

Somewhat more qualitative material balances were performed on two other cells (cells 10Ca1 and Zn1). For cell 10Ca1, the Zinc balance for the cell 10Ca1 closed to within 15%, and the Ca balance closed to within 7%. However, it must be remembered that this cell had been reassembled with its separator, nylon wick and NiOOH electrodes replaced, adding to the risk of material loss. Also, for this cell only the NiOOH

and zinc electrodes were analyzed, so it was assumed that all the other values would be the same as that for cell 25Ca1. The different amounts of electrolyte, nylon wick, and separator used were adjusted for.

The Zinc balance for Zn1 closed to within 6% (also based on the above approximations).

4.6. Complex Formation in the Electrode

Chapter 2 described the formation of complex in a beaker. Zinc supersaturation was found to be necessary for the complex to form at a reasonable rate in the electrolyte investigated. In saturated electrolyte (31% KOH) a small amount of complex would only form after a period of days, whereas in supersaturated electrolyte (~31% KOH), complex formation began after only a few minutes. The same behavior is expected to occur in the electrode, with the complex being formed only during discharge when the electrolyte becomes supersaturated. During a subsequent charge the complex decomposes and is converted into Zn and $Ca(OH)_2$. This postulate was supported by the observation that in all of the discharged cells, Calcium could be found only as the complex, whereas in the charged cell, Calcium was found also as $Ca(OH)_2$. The indication (by AAS) that a slight amount of Calcium (5%) may be uncomplexed in the discharged cells can now be rationalized. When the cell is discharging, the degree of supersaturation will be high, however, as more and more complex is formed, the degree of supersaturation decreases. As all of the ZnO produced by the discharge is required for creating 100% complex (e.g., in a cell where all excess Zinc has migrated away, as in cell 25Ca1), by the time 90% of the complex is formed, the electrolyte should no longer be highly supersaturated. Thus, perhaps 90% of the complex forms quickly, while the

remaining 10% forms at a decreasing rate, perhaps requiring a number of days for the final few percent to form.

Considering the large distance that the Zinc had to migrate in cell 10Ca3 to reform the complex, along with the stable capacity of the cell, it is expected that there must be considerable convective flow during cycling. Diffusion along concentration gradients is not expected to be sufficiently rapid to supply the required amount of Zinc over this distance. This is because virtually all of the Zinc migration and complex formation must occur within the 2.5 h discharge and 10 min open circuit periods. If less than this amount of migration and complex formation occurred on a discharge, it would be expected that the cell would not be able to retain its capacity and that when disassembled (even after a few days) a noticeable variation in the ratio of $Ca(OH)_2$ to complex should be found, even on a fully discharged cell.

The fact that the last part of complex formation occurs slowly suggests that allowing a cell with Calcium which has lost some capacity (by Zinc redistribution) to sit for a few days or a week could restore some of its lost capacity. There of course must be enough Calcium to complex with the amount of Zinc required for full capacity. For example, if cell 25Ca1 was only 70% complexed in the center resulting in a 20% capacity decline, allowing the cell to sit may increase the amount of complex in the center to 80 or 90% after a week, thus increasing its capacity. If a cell is allowed to sit sufficiently long, even the rate of complex formation in an electrolyte which is only at saturation may be enough to regain full capacity.

Another possibility for regenerating a cell with low capacity would be to discard the electrolyte and replace it with a highly supersaturated electrolyte. The supersa-

turated electrolyte could be made by adding deionized H_2O to highly concentrated Zn-saturated KOH solution immediately before injecting it into the cell. This would be a very simple procedure, and for uses such as electric vehicles, could be performed in a few minutes at specially-equipped service stations. The uncomplexed Calcium would react with supersaturated zincate and thus capacity would be restored. A pure deionized H_2O + KOH wash could also be performed to remove some migrated ZnO, as the ZnO dissolves much faster than the complex in KOH.

The above discussion centers on how fast the complex forms and how to create it. It is also important to understand how it forms, and how it decomposes on charge. The fact that supersaturation is important in forming the complex (at high KOH concentrations), and that $Ca(OH)_2$ will not just react with ZnO powder in the solution means that the reaction of $Ca(OH)_2$ occurs with dissolved ZnO (zincate). This is also the method by which ZnO is expected to form Zn in a normal zinc electrode (i.e., $ZnO \rightarrow Zn(OH)_4^=$ $\rightarrow$ Zn). The slight increase in zinc electrode overpotential observed when $Ca(OH)_2$ is added to a zinc electrode can be attributed to the ability of the $Ca(OH)_2$ to lower the concentration of zincate (compared to $Ca(OH)_2$-free cells), causing a concentration overpotential.

There are two obvious mechanisms for $Ca(OH)_2$ to lower the zincate concentration. One would be if there was sufficient excess of $Ca(OH)_2$ (as in the 40% cells) to complex all the Zinc in the electrode and still have excess $Ca(OH)_2$ to combine with the zincate in a saturated solution. This may also occur in cells with less Calcium when the excess Zinc has migrated away. It must also be remembered that normal Zinc cells are supersaturated after a discharge, whereas electrodes with $Ca(OH)_2$ lower the amount of

supersaturation. This decrease in zincate concentration would also increase the concentration overpotential during charge. The second, and probably the largest contribution to the higher overpotential in $Ca(OH)_2$-containing electrodes, is that the complex dissolves at a slower rate (compared to ZnO) in KOH, which means that the equilibrium concentration of zincate in the presence of the complex is probably lower than in the presence of ZnO. This agrees with the results obtained by other researchers.[15,16] Thus, as the electrolyte becomes undersaturated during charge, the complex will keep the zincate concentration lower than ZnO would.

The difference in the rate of dissolution between complex and ZnO also leads to interesting morphologies in the electrode. As mentioned, in the cell disassembled in the charged state, the edge areas were composed of $Ca(OH)_2$ with very little Zinc, and the center area contained complex near the current collector and ZnO and Zn on the surface. A sketch of this arrangement is shown in Figure 47, part A. For this discussion, the net direction for Zinc migration is set to be toward the left in the figure. The structure in part A was observed in the charged cell, but the structure at the end of the previous discharge must have been that shown in part B. The solubility difference between complex and ZnO comes into play when changing from the structure in B to that in A during charge. When the electrode is charged, the Zn is deposited from solution. As the zincate concentration decreases, the ZnO begins to dissolve. Thus, in areas where there is ZnO, most of the complex will stay intact and not dissolve. In the area toward the right, where there is no ZnO, the complex was forced to decompose and create $Ca(OH)_2$ and zincate. As the Zinc migration is toward the left, the zincate moves in that direction (even though that area should have a higher zincate concentration), and

precipitates. The cause of this migration may be electrolyte convection as diffusion would be in the opposite direction. The reason that no or very little Zn metal stays in the region on the right is that there are indications that Zn has a greater tendency to electrodeposit on Zn than on other materials.

This explains the island growths of Zinc seen on all the cycled electrodes. In the Ca-containing cells these Zinc islands were surrounded by areas of complex. In the pure Zn cells, the islands were surrounded by bare current collector. The island in Figure 47 is caused by the small amount of ZnO changing into Zn on charge. This Zn serves as a preferred site for more Zn deposition and thus draws Zinc from surrounding areas. With further cycling, the gradual migration of the Zinc toward the left will make the island smaller and smaller until insufficient material remains to create any excess ZnO on discharge and the island disappears. Thus, neglecting what caused the original movement of Zinc to the left, once it occurred, the Zn present there will always act to draw zincate from areas which have become depleted in Zinc. The Zinc migration consequently no longer occurs solely by the original mechanism.

This idea that the preferential plating of Zn on Zn helps cause shape change also suggests a way to decrease shape change. If a conductive, inert (as far as the cell is concerned) material could be found on which the Zn plates more readily than on Zn itself, then this material could be uniformly incorporated in the electrode. Then, when the cell was charging there would be no non-uniform distributions due to preferential deposition. If Zn plated on this material more readily than on Zn itself, then the material may guarantee that at least there will be a thin layer of Zn over the whole electrode after charge. With $Ca(OH)_2$ serving to create a uniform complex layer after discharge, and

ZnO + some Zn

Zn

Ca(OH)$_2$

Zn

Current
collector

Ca(OH)$_2$ · 2 Zn(OH)$_2$ · 2H$_2$O
+ some Ca(OH)$_2$

Ca(OH)$_2$ · 2 Zn(OH)$_2$ · 2H$_2$O
+
Ca(OH)$_2$

a)

Center

Edge

ZnO + some Zn

ZnO

Ca(OH)$_2$ · 2 Zn(OH)$_2$ · 2H$_2$O

Current
collector

b)
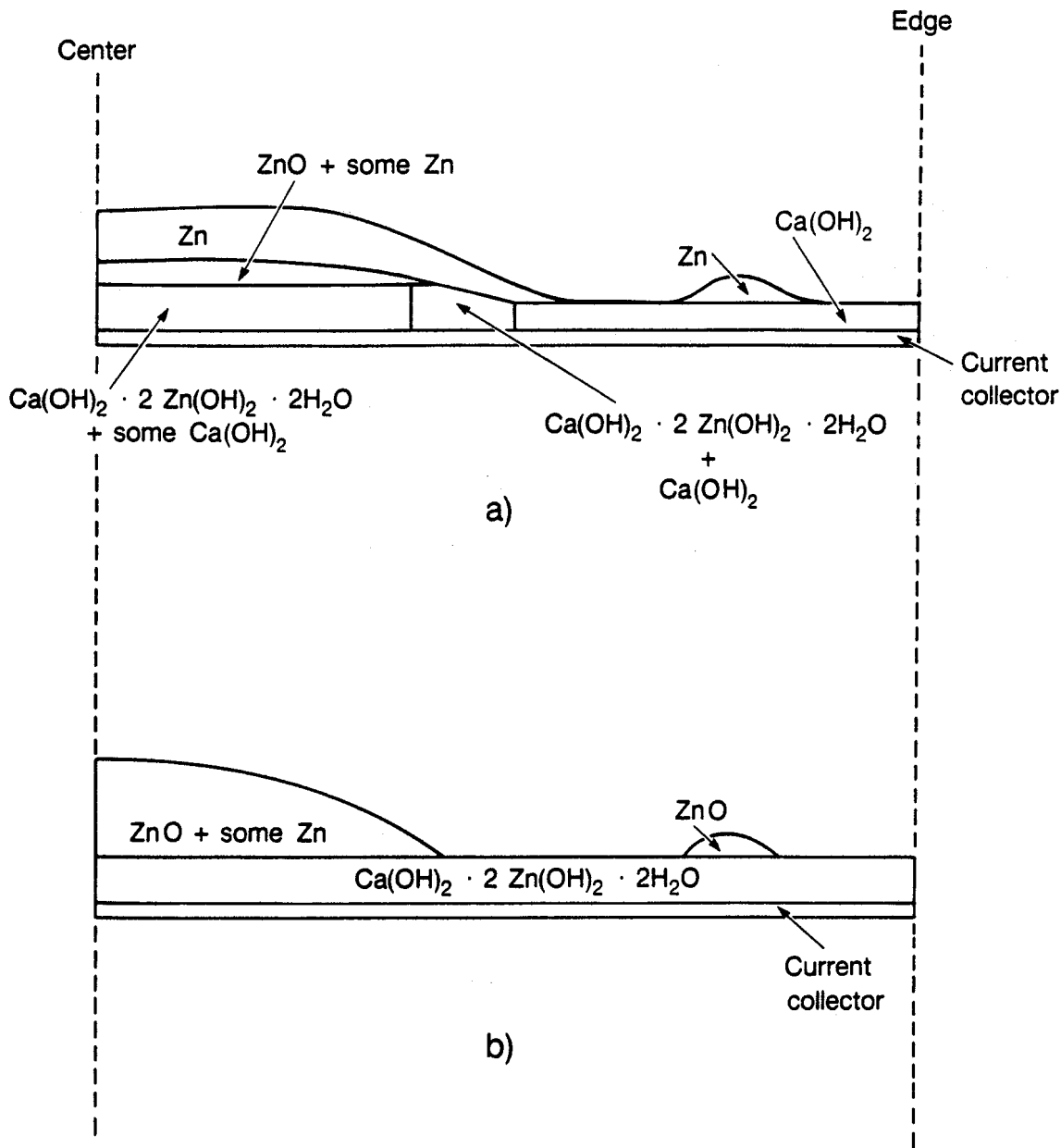
XBL 882-9527

Figure 47. Sketch of Zinc migration in a Ca-containing cell. Part A is in the charged state and Part B is in the discharged state. The migration is toward the left in the sketch.

this material creating a uniform plating layer during charge, Zinc migration could be reduced significantly.

4.7. Zinc Migration into Nickel Oxide Electrodes

As was shown in the material balance in Section 4.5.3, a considerable amount of Zinc migrated into the NiOOH electrodes. This migration accounted for over 90% of the weight loss from the zinc electrodes. A summary of the amount of migration vs the number of cycles is given in Table 6 and plotted in Figure 48. First, it can be seen that the $Ca(OH)_2$ apparently had no effect on the amount of Zinc migration. Second, it is also apparent that the migration occurs rapidly at first and then proceeds slowly. It is expected that after the initial 50 cycles the amount of Zinc in the NiOOH electrodes will increase only at a very slow rate.

The migration of Zinc into the NiOOH electrode was not expected when Zn/NiOOH cells were originally proposed. When the loss of Zinc from the zinc electrode was discovered, it was anticipated that it would be found in the NiOOH electrode.

TABLE 6			
Amount of Zinc Found in Nickel Oxide Electrodes			
Cell	% $Ca(OH)_2$	# of Cycles	Amount of ZnO in each Ni
25Ca1	25	151	.75
10Ca1	10	59	.69
10Ca2	10	5	.49
10Ca3	10	~106	.63
Zn1	0	150	.75
Zn2	0	64	.63

Figure 48. Amount of Zinc migration into NiOOH electrodes.
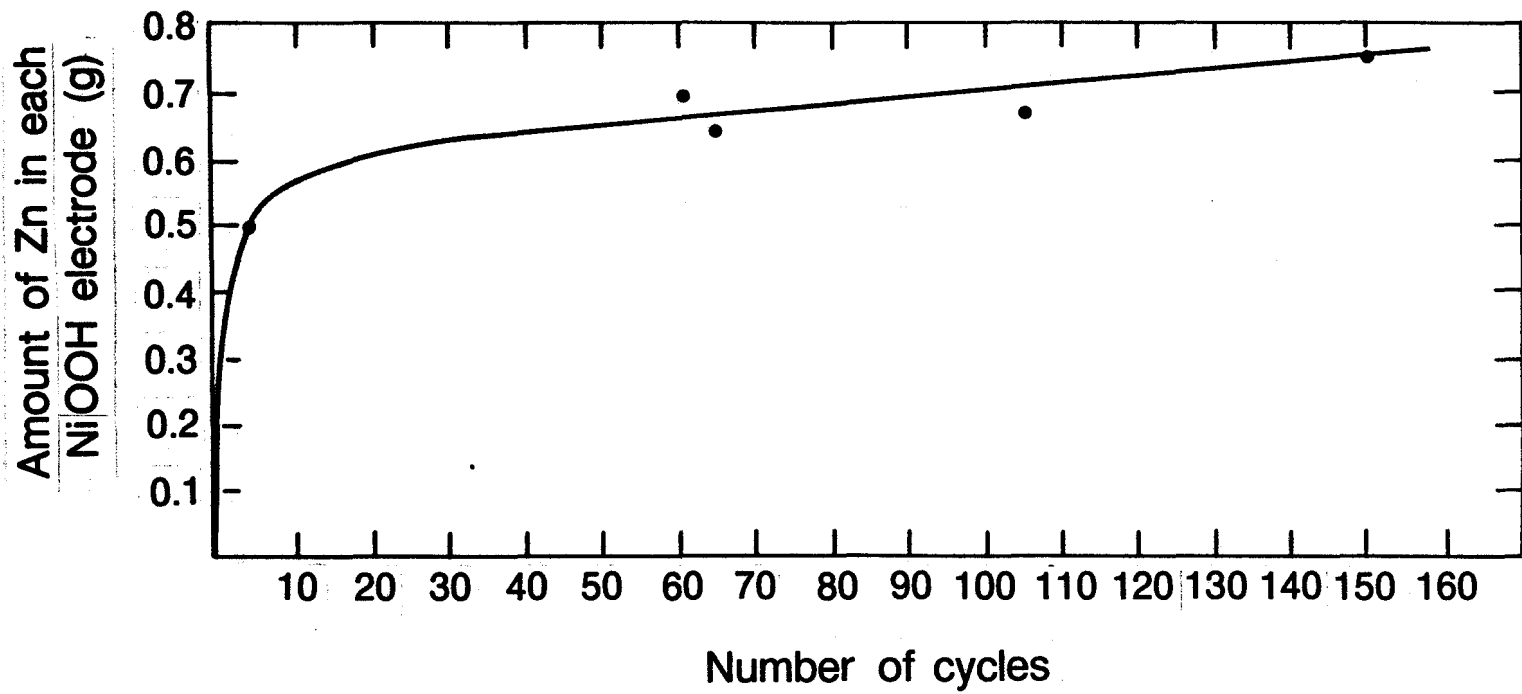
XBL 882-9528

However, there is not any convincing theory as to why this migration occurs. It could be postulated that the migration is due to KOH concentration fluctuations in the NiOOH electrode. In this postulate, the ZnO precipitates because the KOH concentration decreases over the entire cell, and especially in the NiOOH electrode during charge. The decreased KOH concentration causes the zincate to become supersaturated and thus precipitate. But, supersaturated zincate solutions are known to be fairly stable and may not precipitate much ZnO during the charge period. In addition, if this was the cause, then during discharge the higher KOH concentration should cause the precipitated ZnO to redissolve, especially as ZnO dissolves quickly in undersaturated KOH.

Experimental evidence also seems to disagree with this postulate. Powder X-ray diffraction studies of the cycled NiOOH electrodes showed no ZnO, even though a considerable amount of Zinc was known to be present. This may be due to the ZnO particles being very small and well dispersed. But, precipitated ZnO particles show up elsewhere and, with the large amount of Zinc present, the particles should not be isolated. In addition, supersaturated zincate should preferentially precipitate ZnO on existing ZnO. Otherwise, a normal zinc electrode would quickly lose its mass to floating particles of ZnO and to ZnO migration to the separator, etc.. Thus, the particles should not be isolated, but exist in the form of large clumps.

The only material found in the powder X-ray studies was Ni. Both NiOOH and $Ni(OH)_2$ are amorphous and did not appear in the spectrum. Most forms of Zinc are crystalline and readily appear in the powder X-ray patterns. In addition, the material balance in Section 4.5.3 showed that the NiOOH electrode's electrolyte had only 40% the amount of Zinc that should have been present if the electrolyte was saturated. Thus,

the NiOOH electrode seemed to be acting as a Zinc sink.

The only postulate which readily explains this phenomenon is that the Zinc species is forming a bond or otherwise coordinating with the $Ni(OH)_2$ and/or NiOOH. This bond may be a complex similar to that which forms with $Ca(OH)_2$. There are hints of this in the literature.[19] If the ZnO is reacting with the $Ni(OH)_2$, then during charge, when the $Ni(OH)_2$ is converted to NiOOH, the Zinc could remain in the electrode since the KOH concentration would be low. Alternatively, the Zinc may also react with the NiOOH. No charged NiOOH electrodes were examined by powder X-ray analysis so it is unknown if the ZnO reappears in a charged NiOOH electrode. As this Ni-Zn complex may be amorphous, the postulate also explains why nothing was seen in the discharged NiOOH electrode using powder X-ray diffraction.

This idea also explains why no separate Zinc particles or powder could be identified in the discharged NiOOH electrodes examined by SEM and EDS (Zinc was always seen together with Ni). Any such particles of Zinc would have quickly reacted with the NiOOH electrode (up to the stoichiometric limit) and would no longer be physically separate from the Ni. It also explains why the majority of the Zinc migration occurs quickly and then proceeds at a much lower rate. The formation of more complex would require the Zinc to diffuse farther and farther through the complex and into the remaining $Ni(OH)_2$ or NiOOH particles. As this diffusion would continue while the electrode was at open circuit, resulting in the low zincate concentration found in the NiOOH electrode's electrolyte in the disassembled cells. A literature search uncovered no reference to such a complex, but very little was found even on the calcium zincate complex (at the time these experiments were performed). Using the value of 0.75-g ZnO

(same amount in both 150-cycle cells), one calculates that one mole of ZnO reacts with 2.8 moles of either $Ni(OH)_2$ or NiOOH.

Regardless of the reason for the Zinc migration into the NiOOH electrode, it is obvious that a sure and quick way to retard material loss from the zinc electrode is to begin with ZnO saturated NiOOH electrodes. As was mentioned earlier, over 90% of the material loss from the zinc electrode is to the NiOOH electrodes. An easy way to saturate the NiOOH electrodes (if the ZnO does indeed react with $Ni(OH)_2$) may be to allow discharged new NiOOH electrodes to soak for one to two weeks in ZnO-saturated KOH. They should quickly become over 50% saturated with ZnO. Even with no action, however, any further migration of Zinc into the NiOOH electrodes will occur at a relatively slow rate after the first 50 cycles.

4.8. Nickel Oxide Electrode Experiments

As was seen in the voltage vs time plots in Section 4.1, the NiOOH electrodes, especially the ones in the 10% $Ca(OH)_2$ cells, were not well-behaved: they had high and varying overpotentials. It was desired to see if the $Ca(OH)_2$ might have been the cause.

For this purpose, two NiOOH electrodes were assembled and cycled versus each other in various environments. The NiOOH electrodes were created from one of the same NiOOH electrode sheets used for making the NiOOH electrodes in the Ca-containing cell cycling experiments. First, the NiOOH electrodes were cycled in 31% KOH with no ZnO or LiOH present. In this environment they behaved normally. Then, the electrolyte was replaced with one which contained 1% LiOH. Again the electrodes behaved normally. There was no significant change noticed with the addition of

the LiOH.

The next change was to add ZnO to the electrolyte. A ZnO powder reserve was also necessary to insure that the electrolyte remained saturated. The reservoir was created by inserting a zinc electrode (no $Ca(OH)_2$) into the cell. The zinc electrode was partially charged to prevent Cu corrosion and was placed between the cell spacers and one of the NiOOH electrodes. The two NiOOH electrodes still faced each other, and cycling was only performed between the two NiOOH electrodes, with the zinc electrode remaining at open circuit.

Almost immediately, with the continuation of cycling, the NiOOH electrode next to the zinc electrode started to exhibit slightly unusual overpotential behavior during its charge (see Figure 49). After 10 cycles this behavior became rather significant, and would occur when the other NiOOH electrode was discharging and in the transition between exhaustion of NiOOH and evolution of H_2. Once the other electrode's voltage reached the potential for H_2 evolution, the unusual overpotential would disappear. Occasionally, the discharging electrode would also exhibit higher overpotentials in this region. As the cell voltage would also register many of these overpotential spikes, this behavior is not attributable to problems with the reference electrodes. Also, as these unusual overpotentials did not appear in the first two experiments (although cycling conditions were identical) it is believed that the problems are due to the zincate concentration and the proximity of the zinc electrode.

To confirm this, the cell was reassembled with the position of the two NiOOH electrodes interchanged. The unusual overpotentials continued, again affecting the NiOOH electrode closer to the zinc electrode. Removal of the zinc electrode but leav-
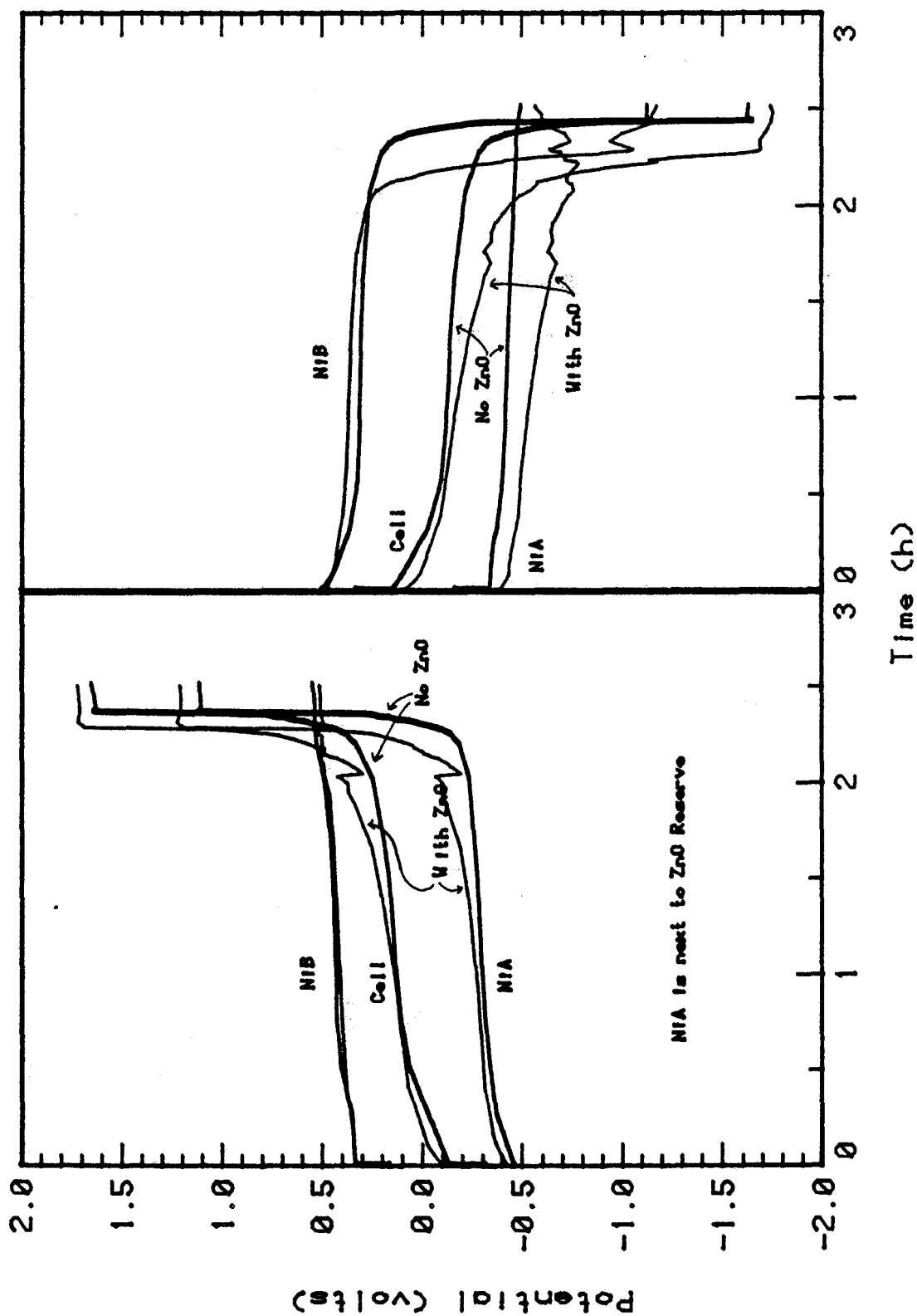
Figure 49. Cycle showing unusual overpotential behavior of a NiOOH electrode. This behavior occurred when a 100% Zn electrode was added (the zinc electrode remained in open circuit) next to the NiOOH electrode.

ing the electrolyte with zincate caused the problems to disappear immediately, and the electrodes returned to normal behavior. It is unknown what caused this behavior. While this is not the same phenomenon seen with the Ca-containing cells, it is similar and indicates that the NiOOH electrodes themselves may have been abnormal.

The next change involved replacing the zinc electrode with a 10% $Ca(OH)_2$ electrode. The electrode and cell were prepared in the same way as in the previous tests. This time, the NiOOH electrodes behaved normally and showed no signs of unusual behavior. This was somewhat unexpected as the 10% $Ca(OH)_2$ electrode should be very similar to a pure Zn electrode.

The last change was to cycle the 10% $Ca(OH)_2$ electrode against the NiOOH electrodes. This cell was designated 10Ca3 and was discussed in previous sections. The structure remained the same and the two NiOOH electrodes were connected together outside of the cell so that they would cycle as one electrode against the $Ca(OH)_2$ electrode. Over 100 cycles were performed in this way, and the NiOOH electrodes behaved normally throughout cycling.

While it was not known exactly what caused the unusual NiOOH electrode overpotentials in the 10 and 25% $Ca(OH)_2$ cells, the above experiment shows that Calcium does not have a detrimental influence on normal NiOOH electrodes. It appears that the problems were caused by defective NiOOH electrodes.

4.9. Summary

Calcium hydroxide was found to react with zincate solutions, forming a crystalline calcium zincate complex. The formation of this complex was fairly rapid in zincate

supersaturated 31% KOH solution, whereas in 31% KOH solutions which are not super-saturated, the reaction, if it occurs at all, is very slow.

The addition of $Ca(OH)_2$ to the zinc electrode was found to dramatically improve cycle life performance. The $Ca(OH)_2$ forms the calcium zincate complex with the zincate-supersaturated KOH solution during the discharge half-cycle. As calcium zincate is relatively insoluble in this solution, the formation of this complex decreases the rate of Zinc redistribution (shape change) since the complexed Zinc is no longer free to migrate.

The decrease in the amount of excess ZnO because of $Ca(OH)_2$ addition (to maintain the kg/kWh for this cell) was found to be more than offset by the benefits of Calcium addition. For similarly constructed cells, the number of Ah the cell cycled per gram excess ZnO increased from only 20 for a 100% Zn electrode to over 75 for a 25% $Ca(OH)_2$ electrode. In addition, the 25% $Ca(OH)_2$ electrode was still functioning well when cycling was terminated at 150 cycles whereas the 100% Zn cell was terminated due to lack of capacity at only 64 cycles.

X-ray images and chemical analyses of the discharged electrodes after cycling showed that for the Ca-containing cells, a uniform layer of "background" calcium zincate was present whereas in the 100% Zn cells there were many regions on the current collector with no Zinc. As was expected, the amount of material in the background layer was found to increase with the amount of $Ca(OH)_2$ initially present. Chemical analysis indicated that one Ca atom reacts with two Zn atoms and experiments indicate that the density of the complex is 2.63 g/cm^3.

The addition of only 10% $Ca(OH)_2$ was found to be insufficient for maintaining cycling capacity, as this small amount of Calcium can not bond with the amount of Zinc required for full capacity. The 25% $Ca(OH)_2$ cells, however, were found to be able to maintain the required capacity and performed well in cycling.

While $Ca(OH)_2$ addition was found to raise the zinc electrode overpotential during charge, the increase was not large enough to cause shorting problems nor enough to lead to a significant decrease in efficiency for the 10 and 25% $Ca(OH)_2$ cells. For the 40% $Ca(OH)_2$ cells, however, the increase in overpotential, and the expansion of the electrode itself resulted in the early failure of those cells. The high overpotential facilitated dendrite formation, and the expansion of the electrode caused the separator to tear. Both processes helped lead to the shorting of the cell. The higher overpotential for the 40% $Ca(OH)_2$ cells may have been caused somewhat by the expected decrease in the zincate concentration for those cells. At a 40% $Ca(OH)_2$ level, there would not have been enough Zinc in the electrode to react with all the Calcium and thus, the $Ca(OH)_2$ is expected to have lowered the zincate concentration to a value below saturation.

A comprehensive material balance was performed on a 25% $Ca(OH)_2$ cell. The Zn balance closed to within 1.6%, and the Ca balance closed to within 2.2%. A chemical species distribution over the zinc electrode for this cell was also performed. The result of the elemental distribution analysis was that at most 5% (by considering the amount of Calcium and assuming 100% complex) of the expected Zinc in the center of the electrode had migrated away after 150 cycles. While this value is smaller than the experimental error, if in fact depletion occurs, further depletion is expected to happen very slowly as the $Ca(OH)_2$ will continue to draw back migrating Zinc, especially if the

cell is allowed to stand for a few days. Even if extensive Zinc depletion does occur, the $Ca(OH)_2$ should allow the use of simple methods for regeneration, such as replacing the electrolyte with a zincate-supersaturated electrolyte.

The chemical balance over the cell showed that over 90% of the Zinc which had migrated from the zinc electrode was in the NiOOH electrodes. Zinc may be forming a bond with $Ni(OH)_2$ (perhaps similar to the bond with $Ca(OH)_2$) and this seems to provide the driving force for the migration. Most of this migration occurs within the first few cycles, and after 50 cycles further migration is expected to occur very slowly. Starting with ZnO-presaturated NiOOH electrodes may alleviate this problem.

Experiments with the NiOOH electrodes showed that the addition of $Ca(OH)_2$ to the zinc electrode does not have any noticeable detrimental effect on the NiOOH electrodes. The unstable high overpotentials witnessed in some cycles of the Ca-containing cells were attributed to defects in the NiOOH electrodes.

Finally, sealing the separator close to the top and sides of the zinc electrode was found to decrease the rate of Zinc redistribution. Cells with a large gap between the electrode and the seal exhibited an enhanced rate of Zinc redistribution, compared to those with a small gap. Significant amounts of Zinc were found to migrate into the gap above the upper edge of the zinc electrode.

Chapter 5

Conclusions

Calcium hydroxide forms a stoichiometric $CaZn_2(OH)_6$ complex with the ZnO-supersaturated electrolyte produced by a discharging zinc electrode, leading to a more uniform distribution of active material after extensive cycling.

Electrodes containing 25 mol% $Ca(OH)_2$ showed the best cycle-life performance of those tested.

The zinc electrode cycle-life depends (among other things) upon the proximity of the separator seals to the edges of the zinc electrode. The closer the seals, the lower the rate of Zinc redistribution.

Nickel oxide electrodes act as a Zinc receptor and account for almost all the Zinc loss from zinc electrodes. $Ni(OH)_2$ and/or NiOOH may be complexing or binding with the ZnO.

Charging of the zinc electrode involves as a source dissolved Zinc species (probably zincate). Zinc oxide does not convert directly to metallic Zn during charge, instead, ZnO dissolves into solution and the zincate in solution plates as metallic Zn upon charge transfer. Also, Zn appears to deposit on Zn more readily than on other material in the electrode.

Chapter 6

Recommendations

Add $Ca(OH)_2$ to the zinc electrode. Add enough to complex with at least the amount of Zinc which corresponds to the design capacity of the cell. Do not add so much that the electrolyte becomes unsaturated in zincate as this may lead to very high zinc electrode overpotentials.

Seal the separator as close to the edges of the zinc electrode as possible, leaving room for some electrode expansion.

Use NiOOH electrodes which have been presaturated with ZnO.

Find a conductive material which is not active in the battery, but upon which the Zn prefers to plate. Uniformly distribute this material over the electrode to help decrease the rate of Zinc redistribution during charge.

Investigate the rejuvenation of low-capacity cells which contain $Ca(OH)_2$ by replacing the electrolyte with a zincate-supersaturated electrolyte.

References

1. J. McBreen, "Zinc Electrode Shape Change in Secondary Cells," *J. Electrochem. Soc.*, **119**, 1620 (1972).

2. K.W. Choi, D.N. Bennion, and J. Newman, "Engineering Analysis of Shape Change in Zinc Secondary Electrodes. I. Theoretical," *J. Electrochem. Soc.*, **123**, 1616 (1976).

3. R.G. Gunther and R.M. Bendert, "Zinc Electrode Shape Change in Cells with Controlled Current Distribution," *J. Electrochem. Soc.*, **134**, 782 (1987).

4. T.P. Dirkse, "Aqueous Potassium Hydroxide as Electrolyte for the Zinc Electrode," *J. Electrochem. Soc.*, **134**, 11 (1987).

5. J.T. Nichols, F.R. McLarnon, and E.J. Cairns, "Active Material Redistribution Rates in Zinc Electrodes: Effect of Alkaline Electrolyte Compositions Having Reduced Zinc Oxide Solubility," Lawrence Berkeley Laboratory Report No. LBL-17397 (November 1983).

6. Mark J. Isaacson, F.R. McLarnon, and E.J. Cairns, "Potentials and Concentrations in Porous Zn Electrodes and Thermodynamics of KOH-K$_2$Zn(OH)$_4$ Electrolytes", PhD Thesis, University of California - Berkeley, April 1988.

7. M.H. Katz, F.R. McLarnon, E. J. Cairns, "Computer Control of Electrochemical Experiments with Application to Zinc/Nickel Oxide Cells," Lawrence Berkeley Laboratory Report No. LBL-15546 (December 1982).

8. T.C. Adler, F.R. McLarnon, E.J. Cairns, "Improvements to the Cycle-Life Performance of the Zn/KOH/NiOOH Cell", Proc. 22nd Intersoc. Energy Conv. Eng. Conf., 1987.

9. R.I. Goldberg, F.R. McLarnon, E.J. Cairns, "Novel Current Collectors for the Zinc Electrode in Zn/NiOOH Cells," Lawrence Berkeley Laboratory Report No. LBID-984 (August 1984).

10. Ken Miller, Private Communication.

11. G. Kawamura and Y. Maki, "A Study of Insoluble Zinc Electrodes for Alkaline Secondary Batteries. I. Insolubilizing the Zincate Ion by Calcium Hydroxides," *Denki Kagaku*, **48**, 592 (1980).

12. W.J. van der Grinten, "Secondary Zinc-Electrodes with Zincate Trapping," The Electrochemical Society Extended Abstracts, Vol. 67-2, Paper No. 38 (1967).

13. R.A. Jones, U.S. Patent No. 4,358,517 (November 1982).

14. Y-M. Wang and G. Wainwright, "Formation and Decomposition Kinetic Studies of Calcium Zincate in 20 w% KOH," *J. Electrochem. Soc.*, **133**, 1869 (1986).

15. E.G. Gagnon, "Effect of KOH Concentration on the Shape Change and Cycle Life of Zinc/NiOOH Cells," *J. Electrochem. Soc.*, **133**, 1989 (1986).

16. R.A. Sharma, "Physio-Chemical Properties of Calcium Zincate," *J. Electrochem. Soc.*, **133**, 2215 (1986).

17. F. Liebau and A. Amel-Zadeh, *Kristall und Technik,* **7-1** 221 (1972). Obtained from the International Centre for Diffraction Data Handbook, pp. 25-1449 (1980).

18. Schwick, Inst. Fur Baustoffkunde und Stahlbetonbau, Private Communication. Obtained from the International Centre for Diffraction Data Handbook, pp. 24-222 (1980).

19. H. Bode, K. Kehmelt and J. Witte, "Zur Kenntnis der Nickelhydroxidelektrode—I. Über das Nickel(II)-Hydroxidhydrat," *Electrochim. Acta,* **11,** 1079 (1966).

20. D.M. MacArthur, "Progress in Development of Zinc/Nickel Oxide Cells with Pasted-Rolled Electrodes," Proc. 20th Intersoc. Energy Convers. Eng. Conf., 1985.

21. R.A. Sharma, "Kinetics of Calcium Zincate Formation," *J. Electrochem. Soc.,* **135,** 1875 (1988).

22. E.G. Gagnon and Y-M. Wang, "Pasted-Rolled Zinc Electrodes Containing Calcium Hydroxide for Use in Zn/NiOOH Cells," *J. Electrochem. Soc.,* **134,** 2091 (1988).

23. J. McBreen, "Investigation of the Zinc Electrode Reaction," Brookhaven National Laboratory Report No. BNL-51370 (1980).

Appendix
Zinc Electrode Manufacture

The following is a procedure for the manufacture of zinc (zinc oxide and zinc oxide with $Ca(OH)_2$) electrodes. This procedure is derived from the procedure given by James Nichols[5] with considerable modifications having been made to improve the electrode strength, consistency, porosity, and other qualities. The procedure was designed to be feasible for conversion to large scale production and care was taken to avoid expensive processing chemicals and/or expensive processing requirements. This procedure was created for the fabrication of the Zn and Zn-$Ca(OH)_2$ electrodes used in this thesis and has been used by other researchers in this group with good success.

The desired outcome of this procedure is an electrode which consists of a current collector surrounded by active material on each side. The active material should be uniformly distributed both by weight and by composition not only over the surface, but also from the interior out. The material should have the desired porosity throughout and should strongly bind with itself and the current collector (to give the electrode physical strength and some flexibility). In addition, the final electrode should be of the required weight and thickness.

To ensure uniform composition, the electrode materials are blended together into a slurry. A PTFE polymer dispersion is added to provide fibers for helping the active material bind with itself and the collector, and wet-pressing of the slurry is performed to ensure that the final electrode is uniformly of the desired porosity and thickness.

In the following procedure, a brief general description of each step will be given (and why it is done or required) followed by a more detailed description of the equipment and methods which were used.

Table A1 is a list of the required materials and equipment along with special information identifying the materials used when appropriate.

Stepwise Procedure:

(1) Weigh current collector for future reference.

(2) Cut to the size of the electrode two sheets of the porous polypropylene. Oversize the sheets ~1 mm. The smooth side of the sheets will be facing the electrode active material from the filtering process until the electrode completion. These sheets are used as they easily separate from the dried electrode, leaving a smooth surface, while still providing the desired filtering action. A steel template and an X-acto knife were used to cut the sheet.

(3) Also, cut to the size of the electrode 6 sheets of hard, smooth paper towels. Oversize these by 1 to 2 mm on each side. These sheets are used later when pressing the electrode, to absorb water while still providing a smooth, uniform surface.

(4) Prepare the filtering table.

The filtering table when set up should consist of the filter paper (Whatman) in the center of the filtering table. Centered on the filter paper should be a single sheet of polypropylene with the smooth side up. Centered on this should be the rubber gasket, then the plastic and/or metal frame. This assembly should be

tightly clamped together to prevent liquid seepage. The open cavity created for the slurry should be large enough to hold at least 40 mls of suspension, and should not leak. The filterant should be forced to uniformly pass the polypropylene sheet leaving the solids on the polypropylene.

Using deionized H_2O, it is best to wet the filter paper and polypropylene before assembly and to rinse the gasket and frame (to prevent contamination of the active material). Once assembled, fill the cavity with deionized H_2O and look for leaks and then turn the vacuum on to remove the H_2O.

The vacuum bottle should be between the filter table and the vacuum source. The bottle should have some sort of small opening such as a tube so that vacuum can be easily controlled by a finger. In other words, without a finger covering the hole, there is no vacuum applied to the filter table and by tightly covering the hole, the strongest vacuum is applied. Lower the amount of draw by the vacuum line (using a valve, etc.) if the filtering rate is too high to be easily controlled by finger pressure at the vacuum bottle. As will be discussed later, the ideal amount of time to filter the slurry is 30 to 60 seconds. The vacuum bottle will also prevent liquid from being pulled into the vacuum source.

(5) Preparing the Slurry

In order to have the electrode's composition as uniform as possible, the active materials are blended together. A normal kitchen Osterizer blender was used in this laboratory with the small, ½ pint size blender cups. First, the weighed amount of ZnO, $Ca(OH)_2$, and PbO are added to the blender. The amounts include extra material to compensate for loss, ranging from 15 to 25%. The loss occurs from

seepage in the filtering table, some material making it through the filter, trimmings removed from the electrode edges, etc. Practice will determine the amount of excess material required.

Then, 60 mls of deionized H_2O are added to the blender. The gasket, blade and cap are attached and the mixture is shaken but not yet blended.

(6) Preparing the PTFE.

All that is required in preparing the PTFE is the required amount of PTFE. For the PTFE suspension used here, the suspension first had to be aggressively shaken for half a minute. Then, following proper pipette techniques, the required amount of PTFE was deposited into a 10 ml beaker. This had to be done quickly to prevent any settling of the suspension. Nothing is added to the PTFE at this point.

The proper preparation of the PTFE has been found to be crucial in the formation of a strong electrode. Improperly prepared PTFE resulted in cracked, flaky electrodes which were very delicate and brittle. Many experiments were performed to determine the best preparation. Adding the PTFE, as obtained from the original suspension, to the blender, without further treatments was found to be almost equivalent to not adding any binder. This is because the PTFE is dispersed with a wetting agent and consists of very small spheres which most probably pass through the filter paper. What was required was a way to have the PTFE particles become "sticky" thus binding with themselves, the active material, and the current collector. It is known that some organic solvents such as isopropanol and acetone can cause this to happen. The first attempt was to add isopropanol to the

PTFE and then blend this mixture into the slurry. This was unsuccessful as the PTFE seemed to bind with itself mainly and provide only limited strength to the electrode. The next attempt was to add the PTFE to the slurry, blend, then add some isopropanol and blend. This unfortunately created considerable foam which was stable and made electrode construction very difficult. Fortunately, it was found that when acetone was added instead of isopropanol, there was very little if any foam formed. Electrodes formed with the following blending scheme with PTFE and acetone were consistently of the required strength.

(7) Blending

First, the powders and liquid in the blender are blended at high speed for three minutes. Then, the PTFE is added (using a little deionized H_2O to wash it out of the beaker) and this mixture is blended for 1 minute at high speed. Finally, 10 mls of acetone are added and the mixture is blended at high speed for 3 more minutes. Care must be taken when adding the acetone as the undiluted acetone can attack the plastic blending cup if it touches the sides when added. If available, a glass blending cup or a similar cup made of some other inert material should be used.

(8) Filtering

This step should be performed as quickly as possible, maintaining care and safety.

Quickly open the blender and pour half the solution into the vacuum table. Close the blender and begin blending at a low setting (no need to time). Begin pulling a vacuum on the slurry, using the vacuum bottle and a finger to regulate

the vacuum. The filtering should not be performed very quickly or very slowly—about 30-60 seconds is optimal. During the filtering process, blow softly on the slurry to eliminate (or at least keep moving) the bubbles. Once cake is seen where one is blowing, turn off the vacuum. By the time this is done, the slurry should be fairly dry (only a very slight moist layer should be seen over parts of the electrode, and no overdried, cracked areas should be visible). As this condition only exists for a short period of time, watch carefully and release the vacuum immediately. Overdrying could cause cracked electrodes or non-uniform porosity distributions. Too-wet electrodes will be difficult to handle and will lose substantial amounts of material when being pressed.

When filtering is completed, turn off the vacuum and disassemble the filter table. Remove the clamp and then slowly remove the plastic and/or metal frame, taking care not to disturb the cake. When removing the rubber gasket, pick up one side slowly and peel the filter paper (Whatman) from the bottom of the gasket. Keep the corner of the filter paper in your hand (trying to hold it as close as possible to the surface of the filter table), and remove the gasket. Now, the cake and polypropylene sheet, which are the only items remaining on the filter paper, will slide off the filter table and onto a paper towel when the filter paper is pulled. Thus, there will be a paper towel on the bottom, then the filter paper, the polypropylene sheet and then finally the cake. Put this to one side and reassemble the filter table as described previously (cleaning as necessary). When ready, stop the blender and pour the second half of solution into the filter table. With a small amount of deionized H_2O (~5 ml), clean the blender blade and cup and pour into the vacuum table. Vacuum filter as described above.

Now, there should be two cakes, each one half of the electrode. Slide these cakes to the dry side of the paper towel before proceeding to the next step.

(9) Assembling the Electrode.

The following steps can proceed more slowly, perhaps ½ hour.

Take the first cake and lay the current collector on top of it. Make sure the mesh and the cake are well aligned. Lightly press the current collector into the cake. Ideally, half the thickness of the current collector should be inside the cake and the other half above it. Now take the second cake, leaving the paper towel behind, and turn it over and align it exactly on top of the current collector. Make sure the top cake, current collector and bottom cake are aligned. Lift and pull on the filter papers in order to do this. Once this is done, press lightly on the top filter paper in order to assure that the cakes stick together (they probably already have). Now, peel off the top filter paper, leaving the polypropylene sheets and cakes underneath.

Fold some paper towels so that they are small enough to fit in between the plates which will be used to press the electrode. However, the final dimensions of the paper towels should be larger than the electrode and there should be no folds over the electrode itself.

Take one folded paper towel and place it where the filter paper had been. Completely cover the electrode and (if possible) the tab. Turn over this entire assembly (paper towels, cakes, etc.) so that everything is now resting on the folded paper towel. Remove the top paper towel and filter paper and replace with a folded paper towel. Place this whole structure in between the stainless steel press-

ing plates.

Take this assembly, along with the stainless steel shims, the two unused folded paper towels, and the 6 cut hard paper towels to the press. Be careful not to shake the electrode assembly.

(10) Pressing the electrode.

Manufacturing the electrode by creating two cakes and assembling them with a current collector inserted between them was done to try and ensure that, as much as possible, equal amounts of active material would be present on both sides of the electrode.

In pressing the electrode, it is desired to obtain an electrode of uniform porosity, thickness, and composition. As the pressing plates are made of a non-porous material (stainless steel) if the electrode was just squeezed between the plates, the liquid and active material would only be forced out the sides. This would not lead to a uniform composition and could lead to substantial loss of material. Thus, except for a final pressing of just a few mils, paper towels are included over the electrode to absorb liquid over the whole surface. So, as the electrode is compressed, the liquid is forced into the paper towels and the active material compresses and becomes less porous (remember that the polypropylene sheets are still present preventing the active material from touching the paper towels).

At the press, take the top stainless steel plate off and replace the top folded paper towel with an unused folded towel. Turn over everything (except the pressing plates which are never turned over). Remove the top paper towel and discard it. Now, shims need to be inserted between the plates. The shims are to be put

between the paper towels so that they will prevent the electrode from becoming too thin in this initial pressing. The total thickness of the shims should be about double the desired electrode thickness (as the part of the paper towels under and above the shims will compress substantially compared to that over the electrode). The shims used for this step added to a thickness of 90 mils for the electrodes made for this project. The shims go on opposite sides of the electrode (all 4 if possible) and rest on the paper towel and must be placed such that they will be between the top and bottom pressing plate as much as possible. Any shims placed on the same side must always be stacked on top of each other and not next to each other. Now, place a fresh folded paper towel on top. Ensure that the shims do not contact nor are they over the electrode. Put the top plate on and center the assembly under the press (making sure nothing moved). Press until you see the pressure needle move slightly (around one hundred pounds). Hold for 20 seconds and remove. The paper towels should be damp, and the electrode should still be thicker than the desired thickness. Turn over the wet paper towel so that the dry side is against the electrode (or replace) and invert the whole electrode structure. Again remove the top paper towel, realign the shims, and put the paper towel back with the dry side against the electrode. Replace the top plate, and repeat the pressing procedure, again holding for about 20 seconds.

Remove from the press and remove everything from between the plates. Now, using the cut hard/smooth paper towels, another pressing will be performed to within a few mils of the final thickness. As the paper towels will compress slightly, the total shim thickness is designed such that the pressing will result in the desired final thickness of the electrode. In other words, the thicknesses of the

(12) Special Instructions for Electrodes with $Ca(OH)_2$.

The addition of $Ca(OH)_2$ into the electrodes adds some complications to this procedure for which there need to be adjustments. First, there usually appears to be less loss of the active material during the manufacture so the amount of excess needs to be decreased accordingly. Secondly, the active material seems to hold water very tightly so the final weight will be higher than expected. Chemical analysis is the best way to determine the amount of active material vs H_2O in the final electrode.

In addition, as $Ca(OH)_2$ is less dense, the final electrode thickness will be greater, requiring slightly more PTFE (6% instead of 4% for the 40% $Ca(OH)_2$ electrodes and 5% for the 25% $Ca(OH)_2$ electrodes). Unfortunately, the cakes obtained from vacuum filtration are thinner than those with just ZnO. This required the porosity to be decreased to 70% in order to ensure a constant porosity and thickness. Some cakes come out at or slightly less than 75% porosity after vacuum filtration itself.

To help make as thick cakes as possible, do not allow the cake to become as dry as the ZnO cakes during vacuum filtration. Stop the filtering process one or two seconds sooner. Also, do not overdry the cakes between paper towels before pressing, and often the initial pressing with folded paper towels can be eliminated.

After the electrode is dried overnight, do not dry in the oven. Drying in the oven dries off some of the trapped H_2O, but this causes the electrode to crack and separate from the current collector. The water seems to be necessary for the electrode.

Finally, the finished $Ca(OH)_2$ electrode is much stiffer than the ZnO-only electrodes. The electrode is not flexible and is somewhat similar to plaster. However, the electrode is fairly strong. The electrode will require stronger force with the knife for trimming.

(13) End.

Following the procedures and with slight adjustments for different materials and equipment, good ZnO and $Ca(OH)_2$ electrodes should be formed on a consistent basis. The procedure also allows for the easy incorporation of other additives and should prove to be very useful in the manufacture of other types of similar electrodes.

Table A1

A list of the required materials and equipment in electrode manufacture. In parenthesis is listed the actual material used when appropriate.

- ZnO power (Mallinckrodt & "Analytical Reagent")

- $Ca(OH)_2$ power (Mallinckrodt & "Analytical Reagent")

- PbO powder (Mallinckrodt & "Analytical Reagent"—yellow, low silver)

- Acetone (Fisher Scientific Certified A.C.S.)

- Deionized H_2O

- PTFE Binder (Dupont TFE-30 Fluorocarbon Resin Dispersion)

- Lead-plated copper expanded mesh current collector

- Blender and small blender cup (Osterizer "Galaxie" with ½ pint (8 ounce) size cups).

- Weighing scale - accurate to at least .001 grams

- Beakers - 10 ml and 400 ml (PYREX)

- 1 to 2 ml graduated pipette with 0.1 ml graduations

- Vacuum filter table with a strong and fairly smooth filtering surface larger than the size of the electrode

- Pliable rubber gasket with the open area in the center being of the desired dimensions of the active material (Handmade by cutting a flexible rubber sheet)

- Strong, stiff plastic and/or metal frame with the open area the same as that of the gasket. Also, a clamping mechanism to attach the mold over the rubber gasket on the filtering table tightly enough to prevent seepage. Clamp should be easy and quick, < 1 min. to remove and reinstall.

- Filtering paper (Whatman 50, hardened 12.5 cm filter paper)

- Porous polypropylene sheet (Kendall Fiber Products Div., Webril non-woven fabric. Grade No. 1583, 0.005" thick).

- Vacuum line (Bldg. vacuum line)

- Vacuum hoses and vacuum bottle between vacuum line and vacuum filtering table

- Individual, soft paper towels (Crown Public Service No. 785, single fold, bleached towels, 10 x 10¼ in).

- Hard, smooth paper towels (Crown Jumbo Certified Natural Roll Towels No. 963-UA5-190-3)

- Press - hydraulic or electric capability of at least 2,000 lbs. and large enough to hold and provide even force on the plates used to press the electrode.

- Stainless steel shims - capable of providing the thickness range from 1 to 100 mils (±1 mil)

- Stainless steel Plates - machined flat to ±1 mil and at least ½" larger than the electrode body on each side. It is advantageous to have guiding rods incorporated to prevent the plates from sliding.

- Oven - capable of 150°C.

- Very sharp scalpel-type knife (X-Acto Knife).